

Tangential homoclinic points locus of the Lozi maps and applications

Kilassa Kvaternik, Kristijan

Doctoral thesis / Disertacija

2022

Degree Grantor / Ustanova koja je dodijelila akademski / stručni stupanj: **University of Zagreb, Faculty of Science / Sveučilište u Zagrebu, Prirodoslovno-matematički fakultet**

Permanent link / Trajna poveznica: <https://um.nsk.hr/um:nbn:hr:217:887608>

Rights / Prava: [In copyright](#)/[Zaštićeno autorskim pravom.](#)

Download date / Datum preuzimanja: **2025-03-14**



Repository / Repozitorij:

[Repository of the Faculty of Science - University of Zagreb](#)





University of Zagreb

FACULTY OF SCIENCE
DEPARTMENT OF MATHEMATICS

Kristijan Kilassa Kvaternik

**Tangential homoclinic points locus of
the Lozi maps and applications**

DOCTORAL DISSERTATION

Zagreb, 2022



University of Zagreb

FACULTY OF SCIENCE
DEPARTMENT OF MATHEMATICS

Kristijan Kilassa Kvaternik

**Tangential homoclinic points locus of
the Lozi maps and applications**

DOCTORAL DISSERTATION

Supervisor:

prof. dr. sc. Sonja Štimac

Zagreb, 2022



Sveučilište u Zagrebu

PRIRODOSLOVNO–MATEMATIČKI FAKULTET
MATEMATIČKI ODSJEK

Kristijan Kilassa Kvaternik

**Područje tangencijalnih homokliničkih
točaka Lozijeve preslikavanja i primjene**

DOKTORSKI RAD

Mentor:

prof. dr. sc. Sonja Štimac

Zagreb, 2022.

ACKNOWLEDGEMENTS

First of all, I would like to thank my supervisor Prof. Dr. Sonja Štimac for the immense support during my doctoral studies. She introduced me to the field, had a lot of patience during our discussions, always gave constructive advice and made sure that I could actively participate in our wonderful international scientific community. Her efforts have left an indelible mark on my professional development.

My friends and colleagues were always here to listen, show support in any way they could and cheer me up whenever I lacked motivation. To address each of these contributions individually would be a very thankless and probably impossible task to accomplish. I just hope you guys know how lucky I am to be surrounded by such people.

Finally, my mother Jasna always fought for me and my grandmother Marija showed me how to see the good in people - thank you for all the life lessons you taught me. Although he was not present on this journey, my grandfather Vlado unquestionably believed in me and I know he would be the proudest of all to see this work. This thesis is dedicated to him.

SUMMARY

In this thesis we consider the dynamics of the two-parameter Lozi family of planar homeomorphisms, more precisely, the relationship between the stable and unstable manifold of the hyperbolic fixed point X of that family in the first quadrant together with their intersections, homoclinic points. We describe the zigzag structure which the stable manifold of X forms in the third quadrant, prove that all homoclinic points in the border case are tangential and construct polygons bounded by the stable and unstable manifold of X which allows us to conclude that all border homoclinic tangencies consist of iterates of two distinct points T_0 and V_0 which are the points at which the stable and the unstable manifold, starting from X , intersect the horizontal and vertical axis for the first time respectively. In addition, by posing analytic conditions on the stable and unstable manifold of X , we compute the equations of the first few curves representing the border of the set of existence of homoclinic points for that fixed point.

The determined border is utilized for the introduction of a region in the parameter space for which there are no homoclinic points for X and the period-two cycle is attracting. In this region we further investigate the unstable manifold of X , construct polygons which are in part bounded by it and invariant under the square of the Lozi map and in addition, prove that every part of the unstable manifold which is a finite polygonal line has an open neighborhood disjoint from its complement. We ultimately prove that the topological entropy of the Lozi map is zero for all parameter pairs in the mentioned region if the unstable manifold of X intersects the coordinate axes at T_0 and its inverse image only. Along with this result, we also show that the topological entropy is zero on the complement of the accumulation set of the unstable manifold of X . These results expand the already known ones about the zero entropy locus by a large set of parameters.

In addition, these results are used to observe the basin of attraction for the Lozi map.

Summary

We turn our attention to the stable manifold of the fixed point Y in the third quadrant: we prove that it intersects the horizontal axis at a point right to T_0 which implies that it tends to infinity and accumulates on the stable manifold of X in the first quadrant. As a consequence, the stable manifold of Y separates the plane into two connected components and we prove that the basin of attraction is contained in one of them.

Keywords: Lozi map, stable manifold, unstable manifold, homoclinic points, homoclinic tangency, topological entropy, basin of attraction.

SAŽETAK

U ovoj disertaciji promatramo dinamiku dvoparametarske Lozijeve familije homeomorfizama ravnine, preciznije, odnos stabilne i nestabilne mnogostrukosti hiperboličke fiksne točke X te familije u prvom kvadrantu zajedno s njihovim presjecima, homokliničkim točkama. Opisujemo cik-cak strukturu koju stabilna mnogostrukost od X tvori u trećem kvadrantu, dokazujemo da su sve homokliničke točke u graničnom slučaju tangencijalne i konstruiramo poligone omeđene stabilnom i nestabilnom mnogostrukosti od X iz čega možemo zaključiti da se sve homokliničke točke u graničnom slučaju sastoje od iterata dviju istaknutih točaka T_0 i V_0 , točaka u kojima stabilna i nestabilna mnogostrukost, krećući od X , redom sijeku horizontalnu i vertikalnu os po prvi put. Uz to, postavljajući analitičke uvjete na stabilnu i nestabilnu mnogostrukost od X , računamo jednadžbe prvih nekoliko krivulja u parametarskom prostoru koje predstavljaju granicu skupa egzistencije homokliničkih točaka za tu fiksnu točku.

Izračunatu granicu možemo iskoristiti za uvođenje regije u parametarskom prostoru za koju ne postoje homokliničke točke za X i ciklus perioda dva je privlačan. U ovoj regiji dalje istražujemo nestabilnu mnogostrukost od X , konstruiramo poligone djelomice omeđene njome i invarijantne za kvadrat Lozijevog preslikavanja te uz to, dokazujemo da je svaki dio nestabilne mnogostrukosti koji je poligonalna dužina ima otvorenu okolinu disjunktne s njegovim komplementom. Ultimativno dokazujemo da je topološka entropija Lozijevog preslikavanja nula za sve parametarske parove u spomenutoj regiji ako nestabilna mnogostrukost od X siječe koordinatne osi samo u točki T_0 i njenoj praslici. Uz taj rezultat pokazujemo i da je topološka entropija jednaka nuli na komplementu skupa gomilišta nestabilne mnogostrukosti od X . Ovi rezultati proširuju već postojeće o području entropije nula za velik skup parametara.

Uz to, ovi rezultati se koriste kako bismo promatrali bazen atrakcije za Lozijevo pre-

Sažetak

slikavanje. Sada pozornost skrećemo na stabilnu mnogostrukost fiksne točke Y u trećem kvadrantu: dokazujemo da siječe horizontalnu os u točki desno od T_0 što povlači da teži u beskonačnost i gomila se na stabilnu mnogostrukost od X u prvom kvadrantu. Kao posljedicu dobivamo da stabilna mnogostrukost od Y dijeli ravninu na dvije komponente povezanosti te dokazujemo da je bazen atrakcije sadržan u jednoj od njih.

Ključne riječi: Lozijevo preslikavanje, stabilna mnogostrukost, nestabilna mnogostrukost, homokliničke točke, homoklinička tangentnost, topološka entropija, bazen atrakcije.

CONTENTS

Introduction	1
1 Preliminaries	6
1.1 Basic definitions and results	6
1.1.1 Orbits of points	6
1.1.2 Hyperbolicity	8
1.2 Lozi maps	11
1.2.1 Fixed and periodic points	11
1.2.2 Notation	16
1.3 Homoclinic points	19
1.4 Topological entropy	23
1.4.1 Definition and basic properties	23
1.4.2 Some results for the Lozi map	27
2 Homoclinic points for the Lozi map	31
2.1 Border of existence of homoclinic points for X	31
2.1.1 Structure of the stable manifold	31
2.1.2 Classification of border homoclinic points	37
2.2 Examples of border curves	47
2.2.1 First case: T_0^2 lies on $\overline{XV_0}^{(s)}$	47
2.2.2 Second case: V_0 lies on $\overline{T_0^2T_1}^{(u)}$	51
2.2.3 Third case: T_0^2 lies on $\overline{V_0^{-1}V_1}^{(s)}$	51
2.2.4 Fourth case: T_0^2 lies on $\overline{V_1V_0^{-2}}^{(s)}$	52
2.2.5 Fifth case: V_0 lies on $\overline{T_0^4T_0^{4,6}}^{(u)}$	53

2.2.6	Sixth case: T_0^4 lies on $\overline{V_0^{-1}V_1^{(s)}}$, i.e. $\overline{V_0^{-1}V_0^{-2}^{(s)}}$	55
2.2.7	Seventh case: V_0^{-1} lies on $\overline{T_0^5 T_{-2}^{(u)}}$	57
2.2.8	Eighth case: T_0^5 lies on $\overline{V_0^{-2}V_0^{-3}^{(s)}}$ in the third quadrant	58
2.2.9	Ninth case: T_0^5 lies on $\overline{V_0^{-2}V_0^{-3}^{(s)}}$ in the second quadrant	60
2.2.10	Tenth case: V_0^{-2} lies on $\overline{T_0^6 T_0^{6,8}^{(u)}}$	60
2.2.11	Eleventh case: T_0^7 lies on $\overline{V_0^{-2}V_0^{-3}^{(s)}}$	63
3	Zero entropy for the Lozi map	66
3.1	Relationship with the attracting period-two cycle	66
3.2	Invariant sets for L^2	69
3.3	Main results	76
4	Basin of attraction	82
4.1	Period two revisited	82
4.2	Relationship between W_Y^s and W_X^s	85
4.3	Approaching infinity	97
	Conclusion	106
	Bibliography	107
	Curriculum Vitae	110

INTRODUCTION

Maps on surfaces play a notable role in chaotic dynamics. One class of such maps was introduced by Hénon in 1976 as a two-parameter family of planar diffeomorphisms $H_{a,b}: \mathbb{R}^2 \rightarrow \mathbb{R}^2$,

$$H_{a,b}(x,y) = (1 + y - ax^2, bx).$$

Numerical computations conducted in [7] for parameter values $a = 1.4$ and $b = 0.3$ suggested the existence of a strange attractor, a set of points in the plane which possesses a neighborhood such that iterates of all points in it converge to that set. These considerations were formalized by Benedicks and Carleson in 1991 when they proved in [2] the existence of parameter pairs (a,b) for which there exists a strange attractor for the Hénon map. Despite the fact that the Hénon family is one of the most studied dynamical systems, still not much is known about its dynamical properties.

This family of maps motivated Lozi to define in his 1978 paper [11] a new two-parameter family $L_{a,b}: \mathbb{R}^2 \rightarrow \mathbb{R}^2$,

$$L_{a,b}(x,y) = (1 + y - a|x|, bx),$$

which is obtained by replacing the quadratic term in the Hénon map by an absolute value one. The results of Lozi's numerical computations for parameter values $a = 1.7$ and $b = 0.5$ also suggested the existence of a strange attractor (see Figure 1).

Although the family of the Lozi maps was initially introduced as a simpler model than the Hénon map family, it turned out that this map induces complicated dynamics and has been an object of research ever since. One of the first breakthroughs in the study of the Lozi maps was in 1980 when Misiurewicz proved in [12] that the Lozi map has a strange attractor for a large open set of parameters which is also known as the Misiurewicz parameter set.

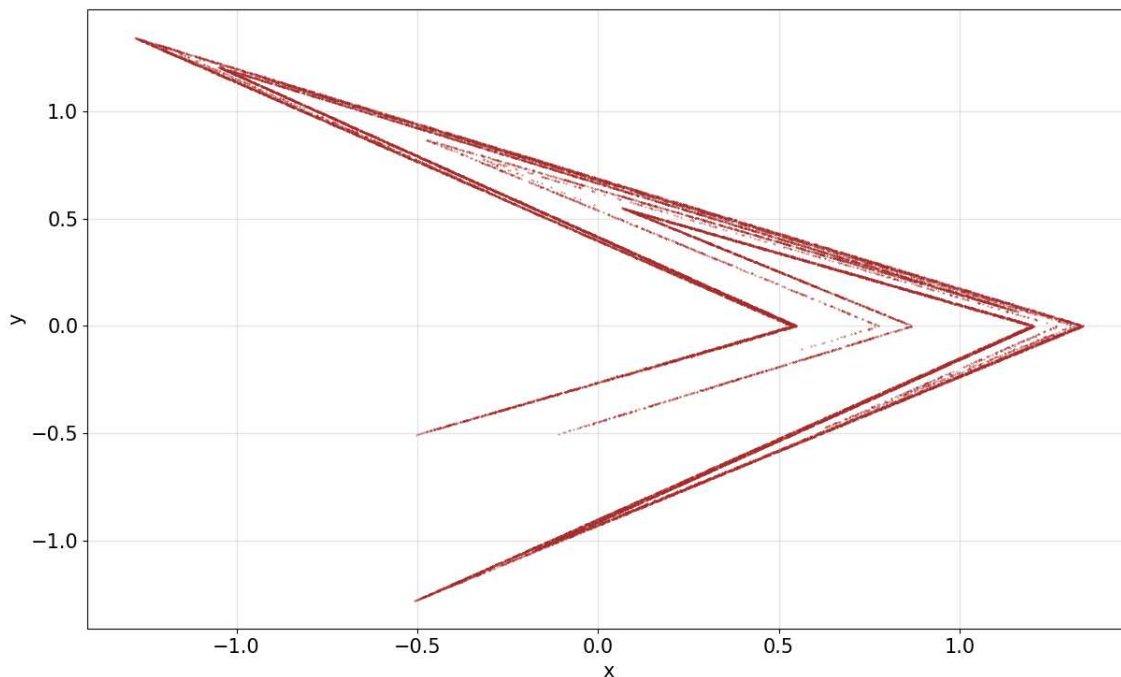


Figure 1: The Lozi attractor for the original choice of parameters $(a, b) = (1.7, 0.5)$.

To enrich and broaden the already existing theory and results about the Lozi map family, we will consider two main dynamical characteristics of that family: homoclinic points (see Definition 1.3.1) and topological entropy (see Section 1.4).

We start with a particular set of interest in the parameter space (see Figure 3.2); more precisely, we determine the most intricate part of its boundary by computing the equations of curves which represent the border of the set of existence of homoclinic points for the fixed point X in the first quadrant (Section 2.2). We also determine all possible homoclinic points for X on that border (Theorem 2.1.10). As we will see in the first chapter, homoclinic points are mainly studied in the context of diffeomorphisms (i.e. one typically requires differentiability of the map in consideration) so these results represent a step towards a comparable theory for homeomorphisms of the plane.

After determining the border of existence of homoclinic points for X , we consider the locus of points in the parameter space for which the corresponding Lozi maps have zero topological entropy. Even though the maximal entropy locus for the Lozi map is already known (see [8]) and some partial results about zero entropy were also obtained (see [21]), we will expand the latter results in Theorem 3.3.1 by proving that the topological entropy

of the Lozi map is zero for a large set of parameters for which there are no homoclinic points for X and the period-two cycle $\{P, P'\}$ is attracting. In addition, we will consider the basin of attraction for the Lozi map and prove that the basin is contained in a subset of the plane bounded by the stable manifold of the other fixed point Y in the third quadrant (Theorem 4.3.3). This result generalizes the one in [1] for the Misiurewicz parameter set.

As a byproduct of all these investigations, we will also obtain various results concerning the geometric structure of the stable and unstable manifolds of the fixed points for the Lozi map which help with the general understanding of the dynamics of that map and some of which can be applied to an even broader set of parameters than the one considered in this work.

Homoclinic points (Section 1.3), together with the dynamical behavior of nearby orbits, are of special interest in dynamical systems. In the case of the Lozi family, Ishii has proved in [8] the existence of homoclinic (heteroclinic) tangencies for all parameter pairs on the boundary of the region H for which the map contains a full Smale horseshoe (see Proposition 1.4.28 and Theorem 1.4.30). In Chapter 2, we investigate homoclinic tangencies associated to the fixed point X in the first quadrant, more precisely, the border of the set of existence of homoclinic points for X . The main result we prove in this chapter is Theorem 2.1.10 in which we determine homoclinic tangencies in the border case: all possible homoclinic points in the border case are iterates of T_0 and V_0 , points at which the unstable manifold W_X^u and stable manifold W_X^s , starting from X , intersect the x - and y -axis respectively for the first time.

The question of *topological entropy*, as a non-negative value which is a measure of complexity of a dynamical system, has also been of interest, but little is still known about the topological entropy of Lozi maps. Buzzi proved in [5] that the topological entropy is lower semi-continuous for piecewise affine homeomorphisms of compact surfaces and asked if the same could be concluded for upper semi-continuity. Yildiz gave a negative answer by using Lozi maps as a counterexample: he proved in [22] that the topological entropy for the Lozi map can jump from zero to a value above 0.1203 as one crosses a particular parameter and is thus not upper semi-continuous in general (see Theorem 1.4.27). A general formula from which the topological entropy of the Lozi map could be derived from the parameters is unknown.

Other results concern the monotonicity of topological entropy. Ishii and Sands have proven in [10] the monotonicity of entropy for the Lozi map in a neighborhood of the a -axis in the parameter space and Yildiz additionally contributed in [21] by showing monotonicity in the vertical direction around $a = 2$ and in some other directions for $1 < a \leq 2$; see Theorems 1.4.21, 1.4.22 and 1.4.23. Moreover, pruning theory enabled Ishii in [9] to establish partial monotonicity of the topological entropy as well as of bifurcations for the Lozi family near horseshoes and in addition, to prove that the Lozi map has maximal entropy (equal to $\log 2$) for parameter values in the aforementioned region H in the parameter space ([8]; see also Theorem 1.4.29).

Zero topological entropy is of special interest for this dissertation. In [21], Yildiz has determined several regions in the parameter space for which the Lozi map has zero topological entropy; see Theorems 1.4.24 and 1.4.25. In the latter theorem, Yildiz proved that $h_{top}(L_{a,b}) = 0$ for parameter values in a small neighborhood of $(a,b) = (1,0.5)$ and his numerical computations suggested that this point belongs to a much bigger region in the parameter space for which $L_{a,b}$ should also have zero entropy (see Figure 1.5). In Chapter 3, we prove in Theorem 3.3.1 that $h_{top}(L_{a,b}) = 0$ for all parameter pairs (a,b) in a region R in the parameter space for which the cycle $\{P, P'\}$ of period two is attracting, there are no homoclinic points for the fixed point X and the unstable manifold W_X^u intersects the coordinate axes only at the point T_0 and its preimage T_0^{-1} . Moreover, by expanding the parameter set to a region \mathfrak{R} for which W_X^u also intersects the coordinate axes at additional points, in Theorem 3.3.7 we show that the topological entropy of the Lozi map, restricted to the complement of the set ℓ of accumulation points of W_X^u , is also zero. We conjecture that $\ell = \{P, P'\}$, which would imply that the whole \mathfrak{R} is the zero entropy locus for the Lozi map when the period-two cycle is attracting.

In this dissertation we take a geometric approach to investigate the aforementioned dynamical properties of the Lozi map; this approach is used throughout the chapters of this dissertation for which we now give an overview:

- In Chapter 1 we give a review of some concepts of interest and known results about them, including elementary notions of topology and dynamical systems, introductory facts concerning the Lozi family (fixed and periodic points, stable and unstable manifolds), tangential homoclinic points and finally, the definition of topological

entropy together with some properties and results about the entropy of Lozi maps. This is the chapter in which we also present the notation used in the following ones;

- In Chapter 2 we investigate *homoclinic points* for the hyperbolic fixed point X in the first quadrant. In Section 2.1, we determine the homoclinic points in the border case: we prove that all such points are tangential in Lemma 2.1.8, describe the zigzag structure which the stable manifold of X forms in the third quadrant in Proposition 2.1.3, and finally, in Theorem 2.1.10, we conclude that all border homoclinic tangencies consist of iterates of T_0 and V_0 . In Section 2.2, we move on to calculating the equations (2.4)-(2.14) of some curves representing the border of the set of existence of those points in the parameter space;
- In Chapter 3 we consider the *zero entropy locus* for the Lozi map. We introduce the regions R and \mathfrak{R} in the parameter space for which there are no homoclinic points for X and the period-two cycle $\{P, P'\}$ is attracting. We further investigate the unstable manifold of X : in Lemma 3.2.5 we construct polygons which are in part bounded by it and invariant under the square of the Lozi map and in addition, we prove in Corollary 3.2.7 that every part of the unstable manifold which is a finite polygonal line has an open neighborhood disjoint from the rest of it. In Section 3.3 we state and prove Theorem 3.3.1, the main result about zero entropy for all parameter pairs in R , Theorem 3.3.7 about zero entropy outside the accumulation set ℓ of W_X^u for all parameter pairs in \mathfrak{R} as well as the corresponding conjecture for the set ℓ ;
- In Chapter 4 the main focus is put on the *basin of attraction* for the Lozi map. We turn our attention to the stable manifold of the fixed point Y in the third quadrant: in Proposition 4.2.3 we prove that it intersects the positive x -axis at a point right to T_0 which implies that it tends to infinity and converges to the stable manifold of X in the first quadrant (Corollary 4.2.6). As a consequence, the stable manifold of Y separates the plane into two connected components \mathcal{A}_1 and \mathcal{A}_2 . In Theorem 4.3.3 we show that all points in \mathcal{A}_2 tend to infinity under the Lozi map which implies that the basin of attraction is contained in \mathcal{A}_1 . Moreover, in Theorem 4.3.7 we prove that $\mathcal{A}_1 \setminus W_X^s$ is the basin of attraction for the accumulation set ℓ from the previous chapter.

1. PRELIMINARIES

In this chapter we introduce elementary notions of interest for the following chapters: preliminaries from topology and dynamical systems, the Lozi map, homoclinic points and topological entropy. We define these notions and give an overview of known relevant results about them.

1.1. BASIC DEFINITIONS AND RESULTS

1.1.1. Orbits of points

Definition 1.1.1. A *dynamical system* is a pair (X, f) , where X is a topological space and $f: X \rightarrow X$ a function.

For every $n \in \mathbb{N}$, we put $f^n = \underbrace{f \circ f \circ \dots \circ f}_{n \text{ times}}$; specially, we define f^0 as the identity map. Additionally, if f is invertible, we also denote $f^{-n} = \underbrace{f^{-1} \circ f^{-1} \circ \dots \circ f^{-1}}_{n \text{ times}}$.

Definition 1.1.2. A set $A \subseteq X$ is *f-invariant* if $f(A) \subseteq A$.

Definition 1.1.3. The *forward orbit* of a point $x \in X$ under the map f is the set $\mathcal{O}^+(x, f)$ of all iterates of x under f , i.e.

$$\mathcal{O}^+(x, f) = \{f^n(x) : n \in \mathbb{N}_0\}.$$

If f is also invertible, the *backward orbit* of x under f is defined as the set $\mathcal{O}^-(x, f)$ of all iterates of x under f^{-1} , i.e.

$$\mathcal{O}^-(x, f) = \{f^{-n}(x) : n \in \mathbb{N}_0\}.$$

The *full orbit* of x under f is the set of all iterates of x under f and f^{-1} , $\mathcal{O}(x, f) = \{f^n(x) : n \in \mathbb{Z}\}$.

Specific points of interest are fixed and periodic points.

Definition 1.1.4. A point $p \in X$ is said to be a *periodic point* for f if there exists $n \in \mathbb{N}$ such that $f^n(p) = p$. The smallest such n will be denoted by $\tau(p)$ and called the *prime period* of p . Specially, if $\tau(p) = 1$, we say that p is a *fixed point* for f .

More generally, one can consider points whose neighborhoods do not "wander away".

Definition 1.1.5. A point $x \in X$ is said to be a *non-wandering point* if for every neighborhood U of x there exists $n \in \mathbb{N}$ such that $f^n(U) \cap U \neq \emptyset$. The set of all non-wandering points for f , the *non-wandering set*, is denoted $\Omega(f)$. A point $y \in X$ is said to be a *wandering point* if there exists an open neighborhood V of y and $n_0 \in \mathbb{N}$ such that $f^n(V) \cap V = \emptyset$ for all $n \in \mathbb{N}, n \geq n_0$.

We next define the notion which describes the "equality" of two dynamical systems.

Definition 1.1.6 (Topological conjugacy). Let (X, f) and (Y, g) be dynamical systems. These systems are *topologically conjugate* if there exists a homeomorphism $h: X \rightarrow Y$ such that

$$g \circ h = h \circ f.$$

The proof of this well-known result about topological conjugacy can be found in e.g. [6].

Proposition 1.1.7. Let (X, f) and (Y, g) be topologically conjugate dynamical systems and $h: X \rightarrow Y$ a conjugacy between f and g .

1. For every $x \in X$, $h(\mathcal{O}^+(x, f)) = \mathcal{O}^+(h(x), g)$, i.e. h maps orbits of f to orbits of g .
2. For every $p \in X$, p is a fixed (periodic) point for f if and only if $h(p)$ is a fixed (periodic) point for g .
3. Conjugacy h maps $\Omega(f)$ to $\Omega(g)$, i.e. a point $x \in X$ is a non-wandering point for f if and only if $h(x)$ is a non-wandering point for g .

1.1.2. Hyperbolicity

Now let M be a smooth surface (two dimensional manifold) and $f: M \rightarrow M$ a diffeomorphism. We denote the differential of f by Df .

Definition 1.1.8. An f -invariant subset $\Lambda \subseteq M$ is said to be a *hyperbolic set* if for every $p \in \Lambda$, the tangent space to M at p admits a splitting

$$T_p M = E_p^s \oplus E_p^u$$

such that:

1. there exist positive constants C and $\lambda < 1$ satisfying

$$\|Df^n(p)\mathbf{v}\| \leq C\lambda^n \|\mathbf{v}\|, \text{ for all } \mathbf{v} \in E_p^s,$$

$$\|Df^{-n}(p)\mathbf{v}\| \leq C\lambda^n \|\mathbf{v}\|, \text{ for all } \mathbf{v} \in E_p^u,$$

for all $n \in \mathbb{N}$,

2. $Df(p)E_p^s = E_{f(p)}^s$ and $Df(p)E_p^u = E_{f(p)}^u$, i.e. the splitting is Df -invariant.

The subspaces E_p^s and E_p^u are respectively called the *stable* and *unstable subspace* at p .

Remark 1.1.9. If M is a surface and E_p^s, E_p^u are both non-trivial spaces, notice that these spaces are lines (and are therefore called the stable and unstable lines).

Definition 1.1.10. Let $f: M \rightarrow M$ be a diffeomorphism and $\Lambda \subseteq M$ a hyperbolic set for f . For $p \in \Lambda$ and $\varepsilon > 0$, the *local stable* and *unstable manifold* of p are defined respectively as

$$W_{p,\varepsilon}^s = \{x \in M: \lim_{n \rightarrow \infty} \text{dist}(f^n(p), f^n(x)) = 0 \text{ and } \text{dist}(f^n(p), f^n(x)) < \varepsilon \text{ for all } n \in \mathbb{N}_0\},$$

$$W_{p,\varepsilon}^u = \{x \in M: \lim_{n \rightarrow \infty} \text{dist}(f^{-n}(p), f^{-n}(x)) = 0 \text{ and } \text{dist}(f^{-n}(p), f^{-n}(x)) < \varepsilon \text{ for all } n \in \mathbb{N}_0\}.$$

The *stable* and *unstable manifold* of p are respectively

$$W_p^s = \bigcup_{n=0}^{\infty} f^{-n}(W_{f^n(p),\varepsilon}^s), \quad W_p^u = \bigcup_{n=0}^{\infty} f^n(W_{f^{-n}(p),\varepsilon}^u).$$

The definition does not depend on the choice of ε . In the case of diffeomorphisms of the Euclidean plane, the following theorem guarantees the existence of local stable and unstable manifolds for hyperbolic sets.

Theorem 1.1.11 (Unstable manifold theorem; [6, Theorem 7.9]). Let $f: \mathbb{R}^2 \rightarrow \mathbb{R}^2$ be a diffeomorphism and Λ a compact, invariant, hyperbolic set for f . Then there exists a $\delta > 0$ such that for any $p \in \Lambda$, there is a smooth curve $\mathbf{c}_p: [-\delta, \delta] \rightarrow \mathbb{R}^2$ satisfying

1. $\mathbf{c}_p(0) = p$,
2. $\mathbf{c}'_p(0) \neq \mathbf{0}$,
3. $\mathbf{c}'_p(0)$ lies along the unstable line E_p^u ,
4. $f^{-1}(\mathbf{c}_p) \subset \mathbf{c}_{f^{-1}(p)}$,
5. $\lim_{n \rightarrow \infty} \text{dist}(f^{-n}(\mathbf{c}_p(t)), f^{-n}(p)) = 0$.

We see that the curve \mathbf{c}_p from the previous theorem corresponds to the local unstable manifold of p . An analogous result can be obtained for the local stable manifold by applying the previous theorem on the inverse of f .

Remark 1.1.12. The notions of hyperbolicity, stable and unstable manifolds are here presented in the two-dimensional setting since that will be the case of interest; however, analogous definitions and results can be obtained in higher dimensions, see e.g. [19].

One special class of diffeomorphisms that is extensively studied in hyperbolic dynamics are the so-called Axiom A diffeomorphisms.

Definition 1.1.13 ([20]). Let M be a smooth manifold. A diffeomorphism $f: M \rightarrow M$ is said to be an *Axiom A* diffeomorphism if

1. the non-wandering set $\Omega(f)$ is hyperbolic and compact,
2. the set of periodic points of f is dense in $\Omega(f)$.

We will conclude this section by giving a classification of hyperbolic periodic points.

Definition 1.1.14. Let M be a smooth manifold and $f: M \rightarrow M$ a diffeomorphism.

1. A periodic point p for f of prime period $\tau(p)$ is *hyperbolic* if all eigenvalues of the differential of $f^{\tau(p)}$, $Df^{\tau(p)}(p)$, have absolute value different than 1.
2. A hyperbolic periodic point p for f is said to be
 - (a) a *sink* or *attractive periodic point* if all eigenvalues of $Df^{\tau(p)}(p)$ have absolute value less than 1,
 - (b) a *source* or *repelling periodic point* if all eigenvalues of $Df^{\tau(p)}(p)$ have absolute value greater than 1,
 - (c) a *saddle point* if it is neither a sink nor a source.
3. If p is a periodic point for f of prime period $\tau(p)$, we say that f is said to be:
 - (a) *area dissipative* at p if $|\det Df^{\tau(p)}(p)| < 1$,
 - (b) *area expansive* at p if $|\det Df^{\tau(p)}(p)| > 1$,
 - (c) *area preserving* at p if $|\det Df^{\tau(p)}(p)| = 1$.

1.2. LOZI MAPS

In this section we will define the central object of this dissertation - the Lozi map family. We will present some elementary notions concerning the dynamics of maps of that family and explain the notation which will be used in the following chapters.

1.2.1. Fixed and periodic points

Definition 1.2.1. The *Lozi map family* is a 2-parameter family of piecewise affine planar homeomorphisms given by

$$L_{a,b}: \mathbb{R}^2 \rightarrow \mathbb{R}^2, \quad L_{a,b}(x,y) = (1 + y - a|x|, bx), \quad (1.1)$$

where $a, b \in \mathbb{R}$, $b \neq 0$.

We will often omit the parameters and write $L := L_{a,b}$.

The inverse of L is given by

$$L^{-1}: \mathbb{R}^2 \rightarrow \mathbb{R}^2, \quad L^{-1}(x,y) = \left(\frac{1}{b}y, x - 1 + \frac{a}{b}|y| \right). \quad (1.2)$$

From (1.1) and (1.2) we directly see how L and L^{-1} act on quadrants in the Cartesian plane for positive values of parameters a and b , see Lemma 2.1.1 and Figure 1.1.

The following result shows that it suffices to consider Lozi maps $L_{a,b}$ such that $|b| \leq 1$ - namely, Lozi maps with $|b| > 1$ are conjugate to inverses of maps with $|b| < 1$.

Remark 1.2.2. Let $|b| > 1$ and $a \in \mathbb{R}$. Then

$$h: \mathbb{R}^2 \rightarrow \mathbb{R}^2, \quad h(x,y) = (-y, -x)$$

is a topological conjugacy between $L_{a,b}$ and $L_{\frac{a}{b}, \frac{1}{b}}^{-1}$, i.e. $L_{a,b} \circ h = h \circ L_{\frac{a}{b}, \frac{1}{b}}^{-1}$.

Furthermore, a direct calculation gives us results about fixed and periodic points of Lozi maps and their hyperbolic character. Notice that the Lozi map is not differentiable on the whole \mathbb{R}^2 so we can consider its hyperbolic structure only at points at which hyperbolic splittings exist. The differential of L at all points in the right half-plane is constant and equals

$$DL_+ = \begin{bmatrix} -a & 1 \\ b & 0 \end{bmatrix},$$

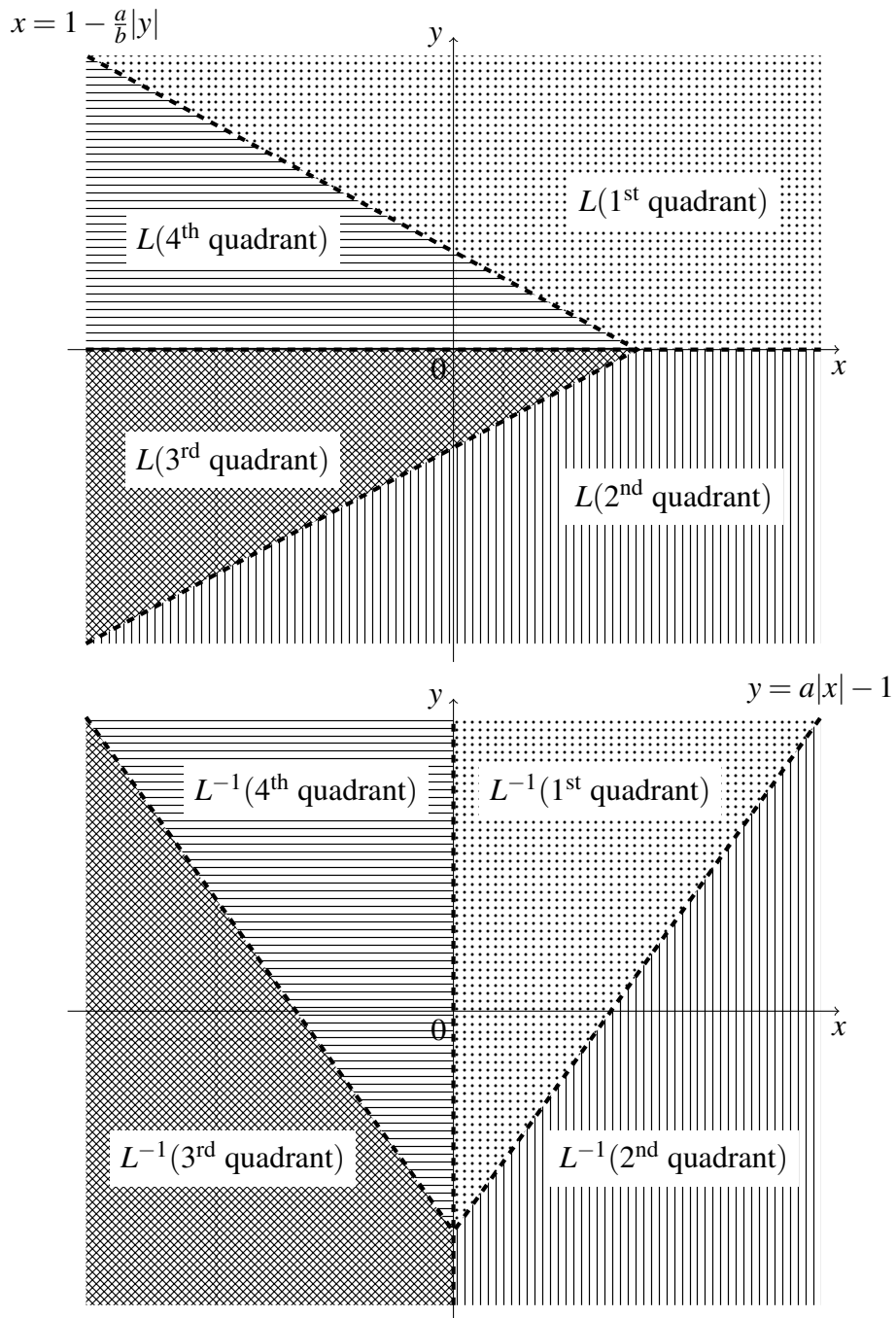


Figure 1.1: Images of quadrants in the Cartesian plane under the Lozi map L (above) and its inverse L^{-1} (below), for positive values of parameters a and b .

and similarly, the differential of L at all points in the left half-plane is equal to

$$DL_- = \begin{bmatrix} a & 1 \\ b & 0 \end{bmatrix}.$$

Remark 1.2.3 (Fixed points for the Lozi map). Let $0 < |b| \leq 1$ and $a \in \mathbb{R}$.

1. If $a \leq b - 1$, then the Lozi map L does not have any fixed points.
2. If $b - 1 < a \leq 1 - b$ and $b \neq 1$, L has one fixed point

$$X = \left(\frac{1}{1+a-b}, \frac{b}{1+a-b} \right).$$

This point lies in the first quadrant for $b > 0$ and in the fourth one for $b < 0$. If $b = -1$ and $a \in (-2, 2)$, or $b = 1 - a$, X is not hyperbolic. For other parameter values in this case, i.e. $b < 1 - a$, X is an attracting fixed point.

3. If $1 - b < a$, L has two fixed points,

$$X = \left(\frac{1}{1+a-b}, \frac{b}{1+a-b} \right), Y = \left(\frac{1}{1-a-b}, \frac{b}{1-a-b} \right).$$

These points lie respectively in the first and third quadrant for $b > 0$, i.e. in the fourth and second quadrant for $b < 0$. Both of these points are hyperbolic saddle points for all parameter values in this case.

Remark 1.2.4 (Periodic points for L of period 2). Let $0 < |b| \leq 1$ and $a \in \mathbb{R}$.

1. If $a < 1 - b$, L does not have any periodic points of prime period 2.
2. If $a = 1 - b$, there is a line segment I of period-two points for L given by

$$I = \left\{ (x, y) \in \mathbb{R}^2 : bx + y = \frac{b}{1-b}, 0 \leq x \leq \frac{1}{1-b} \right\}.$$

The segment I is contained in the first quadrant for $b > 0$ and in the fourth one for $b < 0$. These points are not hyperbolic.

3. If $a > 1 - b$, L has two periodic points of prime period 2,

$$P = \left(\frac{1+a-b}{a^2+(1-b)^2}, \frac{b(1-a-b)}{a^2+(1-b)^2} \right), P' = \left(\frac{1-a-b}{a^2+(1-b)^2}, \frac{b(1+a-b)}{a^2+(1-b)^2} \right).$$

These points lie respectively in the fourth and second quadrant for $b > 0$, i.e. in the first and third quadrant for $b < 0$. If $b \in (0, 1]$ and $a = b + 1$, these points are not hyperbolic. If $b \in (0, 1)$ and $1 - b < a < 1 + b$, these points are attracting. Finally, if $1 - a < b < a - 1$, these points are hyperbolic saddles.

From now on, we will observe parameter pairs (a, b) for which $0 < b < 1$, $a > 0$ and $a + b > 1$. In that case, the differential of L at its two hyperbolic fixed points X and Y in the first and third quadrant respectively is given by $DL(X) = DL_+$ and $DL(Y) = DL_-$.

The eigenvalues of the differential of L are

$$\lambda_X^u = \frac{1}{2}(-a - \sqrt{a^2 + 4b}) \text{ and } \lambda_X^s = \frac{1}{2}(-a + \sqrt{a^2 + 4b}) \text{ at } X,$$

and

$$\lambda_Y^u = \frac{1}{2}(a + \sqrt{a^2 + 4b}) \text{ and } \lambda_Y^s = \frac{1}{2}(a - \sqrt{a^2 + 4b}) \text{ at } Y.$$

Observe that $\lambda_X^u < -1$, $\lambda_Y^u > 1$ and $0 < \lambda_X^s < 1$, $-1 < \lambda_Y^s < 0$. Furthermore, the eigenvector corresponding to the eigenvalue λ is $\begin{pmatrix} \lambda \\ b \end{pmatrix}$.

Recall that the stable manifold of the fixed point X is the set of all points in the plane whose forward iterates under L converge to X :

$$W_X^s = \{T \in \mathbb{R}^2 : L^n(T) \xrightarrow{n \rightarrow \infty} X\}.$$

Similarly, the unstable manifold of X is the set of all points whose backward iterates under L converge to X :

$$W_X^u = \{T \in \mathbb{R}^2 : L^{-n}(T) \xrightarrow{n \rightarrow \infty} X\}.$$

As a direct consequence of these definitions, we see that W_X^s and W_X^u are L - and L^{-1} -invariant sets which both contain X .

Moreover, W_X^s and W_X^u are broken (polygonal) lines in the plane (and therefore not manifolds in the true meaning of that notion), see Figure 1.2. Namely, observe the unstable manifold W_X^u : locally at X , it is a straight line segment whose slope is parallel to the eigenvector corresponding to λ_X^u . This line segment intersects the positive x -axis at the point

$$T_0 = \left(\frac{2 + a + \sqrt{a^2 + 4b}}{2(1 + a - b)}, 0 \right).$$

For $n \in \mathbb{Z}$, put $T_0^n = L^n(T_0)$. Since X and T_0 are both contained in the right half-plane, L will act on the straight line segment $\overline{XT_0}$ as an affine map and therefore, $L(\overline{XT_0})$ is again a straight line segment whose endpoints are X and T_0^1 . Since T_0^1 lies in the second quadrant, $\overline{XT_0^1}$ intersects the positive y -axis and the point of intersection is T_0^{-1} , the inverse image of T_0 . The straight line segment $\overline{XT_0^{-1}}$ is contained in the right and $\overline{T_0^{-1}T_0^1}$ in the left

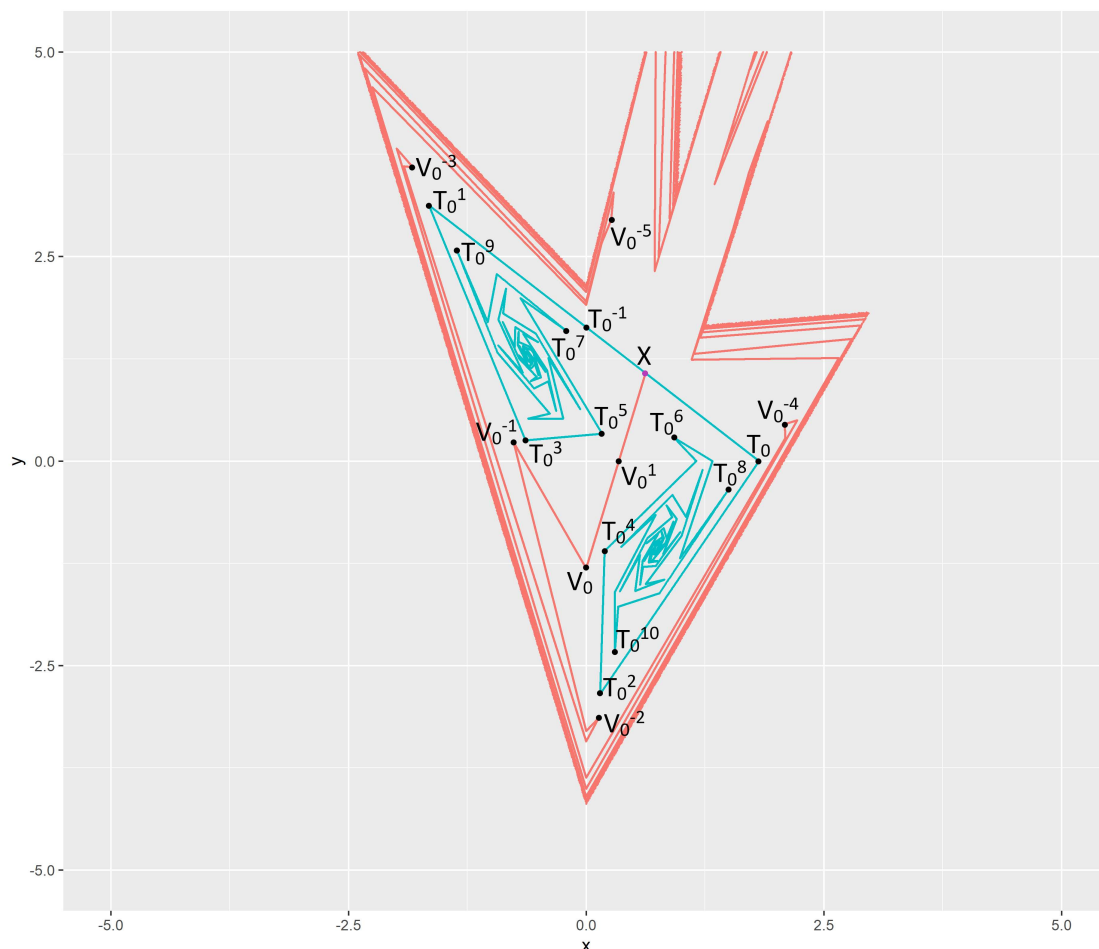


Figure 1.2: The stable (red) and unstable (blue) manifold of the fixed X for parameter values $a = 1.46$, $b = 0.86$, together with some iterates of T_0 and V_0 .

half-plane so L acts on each one of them as an affine map. The image $L(\overline{XT_0^1})$ is thus a broken line and consists of two straight line segments, $\overline{XT_0}$ and $\overline{T_0T_0^2}$. By taking further forward iterations of $\overline{XT_0}$ while considering the intersections with the y -axis we construct the polygonal line W_X^u and we see that

$$W_X^u = \bigcup_{n=0}^{\infty} L^n(\overline{XT_0}).$$

Additionally, we denote by W_X^{u+} the half of W_X^u starting at X and going to the right, passing through T_0 . The other half which starts at X and goes to the left, passing through T_0^{-1} , will be denoted by W_X^{u-} . Observe that

$$W_X^{u-} = \bigcup_{n=-\infty}^{\infty} L^{2n}(\overline{T_0^{-1}T_0^1}), \quad W_X^{u+} = \bigcup_{n=-\infty}^{\infty} L^{2n}(\overline{T_0T_0^2}).$$

Similarly, observe the stable manifold W_X^s which is, locally at X , a straight line segment whose direction vector is parallel to the eigenvector corresponding to λ_X^s . That line intersects the negative y -axis at the point

$$V_0 = \left(0, -\frac{a - 2b + \sqrt{a^2 + 4b}}{2(1 + a - b)} \right).$$

For $n \in \mathbb{Z}$, put $V_0^n = L^n(V_0)$. Then $\overline{XV_0}$ intersects the positive x -axis at V_0^1 , the forward image of V_0 . Since $\overline{XV_0^1}$ is contained in the upper and $\overline{V_0^1V_0}$ in the lower half-plane, L^{-1} will act on these segments as an affine map and $L^{-1}(\overline{XV_0})$ is a broken line consisting of two line segments, $\overline{XV_0}$ and $\overline{V_0V_0^{-1}}$. By taking further backward images of $\overline{XV_0}$ while considering the intersections with the x -axis we construct one half of W_X^s which will be denoted by W_X^{s-} and we have

$$W_X^{s-} = \bigcup_{n=0}^{\infty} L^{-n}(\overline{XV_0}).$$

The other half does not intersect the x -axis, it is a half-line starting from X and going to infinity in the first quadrant. We denote it by W_X^{s+} .

1.2.2. Notation

Before presenting some results about the Lozi map, we will first introduce the notation which is going to be used throughout this dissertation. We start with the notation for the standard number sets: by \mathbb{Z} we denote the set of integers, by \mathbb{N} the set of positive integers and $\mathbb{N}_0 = \mathbb{N} \cup \{0\}$.

Since we are working in the Euclidean plane, we will also use the following notation to denote geometrical objects and their topological characteristics:

- points in the plane will be denoted by capital Latin letters, possibly with indices: $A, B, C, \dots, A_1, B_1, C_1, \dots$. One exception is L which will always denote the Lozi map,
- specially, T_0 and V_0 will always denote points on W_X^u and W_X^s respectively, as defined in the previous subsection (see Figure 1.2), as well as X and Y , the fixed points of L ,

- for a point $A \in \mathbb{R}^2$, A_x and A_y will be the x and y coordinates of A respectively,
- for $A, B \in \mathbb{R}^2$, the straight line segment with A and B as endpoints will be denoted by \overline{AB} ,
- for $A \in \mathbb{R}^2$ and $\varepsilon > 0$, $B_\varepsilon(A)$ will represent the open ball in the plane centered at A of radius ε ,
- small Greek letters α, β, γ , etc. will stand for line segments, straight or polygonal ones,
- capital scripted letters \mathcal{A}, \mathcal{B} , etc. will denote two-dimensional subsets of the plane, typically polygons,
- $\text{dist}: \mathbb{R}^2 \times \mathbb{R}^2 \rightarrow \mathbb{R}$ will be the Euclidean metric in \mathbb{R}^2 ,
- for $\mathcal{A} \subset \mathbb{R}^2$ we will use the following notation:
 - $\text{Int } \mathcal{A}$... interior of \mathcal{A} ,
 - $\text{Cl } \mathcal{A}$... closure of \mathcal{A} ,
 - $\partial \mathcal{A}$... boundary of \mathcal{A} ,
 - $\text{Conv } \mathcal{A}$... convex hull of \mathcal{A} .

Finally, we will use specific notation concerning the Lozi map and the stable and unstable manifolds W_X^s and W_X^u :

- for every $n \in \mathbb{N}$, L^n will denote the composition $\underbrace{L \circ L \circ \dots \circ L}_{n \text{ times}}$ and $L^{-n} = \underbrace{L^{-1} \circ L^{-1} \circ \dots \circ L^{-1}}_{n \text{ times}}$.
Specially, we let L^0 be the identity map,
- for every $k \in \mathbb{Z}$, we put $T_0^k = L^k(T_0)$ and $V_0^k = L^k(V_0)$,
- for points $A, B \in W_X^u$, we put:
 - $[A, B]^{(u)} \subset W_X^u$... polygonal line lying on W_X^u with A and B as endpoints,
 - specially, if $[A, B]^{(u)}$ is a straight line segment, we denote it by $\overline{AB}^{(u)}$,
 - $[A, B]^{(u)} := [A, B]^{(u)} \setminus \{B\}$,

- $(A, B]^{(u)} := [A, B]^{(u)} \setminus \{A\}$,
- $(A, B)^{(u)} := [A, B]^{(u)} \setminus \{A, B\}$,
- for $A, B \in W_X^s$, we define the sets $[A, B]^{(s)}$, $\overline{AB}^{(s)}$, $[A, B)^{(s)}$, $(A, B]^{(s)}$ and $(A, B)^{(s)}$ analogously.

1.3. HOMOCLINIC POINTS

Homoclinic points were first defined by Poincaré in 1899. In his study [16] of the restricted three-body problem, Poincaré considered asymptotic curves of periodic solutions which are nowadays known as stable and unstable manifolds. Poincaré noted that even though these curves can not self-intersect, they can still intersect each other at points which he called homoclinic points, double asymptotic points. In Poincaré's own words, "...., these intersections form a kind of lattice-work, a weave, a chain-link network of infinitely finite mesh; each of the two curves can never cross itself, but it must fold back on itself in a very complicated way so as to recross all the chain-links an infinite number of times."

Definition 1.3.1. Let M be a smooth manifold and $f: M \rightarrow M$ a diffeomorphism with a periodic point p of prime period $\tau(p)$. A point $q \in M$ is said to be a *homoclinic point* for p if $q \neq p$ and q lies in the intersection of W_p^s and W_p^u .

In other words, homoclinic points are points whose forward and backward iterations under $f^{\tau(p)}$ both tend to p . There are two types of homoclinic points: *transversal* homoclinic points at which W_p^u and W_p^s intersect transversally and *homoclinic tangencies* which will be of interest in the second chapter (see Figure 1.3).

Remark 1.3.2. As previously mentioned, Lozi maps are not differentiable on the whole \mathbb{R}^2 and the stable and unstable manifolds of the hyperbolic fixed points are polygonal lines (the differential of L can not be continuously extended to the whole plane). However, transversal and tangential homoclinic intersections can be defined even in this case and these notions are formalized in Definition 2.1.7.

Today we know that homoclinic points are associated with complicated dynamical behaviour which is often linked to chaos. Poincaré noticed that the existence of one homoclinic point implies the existence of infinitely many of them. In addition to that, Smale, [20], presented in 1967 his well-known theorem which states that for every diffeomorphism f of a smooth manifold M which has a transversal homoclinic point x , there exists a Cantor set $\Lambda \subset M$ containing x and a positive integer m such that $f^m|_{\Lambda}$ is topologically conjugate to the shift automorphism on 2 symbols (see Definition 1.4.17). In

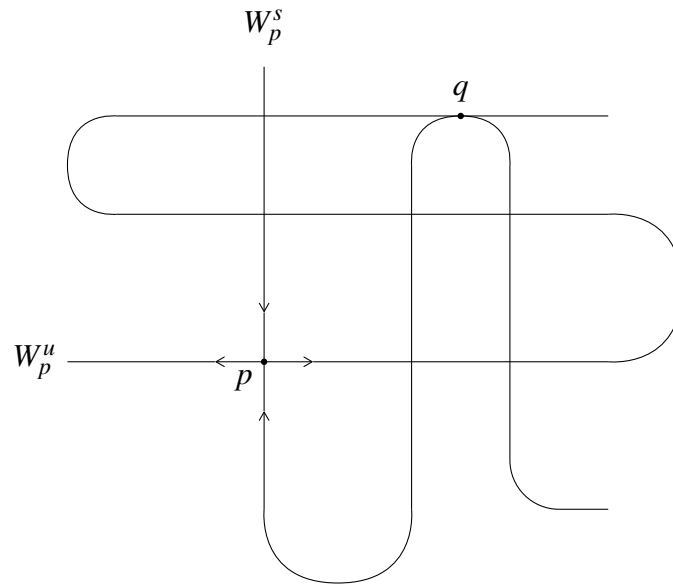


Figure 1.3: Point q is a tangential homoclinic point for p . All other points of intersection of W_p^s and W_p^u different from p on this picture are transversal homoclinic points.

particular, in every neighborhood of a transversal homoclinic point there is a periodic point.

One should note that the assumption of transversality of the homoclinic point in the previous result is essential (see e.g. [4]). In other words, tangential homoclinic points do not pose the same dynamical setting as transversal ones and are therefore subject to a separate study. Survey [15] describes one typical way of creation of homoclinic tangencies: let $\{f_\lambda : \lambda \in [0, 1]\}$ be a parameterized family of C^r -diffeomorphisms of the plane. For such families it frequently occurs that there is a saddle fixed point p_λ continuously depending on λ such that, for some parameter λ_0 , a homoclinic tangency is created at a point q_0 . Specifically, there exists an $\varepsilon > 0$ such that locally, on a small neighborhood of q_0 , the stable manifold $W_{p_\lambda}^s$ and the unstable manifold $W_{p_\lambda}^u$ do not intersect for $\lambda_0 - \varepsilon < \lambda < \lambda_0$, intersect tangentially at q_0 for $\lambda = \lambda_0$ and intersect at two distinct points for $\lambda_0 < \lambda < \lambda_0 + \varepsilon$ (see Figure 1.4).

Tangential homoclinic points are also a source of various dynamical phenomena. Mora and Viana in their 1993 paper [13] have given an answer to a conjecture by Palis by proving that for a one-parameter family $(f_\mu)_\mu$ of C^∞ -diffeomorphisms on a surface such that f_0 has a homoclinic tangency associated to some periodic point, under generic

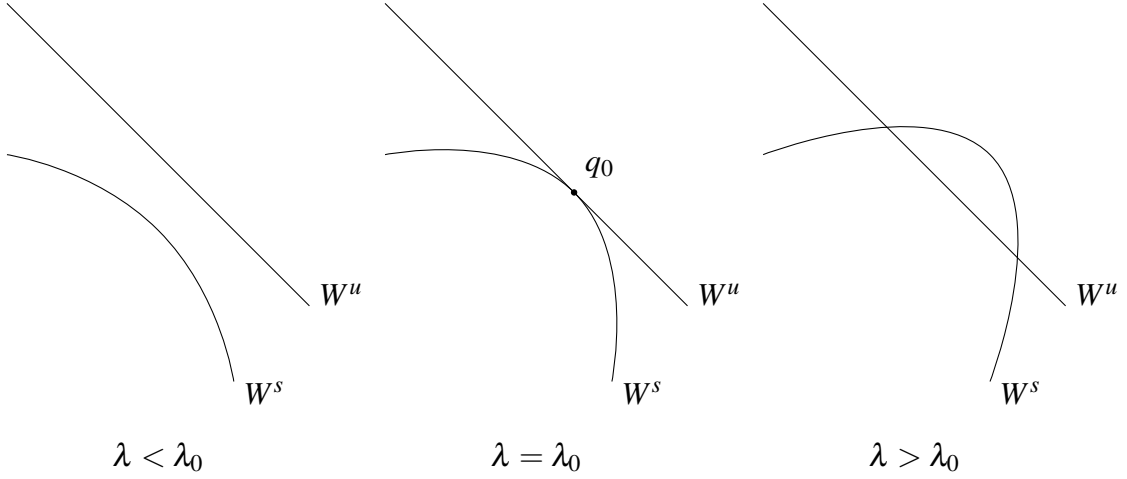


Figure 1.4: Creation of a homoclinic tangency (reworked picture from [15, Figure 7]).

assumptions, there is a positive Lebesgue measure set E of parameter values near $\mu = 0$ such that for $\mu \in E$ the diffeomorphism f_μ exhibits a strange attractor or repeller near the orbit of tangency.

Existence of tangential homoclinic points disrupts the structural stability of a dynamical system, i.e. the qualitative behavior of the trajectories is affected by small perturbations. One of the first results which formalize this statement were given by Newhouse in [14].

Let M be a compact surface and let $\text{Diff}^r M$ be the set of all C^r -diffeomorphisms $f: M \rightarrow M$.

Theorem 1.3.3 (Newhouse [14]; [3, Theorem 3.3]). Let $f: M \rightarrow M$ be any surface diffeomorphism with a homoclinic tangency associated to a saddle point p . Then

1. there exists an open subset \mathcal{U} of $\text{Diff}^2 M$ containing f in its closure, such that every $g \in \mathcal{U}$ may be approximated by a diffeomorphism with a homoclinic tangency associated to the continuation of p ;
2. if f is area dissipative, respectively area expansive at p , then there exists a residual subset $\mathcal{R} \subset \mathcal{U}$ such that every $g \in \mathcal{R}$ has an infinite number of periodic attractors, respectively periodic repellers.

Remark 1.3.4. As stated in [3], no element of \mathcal{U} can be uniformly hyperbolic. On the

other hand, the second claim states that maps with infinitely many sinks or sources are dense in \mathcal{U} .

In addition to that, Pujals and Sambarino in their paper [18] have established the relationship between diffeomorphisms with homoclinic tangencies and Axiom A diffeomorphisms (Definition 1.1.13).

Theorem 1.3.5 ([18, Theorem A]). Let M be a two-dimensional compact manifold and let $f \in \text{Diff}^1 M$. Then f can be C^1 -approximated by a diffeomorphism exhibiting a homoclinic tangency or by an Axiom A diffeomorphism.

As stated by the authors, this result gives a partial answer to a more general conjecture stated by Palis for C^r -diffeomorphisms in higher dimensions.

1.4. TOPOLOGICAL ENTROPY

In this section we present the notion of topological entropy - a numerical quantity which is an invariant of topological conjugacy and measures the complexity of a dynamical system in a certain sense. After giving the definition of topological entropy, we will focus on the known results about the topological entropy of the Lozi family, with a special emphasis on zero topological entropy.

1.4.1. Definition and basic properties

We present the definition in steps as given in [17] using open covers. In addition to that, we will also state one characterization and some basic properties of interest.

Let X be a compact metric space.

Definition 1.4.1 (Topological entropy of an open cover). Let \mathbf{A} be a finite open cover for X . The topological entropy of the cover \mathbf{A} is

$$H(\mathbf{A}) = \log N(\mathbf{A}),$$

the logarithm of the smallest number $N(\mathbf{A})$ of sets that can be used in a subcover of \mathbf{A} (i.e. that still form an open cover of X).

Definition 1.4.2 (Refinement of open covers). Let X be a compact metric space. If $\mathbf{A}^{(r)} = \{A_1^{(r)}, \dots, A_{N_r}^{(r)}\}$, $r = 1, \dots, k$, are finite open covers of X , then their *refinement* is defined as

$$\bigvee_{r=1}^k \mathbf{A}^{(r)} = \{A_{i_1}^{(1)} \cap A_{i_2}^{(2)} \cap \dots \cap A_{i_k}^{(k)} : i_j \in \{1, \dots, N_r\}, j = 1, \dots, k\}.$$

Remark 1.4.3. If $f: X \rightarrow X$ is a continuous map and $\mathbf{A} = \{A_1, \dots, A_n\}$ a finite open cover for X , we know that $f^{-1}(\mathbf{A}) := \{f^{-1}(A_1), \dots, f^{-1}(A_n)\}$ is again an open cover for X . This allows us to consider refinements of the form

$$\begin{aligned} \bigvee_{i=0}^{k-1} f^{-i}(\mathbf{A}) &= \mathbf{A} \vee f^{-1}(\mathbf{A}) \vee \dots \vee f^{-(k-1)}(\mathbf{A}) \\ &= \{A_{i_0} \cap f^{-1}(A_{i_1}) \cap \dots \cap f^{-(k-1)}(A_{i_{k-1}}) : 1 \leq i_0, i_1, \dots, i_{k-1} \leq n\}, \end{aligned}$$

for $k \geq 1$.

The following lemma gives some elementary properties of topological entropy of open covers.

Lemma 1.4.4 ([17, Lemma 3.1]).

1. $H(\mathbf{A}) \geq 0$ for all finite open covers \mathbf{A} .
2. If \mathbf{B} is a subcover of \mathbf{A} , then $H(\mathbf{A}) \leq H(\mathbf{B})$.
3. If \mathbf{A} and \mathbf{B} are two finite open covers for X , then

$$H(\mathbf{A} \vee \mathbf{B}) \leq H(\mathbf{A}) + H(\mathbf{B}).$$

4. If $f: X \rightarrow X$ is continuous and $f(X) = X$, then $H(\mathbf{A}) \geq H(f^{-1}(\mathbf{A}))$.
5. If $f: X \rightarrow X$ is a homeomorphism, then $H(\mathbf{A}) = H(f^{-1}(\mathbf{A}))$.

Definition 1.4.5 (Topological entropy of maps relative to an open cover). Let $f: X \rightarrow X$ be a continuous map. The topological entropy of f relative to an open cover \mathbf{A} is

$$h(f, \mathbf{A}) = \limsup_{n \rightarrow \infty} \frac{1}{n} H \left(\bigvee_{i=0}^{n-1} f^{-i}(\mathbf{A}) \right).$$

Remark 1.4.6 ([17, Lemma 3.2]). The limit from the previous definition is finite; namely, for every $n \in \mathbb{N}$,

$$\frac{1}{n} H \left(\bigvee_{i=0}^{n-1} f^{-i}(\mathbf{A}) \right) \leq H(\mathbf{A}).$$

Definition 1.4.7 (Topological entropy of continuous maps). If $f: X \rightarrow X$ is a continuous map on a compact metric space X , then the *topological entropy* of f is defined by

$$h_{top}(f) = \sup\{h(f, \mathbf{A}) : \mathbf{A} \text{ is a finite open cover for } X\}.$$

One important property of topological entropy is that it is preserved under topological conjugacy, i.e. one can use topological entropy for determining whether two systems are dynamically equivalent.

Proposition 1.4.8 ([17, Proposition 3.11]). Let X_1 and X_2 be compact metric spaces and $f_1: X_1 \rightarrow X_1$, $f_2: X_2 \rightarrow X_2$ continuous. If f_1 and f_2 are topologically conjugate, then $h_{top}(f_1) = h_{top}(f_2)$.

In addition, for a given continuous map f on a compact metric space X , one can also express the topological entropy of iterates of f in terms of $h_{top}(f)$.

Proposition 1.4.9 (Abramov's theorem; [17, Corollary 3.8.1]). Let $f: X \rightarrow X$ be a continuous map on a compact metric space X . Then for every $m \in \mathbb{N}$ we have $h_{top}(f^m) = mh_{top}(f)$.

Topological entropy can be characterized by using the notions of separated and spanning sets.

Definition 1.4.10. Let $f: X \rightarrow X$ be a continuous map on a compact metric space (X, d) and let n be a positive integer and $\varepsilon > 0$.

1. A finite set $S \subset X$ is called an (n, ε) -separated set if for any two distinct points $x, y \in S$ there exists $i \in \{0, 1, \dots, n-1\}$ such that $d(f^i(x), f^i(y)) > \varepsilon$. Let $s(n, \varepsilon)$ denote the maximal cardinality of any (n, ε) -separated set.
2. A finite set $R \subset X$ is called an (n, ε) -spanning set if for every $x \in X$ there exists $y \in R$ such that $d(f^i(x), f^i(y)) < \varepsilon$ for all $i \in \{0, 1, \dots, n-1\}$. Let $r(n, \varepsilon)$ denote the least cardinality of any (n, ε) -spanning set.

Proposition 1.4.11 ([17, Proposition 3.8]). The topological entropy of a continuous map $f: X \rightarrow X$ on a compact metric space X is given by

$$h_{top}(f) = \lim_{\varepsilon \rightarrow 0} \limsup_{n \rightarrow \infty} \frac{1}{n} \log(r(n, \varepsilon))$$

and

$$h_{top}(f) = \lim_{\varepsilon \rightarrow 0} \limsup_{n \rightarrow \infty} \frac{1}{n} \log(s(n, \varepsilon)).$$

Remark 1.4.12. The quantity $s(n, \varepsilon)$ can be interpreted as the number of orbit segments of length n which one can distinguish up to the precision of ε . Therefore, in view of Proposition 1.4.11, $h_{top}(f)$ can be interpreted as the qualitative measure of the average exponential growth of distinguishable orbit segments so we see that topological entropy measures the complexity of a dynamical system in that sense.

The following well-known result should illustrate the interpretation discussed in the previous remark.

Lemma 1.4.13. Let (X, d) be a compact metric space and $f: X \rightarrow X$ a continuous isometry on X . Then $h_{top}(f) = 0$.

Proof. Let $\varepsilon > 0$. Then $\{B_\varepsilon(x) : x \in X\}$ is an open cover for X which, due to compactness, can be reduced to a finite subcover, i.e. there exist $k \in \mathbb{N}$ and $x_1, \dots, x_k \in X$ such that $\{B_\varepsilon(x_i) : i = 1, 2, \dots, k\}$ is a finite open cover for X .

We claim that $\{x_1, \dots, x_k\}$ is an (n, ε) -spanning set for every $n \in \mathbb{N}$. Let $n \in \mathbb{N}$ and $y \in X$ be chosen arbitrarily and fixed. Then we can find $j \in \{1, 2, \dots, k\}$ such that $y \in B_\varepsilon(x_j)$. Because f is an isometry, for every $i \in \{0, 1, \dots, n-1\}$ we have

$$d(f^i(y), f^i(x_j)) = d(y, x_j) < \varepsilon,$$

which proves our claim.

As a consequence, $r(n, \varepsilon) \leq k$ for all $n \in \mathbb{N}$. Proposition 1.4.11 now implies

$$h_{top}(f) = \lim_{\varepsilon \rightarrow 0} \limsup_{n \rightarrow \infty} \frac{1}{n} \log(r(n, \varepsilon)) \leq \lim_{\varepsilon \rightarrow 0} \limsup_{n \rightarrow \infty} \frac{k}{n} = 0.$$

Since $h_{top}(f) \geq 0$ (which is a direct consequence of Lemma 1.4.4(1) and Definition 1.4.7), we conclude that $h_{top}(f) = 0$. ■

Remark 1.4.14. This result is aligned with the intuitive interpretation of topological entropy: the number of distinguishable orbits under isometries does not change. In particular, the topological entropy of the identity map on X is 0.

Another example of maps of significance for dynamical systems for which we can determine the topological entropy are the so-called full shifts on k symbols.

Definition 1.4.15. For $k \geq 2$, let

$$X_k = \{(\dots, x_{-2}, x_{-1}, x_0, x_1, x_2, \dots) \in \mathbb{N}^{\mathbb{Z}} : x_n \in \{1, 2, \dots, k\}, n \in \mathbb{Z}\} = \prod_{n \in \mathbb{Z}} \{1, 2, \dots, k\}.$$

For $x = (x_n)_{n \in \mathbb{Z}}, y = (y_n)_{n \in \mathbb{Z}} \in X_k$, we put

$$N(x, y) = \min\{N \in \mathbb{N}_0 : x_N \neq y_N \text{ or } x_{-N} \neq y_{-N}\}.$$

We define a metric $d: X_k \times X_k \rightarrow \mathbb{R}$ by

$$d(x, y) = \begin{cases} \left(\frac{1}{2}\right)^{N(x, y)}, & \text{if } x \neq y, \\ 0, & \text{otherwise.} \end{cases}$$

Lemma 1.4.16 ([17, Lemma 1.1]). X_k is a compact metric space.

Definition 1.4.17 (Full shift on k symbols). For $x = (x_n)_{n \in \mathbb{Z}}$, we define a map $\sigma: X_k \rightarrow X_k$ by $(\sigma x)_n = x_{n+1}$ for all $n \in \mathbb{Z}$.

Lemma 1.4.18 ([17, Lemma 1.2]). The map $\sigma: X_k \rightarrow X_k$ is a homeomorphism.

The following known result states the topological entropy of the full shift (see [17, Example on p. 22]).

Proposition 1.4.19 ([17]). If $\sigma: X_k \rightarrow X_k$ is the full shift on k symbols, then $h_{top}(\sigma) = \log k$.

1.4.2. Some results for the Lozi map

Remark 1.4.20. The Lozi map is defined on \mathbb{R}^2 which is not compact. To be able to investigate the topological entropy of the Lozi map, we take the one-point compactification of \mathbb{R}^2 and extend the map continuously to this set.

Ishii and Sands in [10] established monotonicity of topological entropy for the Lozi map $L_{a,b}$ in a neighborhood of the a -axis in the parameter space.

Theorem 1.4.21 ([10, Theorem 1]). For every $a_* > 1$ there exists $b_* > 1$ such that, for any fixed b with $|b| < b_*$, the topological entropy of $L_{a,b}$ is a non-decreasing function of $a > a_*$.

Additional results concerning the monotonicity of topological entropy were given by Yildiz in [21]. In contrast to Ishii and Sands, the author showed monotonicity in the vertical direction around $a = 2$ and in some other directions for $1 < a \leq 2$.

Theorem 1.4.22 ([21, Theorem 1.2]). For any fixed a^* in some neighborhood of $a = 2$, there exist $b_1^* > 0$ and $b_2^* < 0$ such that the topological entropy of $L_{a,b}$ is a non-increasing function of b for $0 < b < b_1^*$ and a non-decreasing function of b for $b_2^* < b < 0$.

For the next result we put $G = \{(a, b) \in \mathbb{R}^2: a > 1 + |b|\}$.

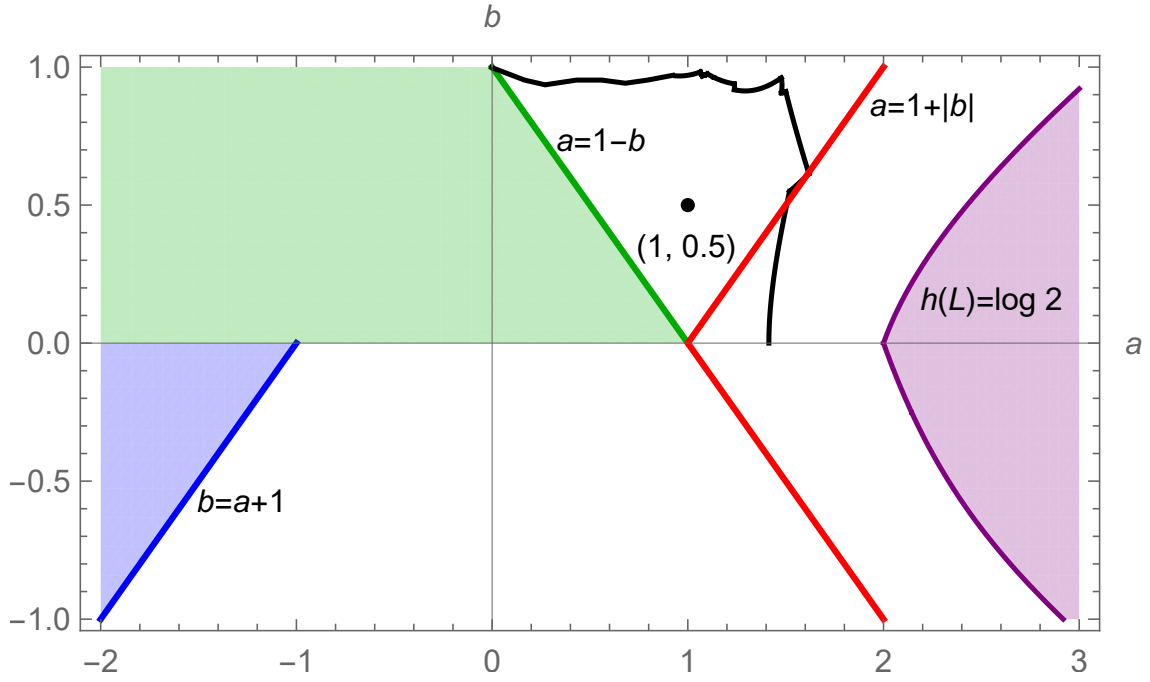


Figure 1.5: Regions (i) (blue), (ii) (green) and (iii) (green line) in the parameter space for which the topological entropy of the Lozi map is zero (Theorem 1.4.24). Point $(a, b) = (1, 0.5)$ belongs to a region bounded by the green, red and black curve in the first quadrant for which it was numerically observed that the topological entropy could also be zero (cf. Figures 2.8 and 3.2). The purple region on the very right is the maximal entropy region determined by Ishii (Proposition 1.4.28, Theorem 1.4.29). This picture is reworked from [21, Figure 6].

Theorem 1.4.23 ([21, Theorem 1.3]). For every $1 < a \leq 2$ there exist $N_a^1, N_a^2 \in \mathbb{R}^+$ and two lines $\mathbf{c}_{1,2}: (-\delta_{1,2}, \delta_{1,2}) \rightarrow G$, $\delta_{1,2} > 0$, given by $\mathbf{c}_1(t) = (a + N_a^1 t, -t)$, $\mathbf{c}_2(t) = (a + N_a^2 t, t)$, such that the topological entropy of $L_{\mathbf{c}_1(t)}$ and $L_{\mathbf{c}_2(t)}$ is a non-decreasing function of t .

In addition to that, Yildiz also states some regions in the parameter space for which the topological entropy of the Lozi map is equal to zero.

Theorem 1.4.24 ([21, Theorem 5.1]). If the Lozi map $L_{a,b}$ satisfies either

- (i) $-1 \leq b < 0$ and $a \leq b - 1$,
- (ii) $0 < b \leq 1$ and $a < 1 - b$,

(iii) $0 < b \leq 1$ and $a = 1 - b$,

then $h_{top}(L_{a,b}) = 0$.

These regions are represented on Figure 1.5. Recall that for $0 < |b| \leq 1$ and $a \leq b - 1$ the Lozi map family does not have any fixed or period-two points. For $0 < b < 1$ and $b - 1 < a \leq 1 - b$ it has a unique fixed point X : if $a < 1 - b$, X is attracting and the map does not have period-two points; if $a = 1 - b$, X is not hyperbolic and it is a midpoint of a line segment of period-two points.

Yildiz has also shown that the topological entropy is zero around a specific point in the parameter space which does not belong to the three aforementioned regions.

Theorem 1.4.25 ([21, Theorem 1.4]). In a small neighborhood of the parameters $a = 1$ and $b = 0.5$, topological entropy of $L_{a,b}$ is zero.

Remark 1.4.26. This case will be of specific interest as the point $(a, b) = (1, 0.5)$ belongs to a larger set R in the parameter space (see Figure 3.2) for which it will be proven in Chapter 3 that the topological entropy of $L_{a,b}$ is also zero.

In order to disprove upper semi-continuity of topological entropy of piecewise affine surface homeomorphisms, Yildiz has also shown in [22] that Lozi maps have a jump up in entropy.

Theorem 1.4.27 ([22, Theorem 1.2]). In general, the topological entropy of the Lozi maps does not depend continuously on the parameters: there exists some $\varepsilon_* > 0$ such that for all $0 < \varepsilon_1 < \varepsilon_*$ and $|\varepsilon_2| < \varepsilon_*$,

1. the topological entropies of the Lozi maps $L_{a,b}$ with $(a, b) = (1.4 + \varepsilon_2, 0.4 + \varepsilon_2)$ are zero.
2. the topological entropies of the Lozi maps, $h_{top}(L_{1.4+\varepsilon_1+\varepsilon_2, 0.4+\varepsilon_2})$, have a lower bound of 0.1203.

Results about maximal topological entropy of the Lozi family were also obtained. Namely, Ishii in his paper [8] defined a region H of points (a, b) in the parameter space for which $a > 1 + |b|$ and the Lozi map, restricted to the set K_L of points whose forward and backward orbits remain bounded, is topologically conjugate to the full shift on two symbols (see Figure 1.5).

Proposition 1.4.28 ([8, Corollary 1.4]). The boundary of H forms an algebraic curve \mathbf{g} . Moreover, \mathbf{g} is a graph of the following functions:

$$\begin{cases} a = \frac{1+b+3\sqrt{1+b^2}}{2} & \text{when } b > 0, \\ b = \frac{-6a^3 + 15a^2 - 8a + \sqrt{4a^6 - 20a^5 + 33a^4 - 16a^3}}{8a^2 - 16a + 8} & \text{when } b < 0. \end{cases}$$

Theorem 1.4.29 ([8, Corollary 1.5]). The topological entropy of $L_{a,b}$ is maximal, i.e. $h_{top}(L_{a,b}) = \log 2$, if and only if (a,b) is in the closure of H .

In the same paper, Ishii also considered tangencies between the stable and unstable manifolds of the Lozi map on the boundary of the set H and gave a solution to the so-called first tangency problem.

Theorem 1.4.30 ([8, Theorem 1.3]). Let $a > 1 + |b|$. For every $(a,b) \in \partial H$, the mapping $L_{a,b}$ has a heteroclinic (resp. homoclinic) tangency when $b > 0$ (resp. $b < 0$). In this case, the combinatorics of $L_{a,b}$ on K_L depends only on the sign of b .

Remark 1.4.31. As stated by the author, all tangencies of the stable and unstable manifolds for parameter values on ∂H are (pre)images of a special tangency on the x -axis.

Specially, in the case $b > 0$, the heteroclinic tangency between W_X^u and W_Y^s corresponds to the point C which we define and investigate in Chapter 4 (see Proposition 4.2.3).

For a fixed $b > 0$, moving along the positive a -axis in the parameter space from greater to smaller values, from the interior of the maximal entropy set H to its boundary (see Figure 1.5), we can conclude that the point C and all of its forward and backward iterates are points of first tangency for the Lozi map.

Remark 1.4.32. In the case $b > 0$, in Chapter 2 we investigate and determine homoclinic tangencies between W_X^u and W_X^s on the boundary of the set of existence of homoclinic points for the fixed point X . As it turns out, all possible tangencies in that case are forward and backward iterates of points T_0 and V_0 defined in Subsection 1.2.1.

As in the previous remark, we can continue to move along the positive a -axis in the parameter space, passing the aforementioned boundary and entering the region where there are no homoclinic points for X . Therefore, in contrast to Theorem 1.4.30, we can consider T_0, V_0 and their iterates as the *points of last tangency*.

2. HOMOCLINIC POINTS FOR THE LOZI MAP

In this chapter we would like to investigate the structure of homoclinic points for the fixed point X of the Lozi map; more precisely, we would like to describe borders of the area of their existence in the parameter space. Recall that a point T is said to be a *homoclinic point* for the fixed point X if T is contained in the intersection of its stable and unstable manifold, $T \in W_X^s \cap W_X^u$. In this chapter we will observe parameter pairs (a, b) such that $0 < b < 1$ and $a + b > 1$.

2.1. BORDER OF EXISTENCE OF HOMOCLINIC POINTS FOR X

2.1.1. Structure of the stable manifold

In this subsection we will describe in greater detail the shape that the stable manifold W_X^s forms in the third quadrant which will give us some insight into the order of appearance of breaking points on it. The two following technical lemmas will be useful during that analysis.

Lemma 2.1.1 (Some geometric properties of L and L^{-1}).

1. The image of the y -axis under L is the x -axis and the image of the x -axis under L is the curve $x = 1 - \frac{a}{b}|y|$.
2. The image of the x -axis under L^{-1} is the y -axis and the image of the y -axis under

L^{-1} is the curve $y = a|x| - 1$.

3. Let α be a line segment in the lower half-plane which lies on a straight line whose slope coefficient equals k_1 . Then the image of α under L^{-1} lies on a straight line whose slope coefficient equals

$$k_2 = b \cdot \frac{1}{k_1} - a.$$

Proof. All claims easily follow from straightforward calculations - we will prove the third one here.

Let (x_1, y_1) and (x_2, y_2) be two points lying on α . Because

$$L^{-1}(x, y) = \left(\frac{1}{b}y, x - 1 + \frac{a}{b}|y| \right)$$

and taking into account that $y_1 < 0$ and $y_2 < 0$, we have that

$$L^{-1}(x_1, y_1) = \left(\frac{1}{b}y_1, x_1 - 1 - \frac{a}{b}y_1 \right), \quad L^{-1}(x_2, y_2) = \left(\frac{1}{b}y_2, x_2 - 1 - \frac{a}{b}y_2 \right).$$

Because α is contained in the lower half-plane, L^{-1} will act on it as an affine map. Hence,

$$k_2 = \frac{x_2 - 1 - \frac{a}{b}y_2 - x_1 + 1 + \frac{a}{b}y_1}{\frac{1}{b}(y_2 - y_1)} = b \cdot \frac{x_2 - x_1}{y_2 - y_1} - \frac{\frac{a}{b}(y_2 - y_1)}{\frac{1}{b}(y_2 - y_1)} = b \cdot \frac{1}{k_1} - a.$$

■

We know that V_0 is the intersection of the y -axis and a straight line through X whose slope coefficient equals $k_0 = \frac{1}{2} (a + \sqrt{a^2 + 4b})$. Furthermore,

$$W_X^{s-} \cup \{X\} = \overline{XV_0}^{(s)} \cup \bigcup_{n=0}^{\infty} L^{-n} \left(\overline{V_0V_0}^{(s)} \right),$$

so we see that the part of W_X^{s-} which doesn't contain $\overline{XV_0}^{(s)}$ consists of preimages of a line segment lying in the lower half-plane. Notice that the third claim of Lemma 2.1.1 gives a recurrence for the slope coefficients for certain parts of those preimages.

Lemma 2.1.2. The sequence $(k_n)_{n \in \mathbb{N}_0}$ given by the recurrence

$$k_{n+1} = b \cdot \frac{1}{k_n} - a, \quad n \geq 0, \tag{2.1}$$

with $k_0 = \frac{1}{2} (a + \sqrt{a^2 + 4b})$, has the following properties:

1. if $k_{n_1} > 0$ for some $n_1 \in \mathbb{N}_0$, then $k_n > 0$ for all $n \leq n_1$,
2. if $k_{n_2} < 0$ for some $n_2 \in \mathbb{N}_0$, then $k_n < 0$ for all $n \geq n_2$,
3. for all $n \in \mathbb{N}_0$, if $k_{2n+1} > 0$, then $k_{2n+2} > 0$,
4. (k_n) converges and $\lim_{n \rightarrow \infty} k_n = \frac{1}{2} \left(-a - \sqrt{a^2 + 4b} \right)$.

Proof. First two claims immediately follow from recurrence (2.1) and $a, b > 0$. In order to prove the third claim, let

$$M_1 := \frac{1}{2} \left(-a - \sqrt{a^2 + 4b} \right), \quad M_2 := \frac{1}{2} \left(-a + \sqrt{a^2 + 4b} \right)$$

be the roots of the equation $M^2 + aM - b = 0$, i.e. fixed points of the function

$$f: \mathbb{R} \setminus \{0\} \rightarrow \mathbb{R}, \quad f(x) = b \cdot \frac{1}{x} - a,$$

which defines recurrence (2.1). Because $a, b > 0$, we see that $M_1 < 0$, $M_2 > 0$ and $|M_2| < |M_1|$. By setting

$$j_n := \frac{k_n - M_1}{k_n - M_2}, \quad n \in \mathbb{N}_0,$$

we see that

$$j_{n+1} \stackrel{(2.1)}{=} \frac{b \cdot \frac{1}{k_n} - a - M_1}{b \cdot \frac{1}{k_n} - a - M_2} = \frac{b \cdot \frac{1}{k_n} - b \cdot \frac{1}{M_1}}{b \cdot \frac{1}{k_n} - b \cdot \frac{1}{M_2}} = \frac{M_2}{M_1} \cdot j_n$$

for every $n \in \mathbb{N}_0$. If $\mu := \frac{M_2}{M_1}$, we have $-1 < \mu < 0$ and $(j_n)_{n \in \mathbb{N}_0}$ satisfies the recurrence

$$j_{n+1} = \mu j_n, \quad n \geq 0; \quad j_0 = \frac{1}{a} \left(a + \sqrt{a^2 + 4b} \right) > 0. \quad (2.2)$$

Therefore, $j_{2n} > 0$ and $j_{2n+1} < 0$ for all $n \in \mathbb{N}_0$. Now assume that $k_{2n+1} > 0$ for some $n \in \mathbb{N}_0$. Due to the fact that

$$k_n = \frac{M_1 - M_2 j_n}{1 - j_n}, \quad n \in \mathbb{N}_0, \quad (2.3)$$

and since $j_{2n+1} < 0$, i.e. $1 - j_{2n+1} > 0$, it follows that $M_1 - M_2 j_{2n+1} > 0$. A direct calculation now gives

$$k_{2n+2} \stackrel{(2.3)}{=} \frac{M_1 - M_2 j_{2n+2}}{1 - j_{2n+2}} \stackrel{(2.2)}{=} \frac{M_1 - M_2 \mu j_{2n+1}}{1 - \mu j_{2n+1}} = \frac{M_1^2 - M_2^2 j_{2n+1}}{M_1 - M_2 j_{2n+1}},$$

which combined together with $M_1^2 - M_2^2 j_{2n+1} > 0$ yields $k_{2n+2} > 0$.

third quadrant below the curve $y = a|x| - 1$. For every $n \in \mathbb{N}$, let $\alpha_n := [V_0^{-(n-1)}, V_0^{-n}]^{(s)}$ and notice that $\alpha_{n+1} = L^{-1}(\alpha_n)$. Since L^{-1} acts as an affine map in the lower half-plane, we see that $\alpha_1 = L^{-1}(V_0^1 V_0^{(s)})$ is a straight line segment and inductively, if α_n is a straight line segment contained in the third quadrant, α_{n+1} is again a straight line segment which may intersect the x -axis. If it intersects the x -axis, it follows that α_{n+2} (and consequently all α_i for $i \geq n+2$) intersects both coordinate axes in the third quadrant - more precisely, its intersection with the third quadrant is a straight line segment whose one endpoint lies on the x -axis and the other one on the y -axis.

In order to prove the first claim of the proposition, we suppose by contradiction that the polygonal segments α_n are all contained in the third quadrant. That implies that they are all straight line segments and the slope coefficient of each α_i is exactly the element k_i of the sequence from Lemma 2.1.2. Since

$$\begin{pmatrix} \lambda_Y^s \\ b \end{pmatrix} = \begin{pmatrix} \frac{1}{2} (a - \sqrt{a^2 + 4b}) \\ b \end{pmatrix} = \frac{1}{2} (a - \sqrt{a^2 + 4b}) \begin{pmatrix} \frac{1}{2} (-a - \sqrt{a^2 + 4b}) \end{pmatrix},$$

we see that the limit of their slope coefficients, $M_1 = \frac{1}{2}(-a - \sqrt{a^2 + 4b})$ (Lemma 2.1.2(4)), is equal to the stable direction for L at its fixed point Y in the third quadrant. By combining this together with the fact that L^{-1} is continuous, it follows that there exist $n' \in \mathbb{N}_0$ and $\eta > 0$ such that

$$\frac{\text{length}(\alpha_{n+1})}{\text{length}(\alpha_n)} > \eta > 1,$$

for all $n \geq n'$ (L^{-1} stretches all vectors in the direction $\begin{pmatrix} \lambda_Y^s \\ b \end{pmatrix}$ by the factor $\frac{1}{|\lambda_Y^s|} > 1$ when it acts as an affine map). The lengths of α_n are thus unboundedly increasing so one of those line segments will eventually intersect the x -axis, which is a contradiction with the original assumption that all segments α_n are contained in the third quadrant. As a consequence, there exists an $n \in \mathbb{N}_0$ for which α_n intersects the x -axis and the smallest $n \in \mathbb{N}$ for which that happens yields the desired n_0 , i.e. iterate $V_0^{-n_0}$ and proves the first claim.

It also immediately follows from previous discussions that $[V_0, V_0^{-(n_0-1)}]^{(s)}$ is contained in the third quadrant, together with the claim about the breaking points of W_X^s lying on it (since $\alpha_1, \alpha_2, \dots, \alpha_{n_0}$ are all straight line segments).

We now claim that $k_{n_0} < 0$. Notice that $V_0^{-(n_0+1)}$ lies in the preimage of the second quadrant, i.e. parts of the first and fourth quadrant below the curve $y = a|x| - 1$ and also,

$[V_0^{-n_0}, V_0^{-(n_0+1)}]^{(s)}$ has a breaking point P on the y -axis below V_0 (it is below the point $(0, -1)$ because α_{n_0} intersects the negative x -axis), i.e. $[V_0^{-n_0}, V_0^{-(n_0+1)}]^{(s)} = \overline{V_0^{-n_0}P}^{(s)} \cup \overline{PV_0^{-(n_0+1)}}^{(s)}$. If k_{n_0} would be positive, $\overline{V_0^{-n_0}P}^{(s)}$ would intersect $[V_0, V_0^{-(n_0-1)}]^{(s)}$ which is not possible. We thus conclude that k_{n_0} is negative.

Let i_0 be the smallest element of the set $\{1, \dots, n_0\}$ such that $k_{i_0} < 0$. The third claim of Lemma 2.1.2 implies that i_0 is odd. Let Q_1 be the intersection of the x -axis and the straight line through $V_0^{-(i_0-2)}$ and $V_0^{-(i_0-1)}$ (see Figure 2.1). Because $V_0^{-(i_0-2)}$ lies on $\overline{V_0^{-(i_0-1)}Q_1}$, $V_0^{-(i_0-1)}$ will lie on $\overline{V_0^{-i_0}L^{-1}(Q_1)}$, i.e. $V_{0,y}^{-i_0} > V_{0,y}^{-(i_0-1)}$. Similarly, if Q_2 is the intersection of the x -axis and the straight line through $V_0^{-i_0}$ and $V_0^{-(i_0+1)}$, then $V_0^{-(i_0+1)}$ lies on $\overline{V_0^{-i_0}L^{-1}(Q_2)}$ so $V_{0,y}^{-i_0} > V_{0,y}^{-(i_0+1)}$.

Because the second claim of Lemma 2.1.2 implies that $k_i < 0$ for all $i \geq i_0$, we conclude by using the same argument that $V_{0,y}^{-n} > V_{0,y}^{-(n-1)}$ for all odd n such that $i_0 \leq n \leq n_0$. Namely, for any such n , let Q' be the intersection of the x -axis and the straight line through $V_0^{-(n-2)}$ and $V_0^{-(n-1)}$. Since $V_0^{-(n-1)}$ lies on $\overline{V_0^{-(n-2)}Q'}$, V_0^{-n} will lie on $\overline{V_0^{-(n-1)}L^{-1}(Q')}$ and thus $V_{0,y}^{-n} > V_{0,y}^{-(n-1)}$ since the slope coefficient of the straight line through $V_0^{-(n-1)}$ and $L^{-1}(Q')$, k_n , is negative.

Since $V_{0,y}^{-n_0} > 0 > V_{0,y}^{-(n_0-1)}$, it follows that n_0 is odd, which finishes the proof. ■

Remark 2.1.4. Even though the first claim of Proposition 2.1.3 holds in general, notice that it can be proven more easily in the case when there exist homoclinic points for X - in that case W_X^s has a non-empty intersection with $\overline{T_0^1 T_0^{-1}(u)}$, the latter of which is a straight line segment in the second quadrant and thus disjoint from W_X^{s+} . This implies that W_X^{s-} intersects that line segment so one negative iterate of V_0 will eventually lie in the second quadrant in order for that to happen.

Definition 2.1.5. The broken line $[V_0, V_0^{-n_0}]^{(s)}$ from Proposition 2.1.3 will be called the *zigzag part* of W_X^s .

Corollary 2.1.6. W_X^s accumulates on W_Y^s .

Proof. Let n_0 and the polygonal segments α_n , $n \in \mathbb{N}$, be as in the proof of Proposition 2.1.3 and moreover, let β_n , $n \in \mathbb{N}$, denote the intersection of α_n with the third quadrant - notice that all β_n are straight line segments and that all β_n , $n > n_0$, intersect both coordinate axes.

Now observe the triangle OA_1A_2 , where O is the origin of the coordinate system and A_1, A_2 are the intersections of β_{n_0+1} with the x - and y -axis, respectively. If Y would be contained in that triangle, then the part of its stable manifold W_Y^s which is a part of a straight line passing through Y would intersect the zigzag part of W_X^s or α_{n_0+1} . Since W_X^s and W_Y^s cannot intersect, this is a contradiction and we thus conclude that Y is contained in the third quadrant outside of the aforementioned triangle.

On the other hand, the part of the unstable manifold of Y , W_Y^u , which is a part of a straight line passing through Y intersects the y -axis in the point

$$\left(0, \frac{a + 2b - \sqrt{a^2 + 4b}}{2(1 - a - b)} \right) = \left(0, -\frac{2b}{a + 2b + \sqrt{a^2 + 4b}} \right),$$

for which we easily see that is higher (has a larger y -coordinate) than V_0 . Therefore, W_Y^u intersects β_{n_0+1} and consequently, due to L^{-1} -invariance, every β_n . The sequence of those intersection points converges to Y which, combined together with the convergence of the slope coefficients of β_n (Lemma 2.1.2.4), implies that β_n accumulate on the arc component of W_Y^s in the third quadrant passing through Y . Since W_Y^s can be obtained as a countable union of iterates of that arc component under L^{-1} , the result follows. ■

2.1.2. Classification of border homoclinic points

To further investigate and characterize the border of the set of existence of homoclinic points for the fixed point X , we will first define two possible types of intersections of lines in the plane.

Definition 2.1.7. Let γ and δ be two (broken) lines in the plane intersecting at a point T . For $\varepsilon > 0$, let $\gamma_{T,\varepsilon}, \delta_{T,\varepsilon}$ be connected components of $\gamma \cap B_\varepsilon(T), \delta \cap B_\varepsilon(T)$ containing T , respectively.

We say that the intersection of γ and δ at T is *tangential* if there exists $\varepsilon > 0$ such that $B_\varepsilon(T) \setminus \gamma_{T,\varepsilon}$ consists of two connected components only one of which contains $\delta_{T,\varepsilon}$. If such ε does not exist, we say that the intersection at T is *transversal*.

As already mentioned, W_X^u and W_X^s are broken lines in the plane. Points at which these lines break, i.e. endpoints of maximal line segments contained in W_X^u and W_X^s , will be called *breaking points*.

Lemma 2.1.8. The border of existence of homoclinic points for X consists of exactly those parameter pairs (a, b) for which each intersection point of W_X^u and W_X^s different from X is tangential, i.e. is a breaking point of at least one of those manifolds.

Proof. We know that the border of existence of homoclinic points for X consists of parameter pairs (a, b) in each open neighborhood of which there are corresponding Lozi maps which do and do not exhibit homoclinic points. Notice that all breaking points of W_X^s and W_X^u , and thus W_X^s and W_X^u themselves, depend continuously on (a, b) . Therefore, if $L_{a', b'}$ has a transversal homoclinic point for some (a', b') , that intersection will be transversal on some open neighborhood of (a', b') in the parameter space which implies that this point lies in the interior of the set of existence of homoclinic points for X . Hence, on the border of that set all homoclinic intersections are tangential. ■

In order to finally determine homoclinic points in the border case, we first describe the general structure of the unstable manifold W_X^u .

Observe the forward orbit $(T_0^n)_{n \in \mathbb{N}_0}$ of T_0 . Because

$$T_0 = \left(\frac{2 + a + \sqrt{a^2 + 4b}}{2(1 + a - b)}, 0 \right) = \left(\frac{2}{2 + a - \sqrt{a^2 + 4b}}, 0 \right)$$

and $a - \sqrt{a^2 + 4b} < 0$ for $b > 0$, we see that T_0 lies on the positive x -axis and $T_{0,x} > 1$.

Therefore,

$$T_0^1 = \left(\frac{2 - a - \sqrt{a^2 + 4b}}{2 + a - \sqrt{a^2 + 4b}}, \frac{2b}{2 + a - \sqrt{a^2 + 4b}} \right).$$

Notice that for $a + b > 1$ and $b < 1$ we have

$$a > 1 - b \Rightarrow a^2 > 1 - 2b + b^2$$

which implies

$$\begin{aligned} a^2 + a\sqrt{a^2 + 4b} + 2b &> 1 - 2b + b^2 + a\sqrt{1 - 2b + b^2 + 4b} + 2b \\ &= 1 + b^2 + a(1 + b) \\ &= 1 + b(a + b) + a \\ &> 1 + a + b > 2. \end{aligned}$$

Hence,

$$0 > \frac{2 - a^2 - a\sqrt{a^2 + 4b} - 2b}{2(1 + a - b)} = \frac{2 - a - \sqrt{a^2 + 4b}}{2 + a - \sqrt{a^2 + 4b}} = T_{0,x}^1$$

and T_0^1 lies in the second quadrant - that is why T_0^2 will lie in the fourth or third quadrant and $[T_0, T_0^2]^{(u)}$ will not contain T_0^1 . In general, because L is order reversing, $[T_0, T_0^{2k}]^{(u)}$ will not contain any odd iterates of T_0 (for any given $k \in \mathbb{N}$) and vice versa. We will put $\gamma_n = [T_0^{2n-1}, T_0^{2n+1}]^{(u)}$, $\delta_n = [T_0^{2n}, T_0^{2n+2}]^{(u)}$ for every $n \in \mathbb{N}_0$, and

$$\Gamma = \bigcup_{n=0}^{\infty} \gamma_n, \quad \Delta = \bigcup_{n=0}^{\infty} \delta_n.$$

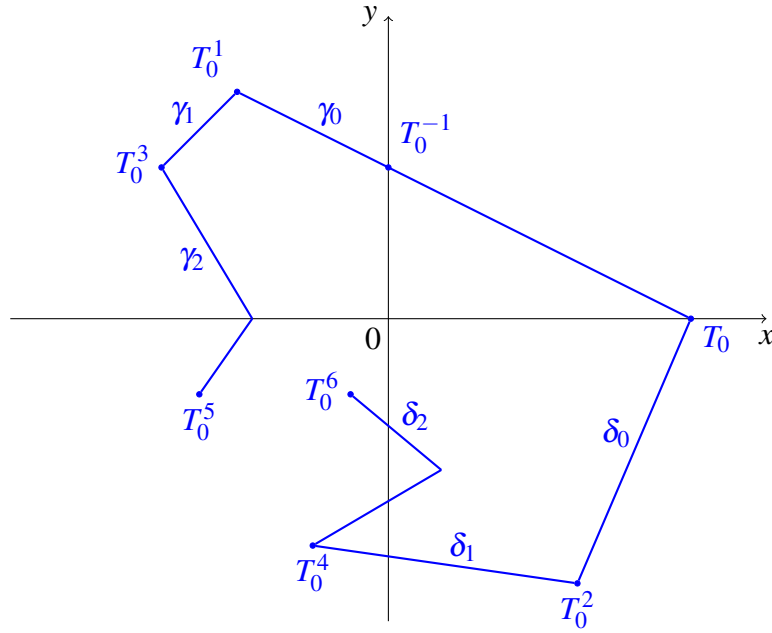


Figure 2.2: Sketch of the general structure of W_X^u .

With this notation we have $\Gamma = W_X^{u-} \setminus [X, T_0^{-1})^{(u)}$ and $\Delta = W_X^{u+} \setminus [X, T_0)^{(u)}$. In general, if T_0^{2n+1} is in the second quadrant above the curve $y = a|x| - 1$ (i.e. in the half-plane $y > -ax - 1$) for some $n \in \mathbb{N}_0$, T_0^{2n+2} is mapped to the fourth quadrant and T_0^{2n+3} to the second or the first quadrant. Therefore, neither Γ or Δ do not have to intersect the y-axis except at T_0^{-1} which lies on Γ . However, if there exist homoclinic points for X , notice that Γ intersects that axis at additional points because, due to Lemma 2.2.1, it intersects W_X^s on $\overline{XV_0}^{(s)}$ in the first or fourth quadrant. This leads us to our two main cases of interest: either Δ intersects the y-axis or it doesn't.

Lemma 2.1.9. Assume that Δ intersects the y-axis. If i_0 is the smallest $i \in \mathbb{N}_0$ such that δ_i intersects that axis, then δ_{i_0} is a straight line segment, $\delta_{i_0} = \overline{T_0^{2i_0} T_0^{2i_0+2}}^{(u)}$.

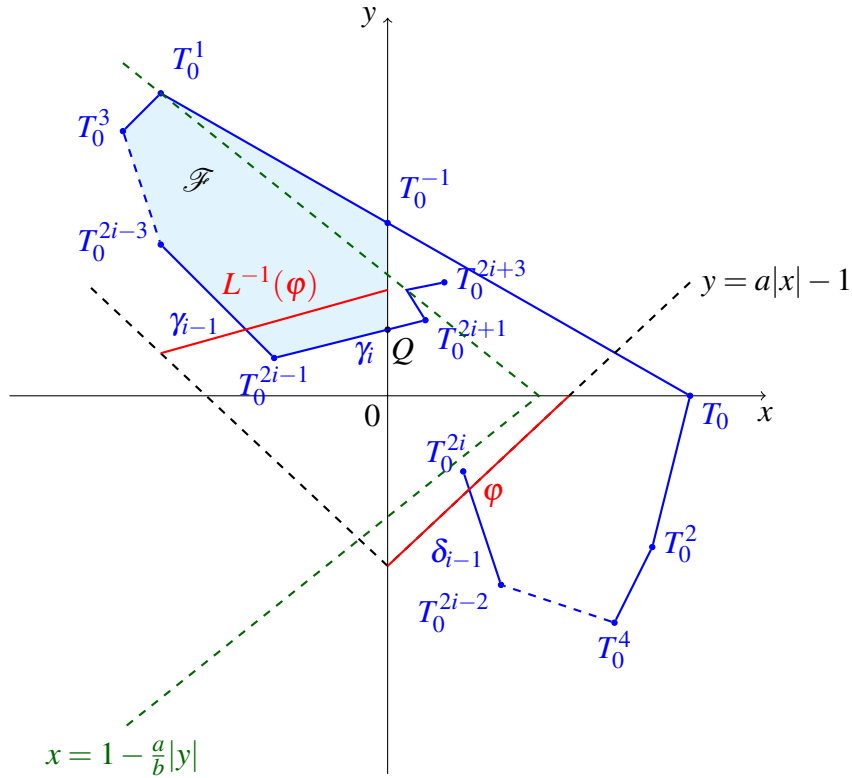


Figure 2.3: Proof of Lemma 2.1.9 - further iterations of γ_i under L^2 do not intersect $L^{-1}(\varphi)$ outside the shaded polygon \mathcal{F} .

Proof. We claim there are no other breaking points of W_X^u on δ_{i_0} apart from the corresponding iterates of T_0 . If the converse would hold, γ_i would transversally intersect the y -axis for some $i \in \mathbb{N}_0$, $i \leq i_0$ (notice that this implies $i > 0$). Observe the broken line $[T_0^1, T_0^{2i+1}]^{(u)}$ - it doesn't intersect the curve $y = a|x| - 1$ (because of the choice of i_0) and therefore it doesn't intersect the x -axis either (which is the second image under L of the aforementioned curve). Therefore, the straight line segment γ_i will intersect the positive y -axis at some point Q . Let \mathcal{F} denote the polygon in the second quadrant with boundary $\partial\mathcal{F} = [T_0^{-1}, Q]^{(u)} \cup \overline{QT_0^{-1}}$. Observe that, because $T_{0,x} > 1$, $\overline{T_0^{-1}T_0^1}^{(u)}$ is above and $[T_0^1, Q]^{(u)}$ is below the curve $x = 1 - \frac{a}{b}|y|$ in the upper half-plane (because that part is obtained from images of the corresponding δ_n which lie in the fourth quadrant; see Figure 2.3).

Notice that if γ_i intersects the positive y -axis, then δ_{i-1} intersects the intersection of the curve $y = a|x| - 1$ with the fourth quadrant, i.e. a straight line segment which will

be denoted by φ . In that case, γ_{i-1} intersects $L^{-1}(\varphi)$ which is a line segment in the left half-plane (with one endpoint lying on $y = a|x| - 1$ and the other one on the y -axis). In general, if γ_l intersects the y -axis below Q for some $l \in \mathbb{N}$, then γ_{l-1} intersects $L^{-1}(\varphi)$ outside \mathcal{F} .

On the other hand, observe the forward images of γ_i under L^2 . Notice that points in the first quadrant are mapped under L to the first and second quadrant above the line $x = 1 - \frac{a}{b}|y|$ and those in the second quadrant to the right of the line $y = a|x| - 1$ to those in the fourth quadrant. Therefore, in order for some γ_j to reach the second quadrant, it will first intersect $\overline{QT_0^{-1}}$, i.e. \mathcal{F} . Since W_X^u has no self-intersections, further forward images of γ_j can only intersect $L^{-1}(\varphi)$ inside \mathcal{F} which leads us to the conclusion that no further forward images of γ_i under L^2 intersect the y -axis below Q , and, by consequence, neither the curve $y = a|x| - 1$ in the second quadrant. This is a contradiction with the assumption that Δ intersects the negative y -axis so δ_{i_0} is indeed a straight line segment. ■

Theorem 2.1.10. If all intersections of W_X^s and W_X^u different from X are tangential, the only possible homoclinic points are iterates of T_0 and V_0 .

Proof. 1° *Main idea of proof*

Lemma 2.2.1 implies that it suffices to observe homoclinic points on $\overline{XV_0}^{(s)}$. Furthermore, because $\overline{XV_0}^{(s)} = \{X\} \cup \bigcup_{n=1}^{\infty} L^n(\overline{V_0V_0}^{(s)})$, it suffices to observe homoclinic points on $\overline{V_0V_0}^{(s)}$. Lemma 2.1.8 now implies that two possibilities can occur in this case: V_0 can be a homoclinic point as a breaking point of W_X^s or there is a breaking point of W_X^u lying on $\overline{V_0V_0}^{(s)}$. For the latter case, notice that every breaking point of W_X^u is an iterate of a transversal intersection point of W_X^u with the y -axis. We will show that these intersection points are contained in polygons whose boundary consists of parts of W_X^u and the zigzag part of W_X^s and which do not contain any other parts of W_X^s . If so, notice that there are two ways in which W_X^s can intersect W_X^u at these points: either the boundary of the aforementioned polygon intersects it or some other part of W_X^s does. In the former case, Proposition 2.1.3 and Lemma 2.1.8 imply that these points coincide with some iterates of V_0 , i.e. V_0 is a homoclinic point. In the latter one, W_X^s intersects transversally the boundary of the polygon in order to pass through its interior point. Since W_X^s has no self-intersections, it will intersect the part of the boundary belonging to W_X^u which contradicts the assumption of the theorem. The only remaining possibility is that these points lie on the boundary of

the polygon, in which case it will be clear by construction that the only such point is T_0^{-1} , i.e. T_0 is a homoclinic point.

Let $[V_0, V_0^{-n_0}]^{(s)}$ be the zigzag part of W_X^s . Because $\overline{XV_0}^{(s)} = \{X\} \cup \bigcup_{n=0}^{\infty} L^n(\overline{V_0V_0^1}^{(s)})$, we see that there exists a homoclinic point for X on $\overline{V_0V_0^1}^{(s)}$ and thus also on each of the iterates (positive or negative) of that line segment. Specially, there exists a homoclinic point on $\overline{V_0^{-(n_0-1)}V_0^{-n_0}}^{(s)}$.

Furthermore, let Γ , Δ , γ_n and δ_n be as defined at the beginning of this section. As already stated, we will consider two main cases of interest depending on whether Δ intersects the y -axis or not.

2° *First case: Δ does not intersect the y -axis*

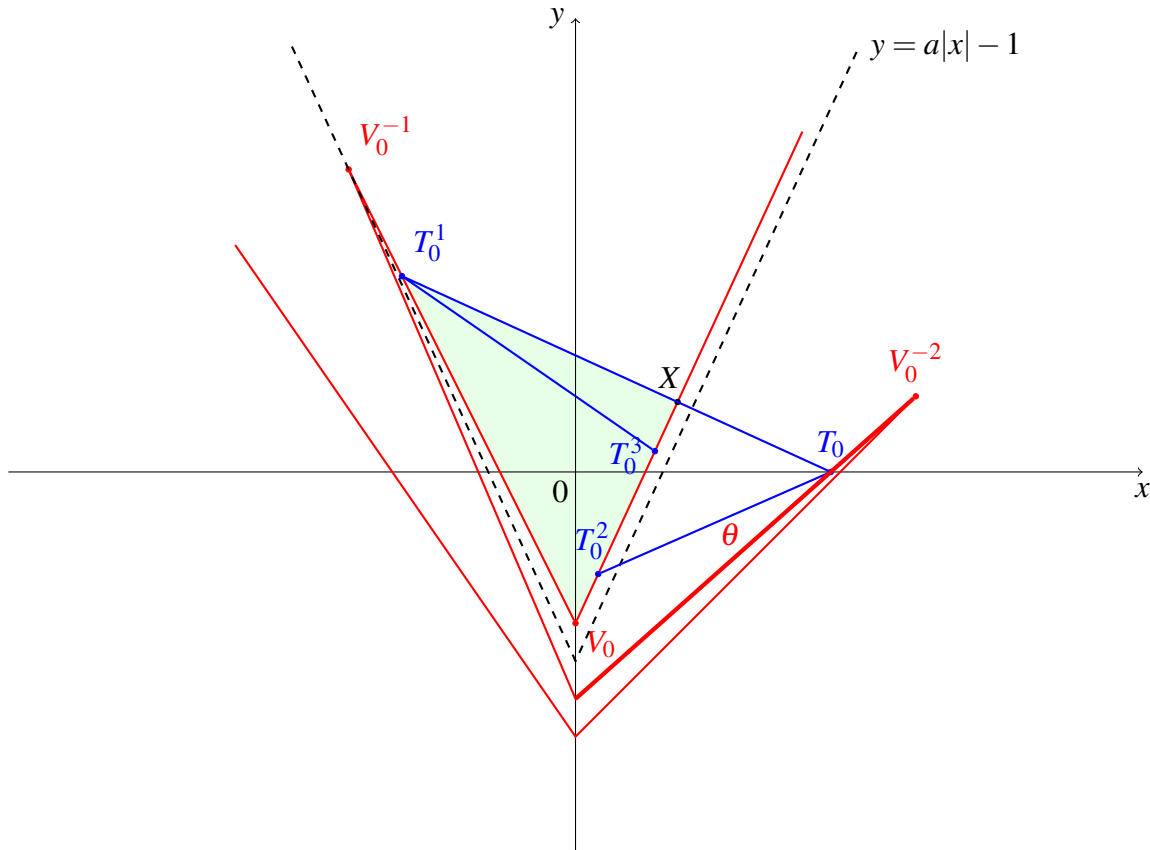


Figure 2.4: Proof of Theorem 2.1.10 in the case when Δ does not intersect the y -axis: T_0 lies on the line segment θ , T_0^2 on $\overline{V_0V_0^1}^{(s)}$ and Γ , together with all its intersections with the y -axis, is contained in the shaded triangle $XV_0T_0^1$.

Assume now that Δ does not intersect the y -axis, i.e. it is contained in the first and

fourth quadrant. Notice that if $n_0 > 1$, Proposition 2.1.3 implies that $n_0 \geq 3$. In that case, $L(\overline{V_0^{-(n_0-1)}V_0^{-n_0}}^{(s)})$ and $L^2(\overline{V_0^{-(n_0-1)}V_0^{-n_0}}^{(s)})$ are two line segments that both belong to the zigzag part of W_X^s , i.e. they are both contained in the third quadrant and there is a homoclinic point on each one of them. Notice that, because $L(\gamma_n) = \delta_n$ and $L(\delta_n) = \gamma_{n+1}$ for $n \in \mathbb{N}_0$, one of those points belongs to Δ . This is a contradiction with the assumption that Δ does not intersect the y-axis, so it follows that $n_0 = 1$.

Furthermore, if Δ does not intersect the y-axis, Γ does not intersect its image nor its preimage under L , i.e. the x-axis and the curve $y = a|x| - 1$. Moreover, notice that V_0^{-1} lies on the latter curve and because $V_{0,y}^{-1} > -1$, $\overline{V_0V_0^{-1}}^{(s)}$ lies above that curve in the second and the third quadrant. However, because parts of further preimages of that line segment under L in the third quadrant have negative slope coefficients (Proposition 2.1.3) and intersect the negative y-axis, they will all be below that curve in the third and intersect it in the second quadrant (those intersections will be preimages of breaking points of W_X^s on the negative y-axis).

Because $W_X^u = \bigcup_{n=0}^{\infty} L^n(\overline{XT_0}^{(u)})$ and $\overline{XT_0}^{(u)} = \{X\} \cup \bigcup_{n=0}^{\infty} L^{-2n}(\overline{T_0T_0^{-2}}^{(u)})$, it follows that in the case there exist homoclinic points for X , there also exists a homoclinic point for X lying on $\overline{T_0T_0^{-2}}^{(u)}$ and consequently, there exists a homoclinic point on all of its iterates under L . Specially, there exist a homoclinic point for X on γ_n and δ_n for all $n \in \mathbb{N}_0$.

Now observe δ_0 - because γ_0 is a line segment in the second quadrant, δ_0 will also be a line segment (in the fourth quadrant due to the assumption that Δ does not intersect the y-axis). We know there exists a homoclinic point for X lying on δ_0 which implies that this line segment intersects W_X^s in the fourth quadrant. On the other hand, parts of W_X^s in the fourth quadrant are $\overline{V_0V_0^1}^{(s)}$ and the preimages of intersections of $L^{-n}(\overline{V_0^{-(n_0-1)}V_0^{-n_0}}^{(s)}) = L^{-n}(\overline{V_0V_0^{-1}}^{(s)})$ with the second quadrant. If δ_0 intersects one of those preimages for some $n > 1$, then Γ (more precisely, γ_1) will intersect $L^{-n}(\overline{V_0V_0^{-1}}^{(s)})$ in the second quadrant below the curve $y = a|x| - 1$. This contradicts our assumption and so it follows that δ_0 intersects either $\overline{V_0V_0^1}^{(s)}$ or the intersection of $L^{-1}(\overline{V_0V_0^{-1}}^{(s)})$ with the fourth quadrant which we will denote by θ . However, notice that both $\overline{V_0V_0^1}^{(s)}$ and θ are both line segments with endpoints V_0, V_0^1, V_0^{-2} (which can lie in the fourth or first quadrant) and a breaking point of W_X^s on the y-axis (the preimage of the intersection of $\overline{V_0V_0^{-1}}^{(s)}$ with the x-axis). Since Δ does not intersect the y-axis and the homoclinic inter-

section on δ_0 is tangential, the only possibility is that the homoclinic point is a breaking point of W_X^u lying on δ_0 , i.e. T_0 and T_0^2 . In this case we see that T_0 will lie on θ and T_0^2 on $\overline{V_0 V_0^1}^{(s)}$. Therefore, T_0^1 lies on $\overline{V_0 V_0^{-1}}^{(s)}$ in the second and T_0^3 lies on $\overline{V_0^1 V_0^2}^{(s)}$ in the first quadrant so γ_1 is the first element of the sequence $(\gamma_n)_{n \in \mathbb{N}}$ which intersects the y -axis.

Finally, observe now the triangle $XV_0T_0^1$ and its boundary, $[X, T_0^1]^{(s)} \cup [T_0^1, X]^{(u)}$. Notice that Γ is contained in that triangle since it cannot (transversally) intersect its sides. Therefore, all intersections of W_X^u with the y -axis are contained in that triangle. This fact, together with the discussion at the beginning of the proof, finishes the proof in this case.

3° *Second case: Δ intersects the y -axis*

In the second case, when Δ intersects the y -axis, we define i_0 as in Lemma 2.1.9. Notice that γ_{i_0} then intersects the preimage of the y -axis, $y = a|x| - 1$, in the second or third quadrant.

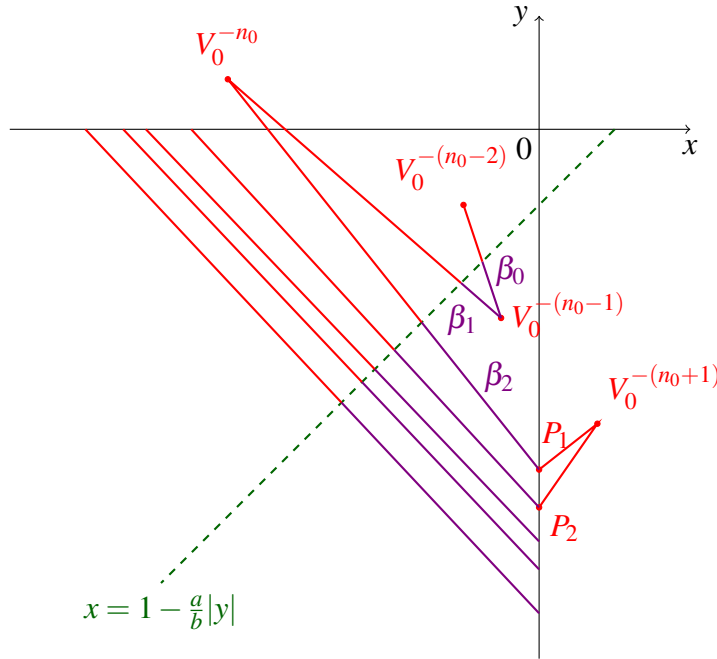


Figure 2.5: Parts of W_X^s in the third quadrant: segments β_n (violet) and α_n . All possible homoclinic points on δ_{i_0} in the third quadrant can lie only on β_0 , β_1 or β_2 .

3.1° *Claim: the first homoclinic point on Δ in the third quadrant lies on the zigzag part or on the preimage of its last segment*

Like before, let $[V_0, V_0^{-n_0}]^{(s)}$ be the zigzag part of W_X^s . We claim that the first homoclinic point which occurs on Δ in the third quadrant lies either on the zigzag part of W_X^s or

on the preimage of the segment $\overline{V_0^{-(n_0-1)}V_0^{-n_0}}^{(s)}$.

Now observe δ_{i_0} and homoclinic points lying on it. If none of them are lying in the third quadrant or on the y -axis, then by Lemma 2.1.8 it follows that the homoclinic point on δ_{i_0} is a negative iterate of V_0 . Notice that δ_{i_0+1} lies in the third and also possibly fourth quadrant and has a breaking point on the curve $x = 1 - \frac{a}{b}|y|$. If the aforementioned iterate of V_0 would be V_0^{-n} for some $n > n_0 + 1$, then $V_0^{-(n-2)}$ would lie on δ_{i_0+1} in the fourth quadrant. In that case W_X^s would transversally intersect $[T_0, R]^{(u)}$, where R is the intersection of δ_{i_0} with the y -axis. This is a contradiction with the assumption of the theorem and hence we see that $V_0^{-(n_0+1)}$ is the homoclinic point lying on δ_{i_0} . In this case $V_0^{-(n_0-1)}$ lies on δ_{i_0+1} as a breaking point of the zigzag part.

If there is a homoclinic point on δ_{i_0} in the third quadrant, Lemma 2.1.8 again implies that this point is either a breaking point of δ_{i_0} , i.e. an iterate of T_0 (due to Lemma 2.1.9), or a breaking point of W_X^s on the y -axis. In this case, for every $n \in \mathbb{N}_0$, let α_n be the intersection of $L^{-n}(\overline{V_0^{-(n_0-2)}V_0^{-(n_0-1)}}^{(s)})$ with the third quadrant and let β_n be the intersection of α_n with the half-plane $x \geq 1 + \frac{a}{b}y$ (i.e. the part of α_n below the curve $x = 1 - \frac{a}{b}|y|$). Observe that, by construction of the zigzag part, all β_n are non-empty for all $n \in \mathbb{N}_0$ and all α_n are straight line segments with endpoints lying on the coordinate axes for all $n \geq 2$. Moreover, notice that $L^{-1}(\alpha_n \setminus \beta_n) = \alpha_{n+1}$ for all $n \in \mathbb{N}_0$ (see Figure 2.5).

Notice that the homoclinic point on δ_{i_0} in the third quadrant lies on some β_n (because it is an image of the corresponding homoclinic point on δ_{i_0-1} in the second quadrant). If n would be greater than 2, then δ_{i_0+1} would transversally intersect α_{n-1} in the third quadrant in order to intersect α_{n-2} and the curve $x = 1 - \frac{a}{b}|y|$. Hence, $n \leq 2$, so the claim follows.

Now suppose that a homoclinic point P_1 on δ_{i_0} is a breaking point of W_X^s on the y -axis. From previous conclusions it follows that P_1 is the preimage of the intersection of $\overline{V_0^{-(n_0-1)}V_0^{-n_0}}$ with the x -axis. Observe the triangle $P_1V_0^{-(n_0+1)}P_2$, where P_2 is the preimage of the intersection of $\overline{V_0^{-n_0}P_1}^{(s)}$ with the x -axis. If P_1 would not be a breaking point of δ_{i_0} , δ_{i_0} would transversally intersect one of the sides of that triangle that doesn't lie on the y -axis, i.e. the polygonal line $[P_1, P_2]^{(s)}$ in order to tangentially intersect W_X^s at P_1 . Therefore, P_1 is a breaking point of δ_{i_0} and thus an iterate of T_0 .

3.2° *Construction of the corresponding polygons in the second case; end of proof*

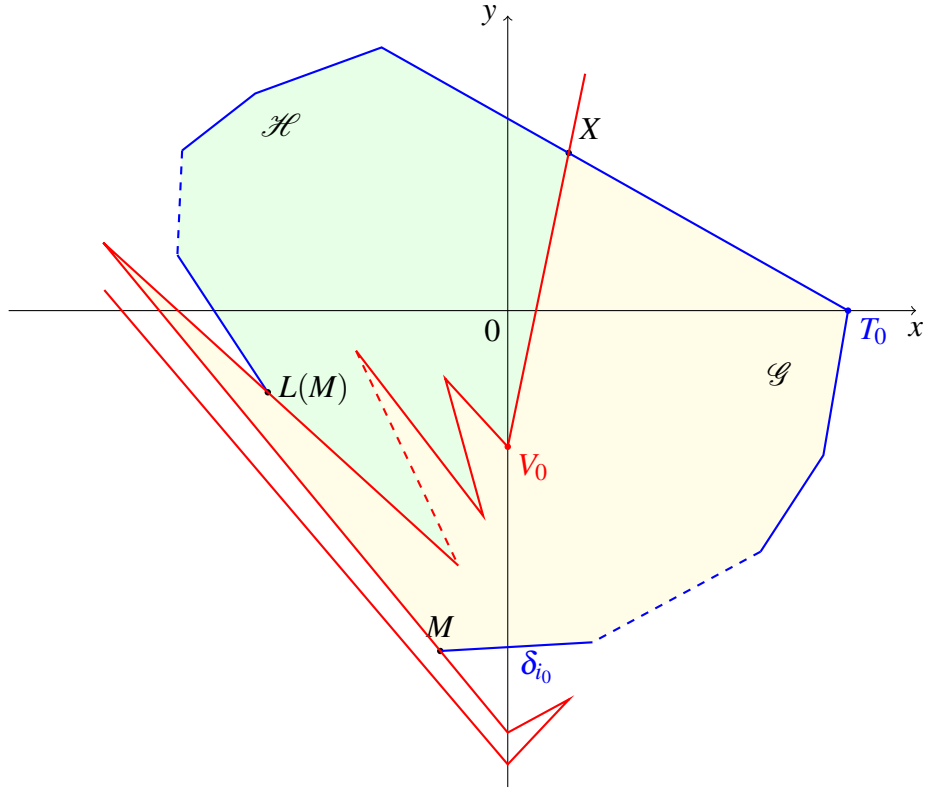


Figure 2.6: Polygons \mathcal{G} and \mathcal{H} in the second case of the proof of Theorem 2.1.10. Point M is the first homoclinic point on Δ in the third quadrant.

Finally, let M be the first homoclinic point on Δ lying in the third quadrant. Let \mathcal{G} be a polygon whose boundary is $\partial\mathcal{G} = [X, M]^{(u)} \cup [M, X]^{(s)}$ (Figure 2.6). Notice that the only breaking points of W_X^s contained in $[M, X]^{(s)}$ are iterates of V_0 and possibly M itself (and the previous argument implies that M coincides with some iterate of T_0 in that case). Moreover, because W_X^u doesn't intersect transversally the sides of \mathcal{G} and $[M, L^2(M)]^{(u)}$ is contained in it, \mathcal{G} contains Δ and all of its intersections with the y -axis. Similarly, if we let \mathcal{H} be a polygon whose boundary is $\partial\mathcal{H} = [X, L(M)]^{(u)} \cup [L(M), X]^{(s)}$, then \mathcal{H} contains Γ and all of its intersections with the y -axis (notice that $[X, L(M)]^{(u)}$ intersects the y -axis only at T_0^{-1}). Applying the argument from the beginning on these two polygons finishes the proof. ■

2.2. EXAMPLES OF BORDER CURVES

In this section we compute and describe some curves in the parameter space which represent a part of the border of the region of homoclinic points for the fixed point X , i.e. the locus of tangential homoclinic points for X (Lemma 2.1.8). We obtain the equations of all those curves in the form

$$C_n \dots P_n(a, b) + Q_n(a, b) \sqrt{a^2 + 4b} = 0,$$

where P_n and Q_n are polynomials in a and b . Since these equations can be written in the form $(P_n(a, b))^2 - (Q_n(a, b))^2(a^2 + 4b) = 0$, we see that these curves are algebraic curves. They are represented in the parameter space on Figure 2.8 and the corresponding configurations of W_X^s and W_X^u for a few curves can be seen on Figure 2.7.

The following simple result will allow us to start the analysis.

Lemma 2.2.1. Assume there exists a homoclinic point for the fixed point X different from X . Then there exists a homoclinic point for X different from X on the line segment $\overline{XV_0}^{(s)}$.

Proof. If $T, T \neq X$, is a homoclinic point for X , then, because $T \in W_X^s$, it follows that there exists an $n \in \mathbb{N}_0$ such that $T \in L^{-n}(\overline{XV_0}^{(s)})$. Therefore, $L^n(T) \in \overline{XV_0}^{(s)}$, $L^n(T) \neq X$ since L is a homeomorphism, and because W_X^u is L^n -invariant, $L^n(T)$ is the desired homoclinic point. ■

Notice that the line segments $\overline{T_0T_0^1}^{(u)}$ and $\overline{XV_0}^{(s)}$ intersect only at the point X - that is why the previous lemma implies that the first possibility for a homoclinic point (different from X) to occur happens when the line segments $\overline{T_0T_0^2}^{(u)}$ and $\overline{XV_0}^{(s)}$ intersect. Considering the border case leads us to our first case of interest.

2.2.1. First case: T_0^2 lies on $\overline{XV_0}^{(s)}$

This happens if the slope coefficients of the lines XT_0^2 and XV_0 are equal, that is

$$\frac{T_{0,y}^2 - X_y}{T_{0,x}^2 - X_x} = \frac{V_{0,y} - X_y}{V_{0,x} - X_x} = \frac{1}{2} \left(a + \sqrt{a^2 + 4b} \right).$$

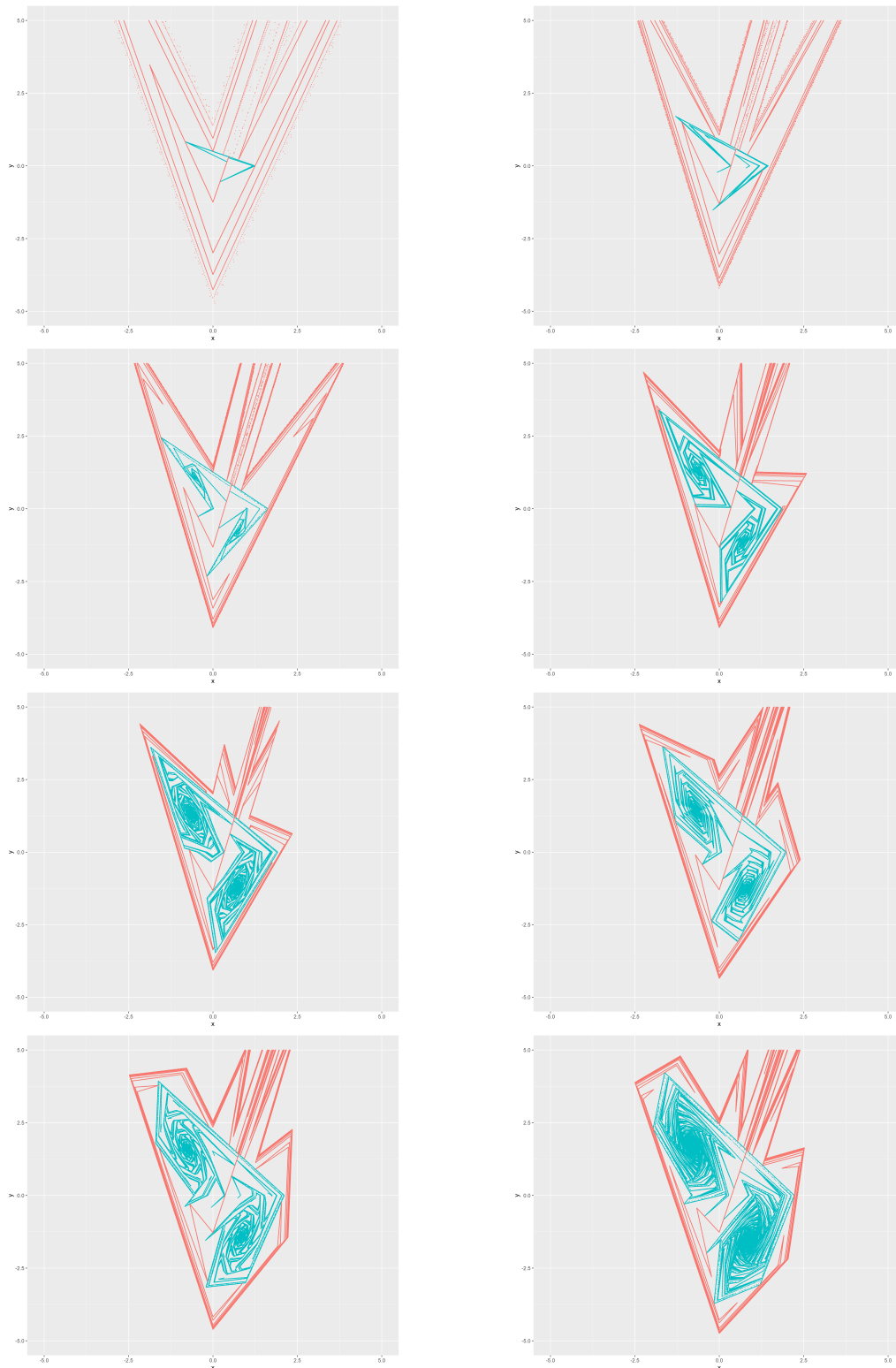


Figure 2.7: The stable (red) and unstable (blue) manifold of X for parameter pairs on the border curves $C_1 - C_8$ (left to right, top to bottom).

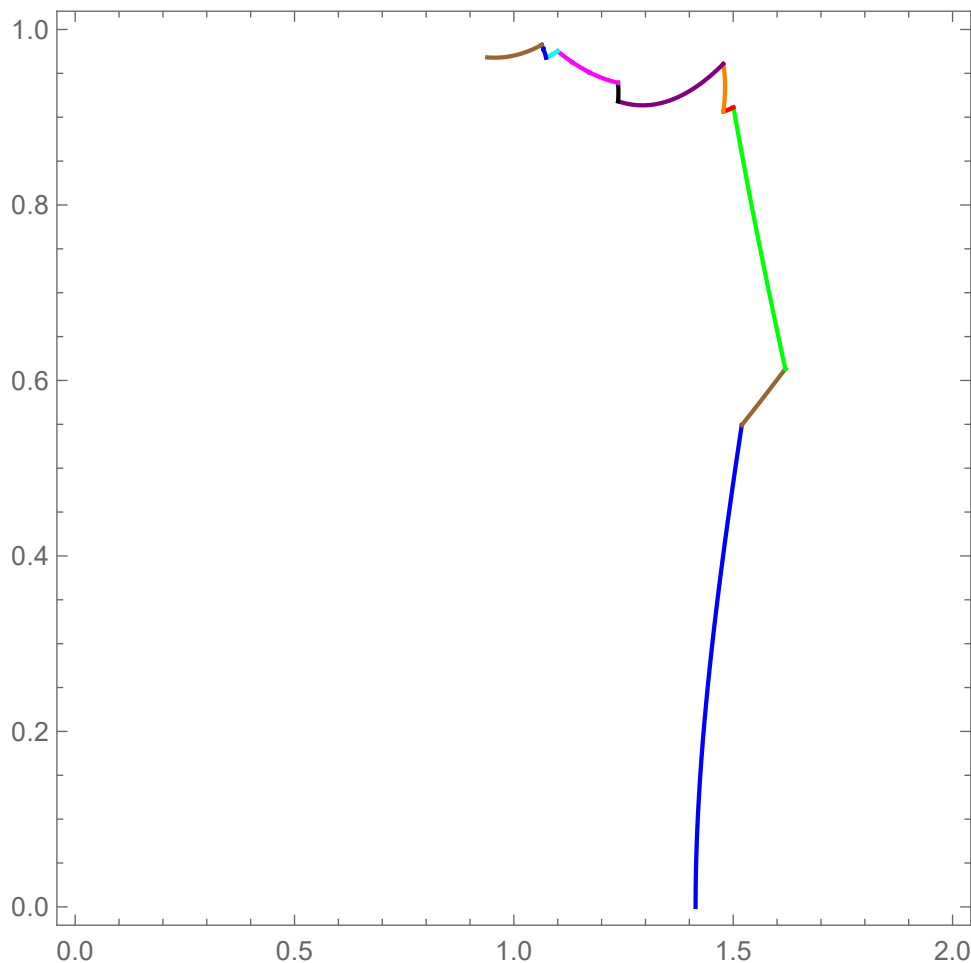


Figure 2.8: Borders for the area of existence of homoclinic points: curves C_1 (blue), C_2 (brown), C_3 (green), C_4 (red), C_5 (orange), C_6 (purple), C_7 (black), C_8 (magenta), C_9 (cyan), C_{10} (blue) and C_{11} (brown). The values of parameter a are presented on the horizontal and those of b on the vertical axis.

A straightforward computation tells us that this condition is satisfied on a curve C_1 in the parameter space described by the implicit equation

$$C_1 \dots a^3 - 4a + (a^2 - 2b)\sqrt{a^2 + 4b} = 0. \tag{2.4}$$

The curve is given on Figure 2.8. Since T_0^2 lies either in the third or fourth quadrant, the corresponding border is only a part of the curve starting at the point for which T_0^2 coincides with $L(V_0)$, $(a_0, b_0) = (\sqrt{2}, 0)$, and ending at the point (a_1, b_1) for which T_0^2 coincides with V_0 . In the former case, all points T_0^n fall on the same point on the x -axis and W_X^u is a line segment. For the latter case, numerical computations give approximate values

$(a_1, b_1) = (1.51950144, 0.549133899)$ and parts of the stable and unstable manifold in that case are presented on Figure 2.9.

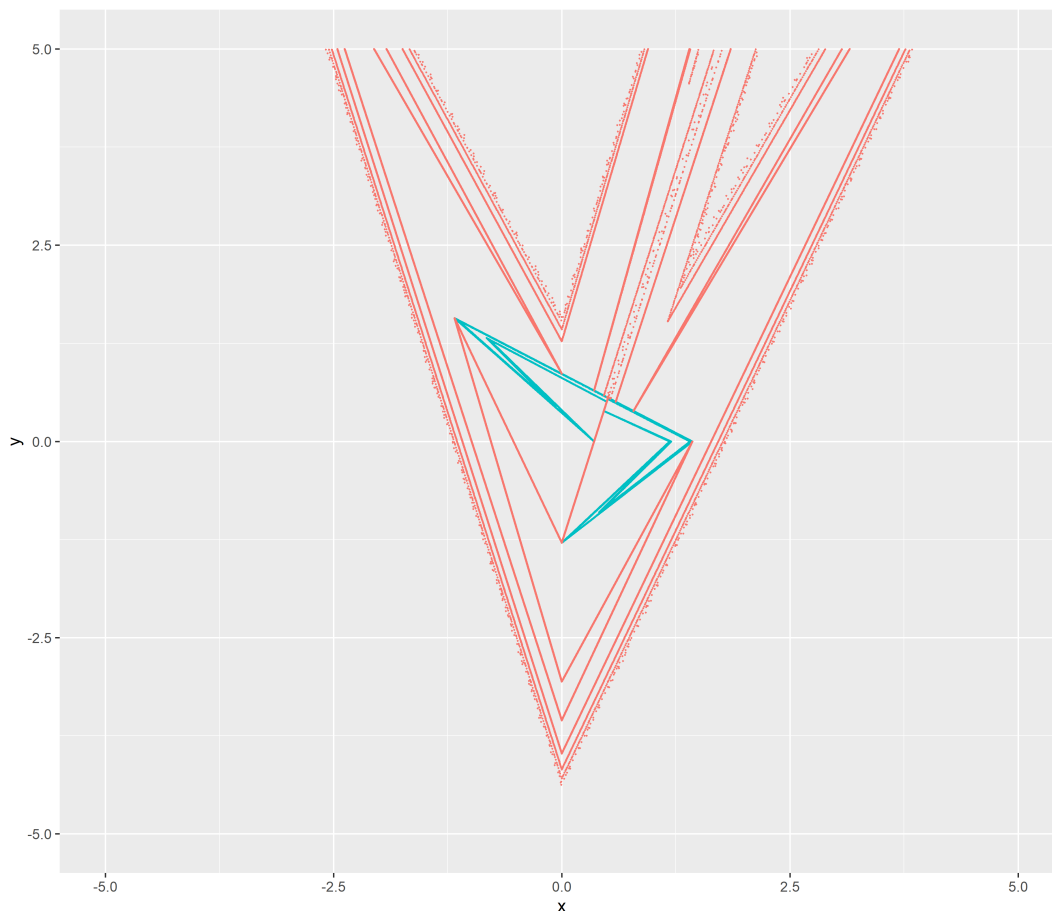


Figure 2.9: The stable (red) and unstable (blue) manifold in case when T_0^2 and V_0 coincide (endpoint (a_1, b_1) of the curve C_1).

Remark 2.2.2. By writing down (2.4) in its algebraic form, we obtain the equation

$$2a^4 - 4a^2 - 3a^2b + 4b^3 = 0,$$

which corresponds to the curve

$$2a = \sqrt{3b^2 + 4 + \sqrt{(3b^2 + 4)^2 - 32b^3}}$$

used in [12, p. 349] as the fourth condition for the construction of the Misiurewicz parameter set. Notice that this curve and the curve C_1 in our case are derived from posing the same geometric condition on W_X^u and W_X^s (see [12, p. 358]).

2.2.2. Second case: V_0 lies on $\overline{T_0^2 T_1}^{(u)}$

Notice that in the first case, both T_0^2 and V_0 are homoclinic points. Therefore, the next homoclinic point that occurs is V_0 . In this case, T_0^2 lies in the third quadrant so there exists an intersection point of $\overline{T_0 T_0^2}^{(u)}$ whose forward image under L will be denoted by T_{-1} . Furthermore, $\overline{T_0^1 T_{-1}}^{(u)}$ is a part of the unstable manifold W_X^u with the y -axis which intersects the y -axis at a point whose forward image will be called T_1 . Point V_0 will remain a homoclinic point when it lies on $\overline{T_0^2 T_1}^{(u)}$.

Equating the slope coefficients of lines $V_0 T_0^2$ and $V_0 T_1$ yields a curve C_2 in the parameter space with an implicit equation given by

$$\begin{aligned} C_2 \dots \quad & 4ab^5 - (8a^4 - 4)b^4 - (4a^5 + 8a^3 + 15a^2 + 4a + 4)b^3 + (15a^4 + 16a^3 + 11a^2)b^2 \\ & + (4a^7 + 2a^6 - 8a^5 - 10a^4)b - (2a^8 - 2a^6) + [(-4a^4 + 4a^2 - a)b^3 \\ & - (8a^4 + a^3 - 3a)b^2 + (4a^6 + 6a^5 - 6a^3)b - (2a^7 - 2a^5)] \sqrt{a^2 + 4b} = 0. \quad (2.5) \end{aligned}$$

The border of the area of existence of homoclinic points is a part of this curve starting at (a_1, b_1) (the point of intersection with the curve C_1) and ending at the point (a_2, b_2) for which T_0^2 again lies on W_X^u , this time on the segment $\overline{V_0^{-1} V_1}^{(s)}$, where V_1 is the image under L^{-1} of the intersection of $\overline{V_0 V_0^{-1}}^{(s)}$ and the x -axis. Numerical computations again give $(a_2, b_2) = (1.61870652, 0.613234325)$ and this case is depicted on Figure 2.10.

2.2.3. Third case: T_0^2 lies on $\overline{V_0^{-1} V_1}^{(s)}$

After hitting the segment $\overline{V_0^{-1} V_1}^{(s)}$, the point T_0^2 will stay on it and thus remain a homoclinic point. This is achieved for parameter values on the curve C_3 given by

$$\begin{aligned} C_3 \dots \quad & (4b^3 + 3a^2b^2 - (a^4 + 6a^2 + 4a)b - (4a^4 + 4a^3 + 2a^2)) \\ & + [-3ab^2 - (a^3 - 2a)b + (4a^3 + 4a^2 + 2a)] \sqrt{a^2 + 4b} = 0. \quad (2.6) \end{aligned}$$

The border is a part of this curve starting at (a_2, b_2) and ending at the point (a_3, b_3) for which T_0^2 and V_1 coincide, where V_1 is the backward image under L of the point of intersection of $\overline{V_0 V_0^{-1}}^{(s)}$ and the x -axis. Approximate numerical values for the latter endpoint are $(a_3, b_3) = (1.50065366, 0.911203728)$ and this case is shown on Figure 2.11.

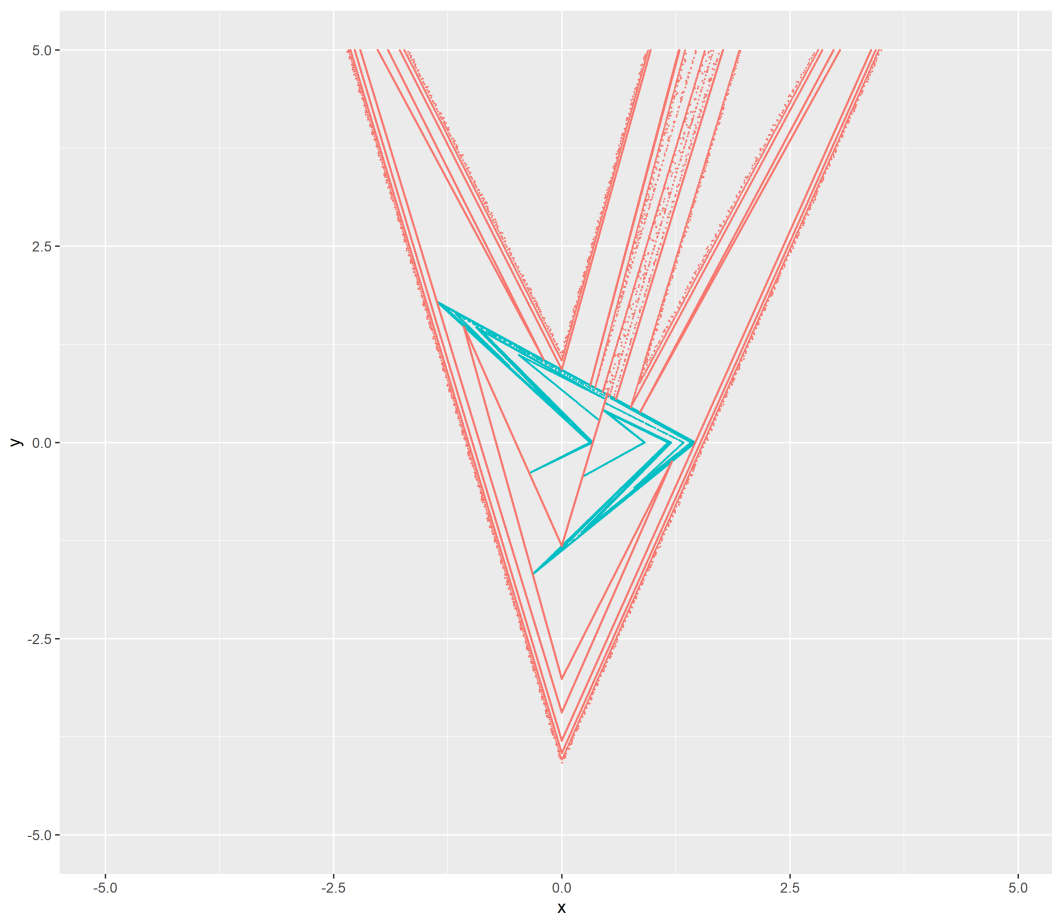


Figure 2.10: The stable (red) and unstable (blue) manifold in the border case $(a, b) = (a_2, b_2)$ (second endpoint of the curve C_2).

2.2.4. Fourth case: T_0^2 lies on $\overline{V_1 V_0^{-2}(s)}$

After coinciding with V_1 , T_0^2 will continue to lie on the segment $\overline{V_1 V_0^{-2}(s)}$ until it coincides with V_0^{-2} . In order for V_1 to exist, notice that there has to exist a point of intersection of $\overline{V_0 V_0^{-1}(s)}$ and the x -axis, i.e. V_0^{-1} has to be above the x -axis. This condition permits a slightly simpler calculation of V_{0x}^{-2} and V_{0y}^{-2} and the standard equating of slope coefficients of straight lines $V_0^{-2} T_0^2$ and $V_0^{-2} V_1$ gives the equation of the fourth boundary curve in the parameter space

$$C_4 \dots 4ab^3 + (-9a^3 + 4a)b^2 + (2a^5 - 4a^3 + 4a)b + (4a^5 - 2a^3) + [2b^3 - 5a^2b^2 + (2a^4 + 4a^2)b + (-4a^2 + 2a^2)] \sqrt{a^2 + 4b} = 0. \quad (2.7)$$

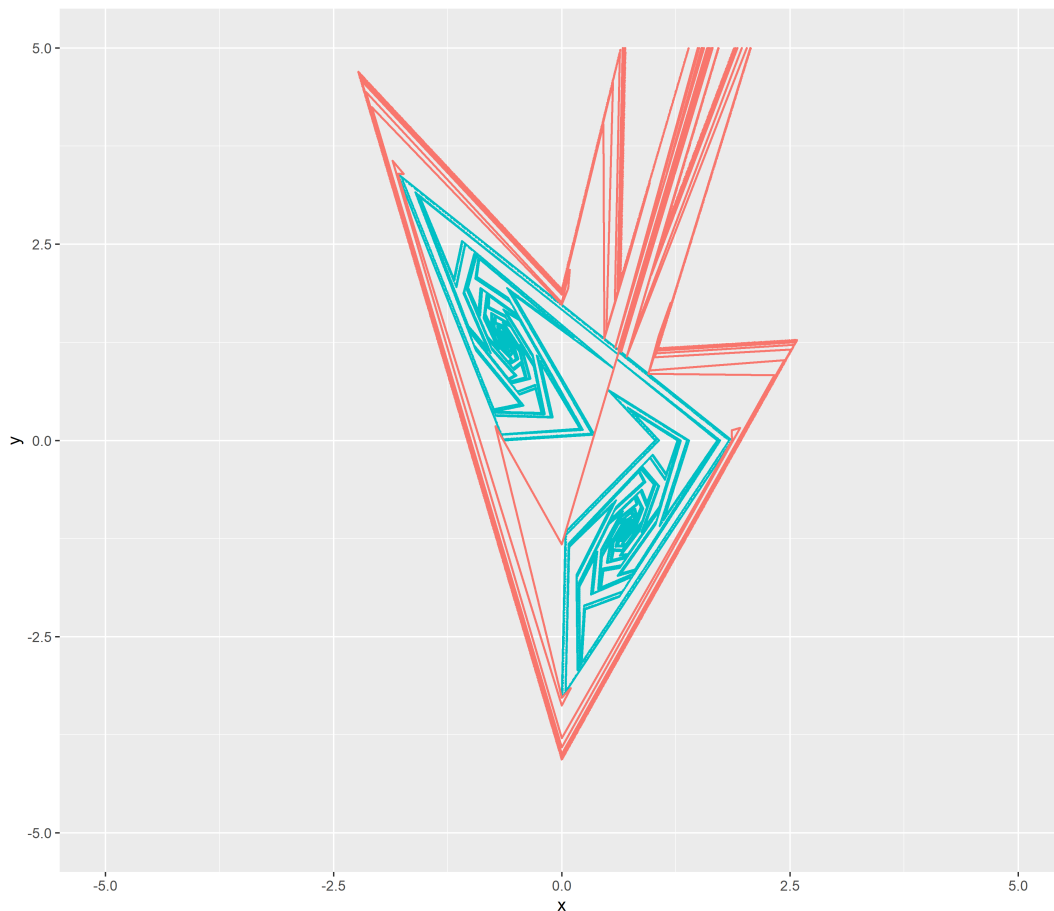


Figure 2.11: The stable (red) and unstable (blue) manifold in the border case $(a, b) = (a_3, b_3)$ (second endpoint of the curve C_3).

This curve propagates from (a_3, b_3) to the point (a_4, b_4) at which T_0^2 and V_0^{-2} coincide. Numerical calculations give $(a_4, b_4) = (1.4778227, 0.906571953)$ and the corresponding case is depicted on Figure 2.12.

2.2.5. Fifth case: V_0 lies on $\overline{T_0^4 T_0^{4,6}}(u)$

Because L is a homeomorphism, the condition that T_0^2 and V_0^{-2} coincide is equivalent to the one that V_0 and T_0^4 coincide. Notice that after that happens, V_0 will remain being a homoclinic point and a situation similar to the one in the second case occurs: in this case, $\overline{T_0^4 T_0^{2,5}}(u)$ intersects the y -axis because T_0^4 and T_0^2 are respectively in the third and second quadrant. We will denote by $T_0^{3,5}$ the image of that intersection under L and $T_0^{4,6} = L(T_0^{3,5})$. Point V_0 will remain being a homoclinic point when it lies on the line

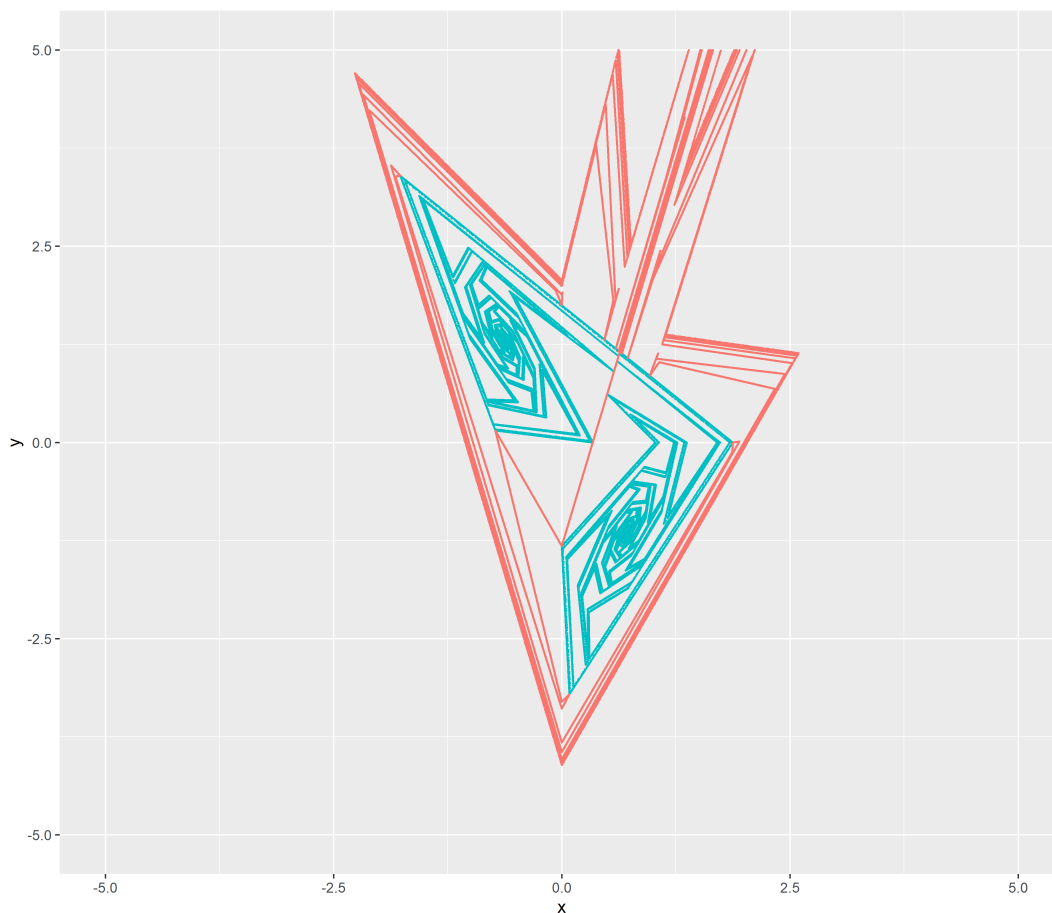


Figure 2.12: The stable (red) and unstable (blue) manifold in the border case $(a, b) = (a_4, b_4)$ (second endpoint of the curve C_4).

segment $\overline{T_0^4 T_0^{4,6}(u)}$.

The implicit equation of the fifth boundary curve is obtained by equating the slope coefficients of the straight lines $V_0 T_0^4$ and $T_0^4 T_0^{4,6}$ and it is of the form

$$C_5 \dots P_5(a, b) + Q_5(a, b) \sqrt{a^2 + 4b} = 0, \quad (2.8)$$

where polynomials P_5 and Q_5 are given by

$$\begin{aligned} P_5(a, b) &= 7a^2 b^7 + (-11a^4 + 9a^2) b^6 + (3a^6 - 27a^4 + 11a^2 + 6a) b^5 + (20a^6 - 52a^4 - 35a^3) b^4 \\ &\quad + (-4a^8 + 64a^6 + 56a^5) b^3 + (-28a^8 - 36a^7) b^2 + (4a^{10} + 10a^9) b - a^{11}, \\ Q_5(a, b) &= ab^7 + (-3a^3 + a) b^6 + (a^5 - a^3 + a + 1) b^5 - 9a^2 b^4 + 24a^4 b^3 - 22a^6 b^2 + 8a^8 b - a^{10}. \end{aligned}$$

This curve starts at the point (a_4, b_4) and ends at a point (a_5, b_5) at which T_0^4 lands on

$\overline{V_0^{-1}V_1^{(s)}}$. We have approximately $(a_5, b_5) = (1.47728163, 0.960699507)$ and this case is presented on Figure 2.13.

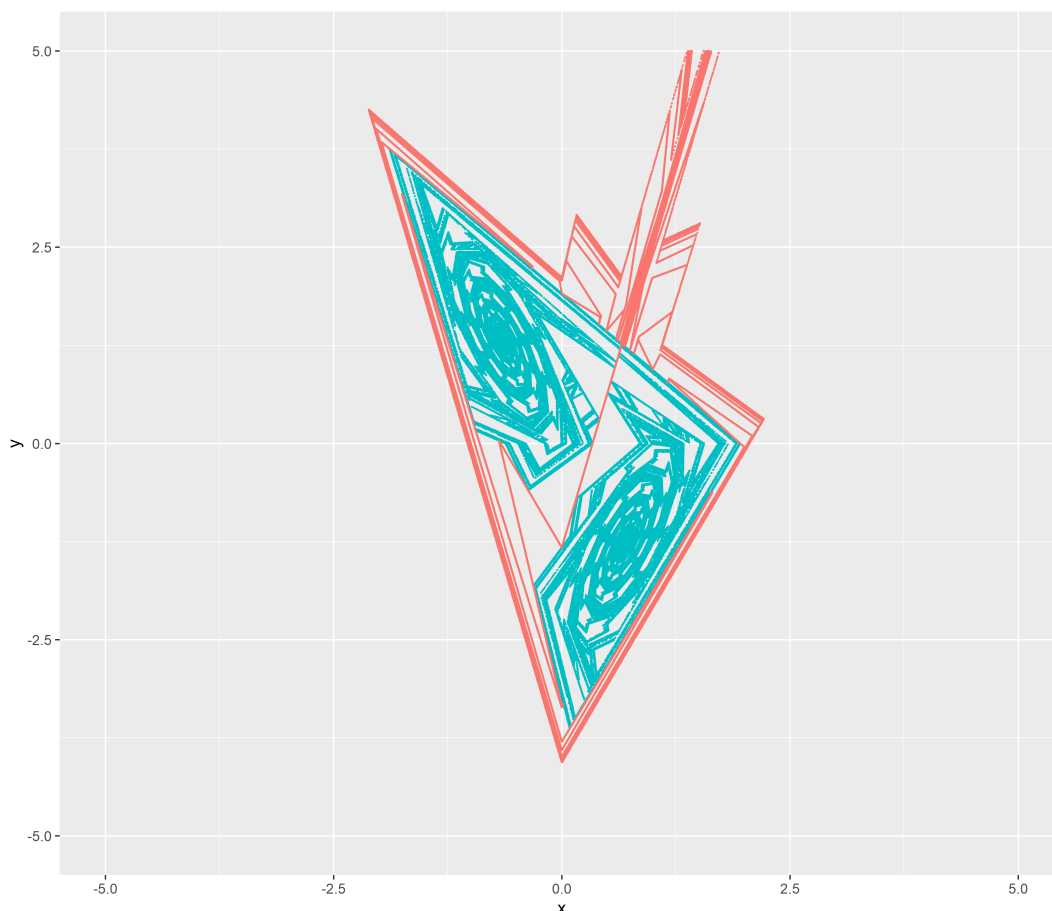


Figure 2.13: The stable (red) and unstable (blue) manifold in the border case $(a, b) = (a_5, b_5)$ (second endpoint of the curve C_5).

2.2.6. Sixth case: T_0^4 lies on $\overline{V_0^{-1}V_1^{(s)}}$, i.e. $\overline{V_0^{-1}V_0^{-2}^{(s)}}$

After landing on $\overline{V_0^{-1}V_1^{(s)}}$, T_0^4 will remain on that segment. Equating the slope coefficients of $V_1V_0^{-1}$ and $V_1T_0^4$ results in the implicit equation of the sixth boundary curve

$$C_6 \dots 4ab^3 + (a^3 - 4a)b^2 + (4a^3 - 4a)b + (-a^7 + 6a^5 - 6a^3 - 6a - 4) + [-2b^3 + 3a^2b^2 + 2a^4b + (-a^6 - 2a^4 + 2a^2 + 2a)]\sqrt{a^2 + 4b} = 0. \quad (2.9)$$

In this case, a particular thing happens: at the point (a^*, b^*) of this curve for which

we approximately have $(a^*, b^*) = (1.42928120, 0.939623413)$, V_0^{-1} will land on the x -axis and will rest in the third quadrant after we pass that point. Therefore, point V_1 , as described in the second case, will no longer exist and T_0^4 will lie on $\overline{V_0^{-1}V_0^{-2}}^{(s)}$ (which is a segment that doesn't intersect the y -axis). However, if we still define V^* as the image under L^{-1} of the intersection of the straight line $V_0V_0^{-1}$ and the x -axis, we see that points V_0^{-1} , V_0^{-2} and V^* must be collinear because L^{-1} , restricted to the lower half-plane, is an affine map. It follows that the curve C_6 is well-defined by the previous equation even when V_0^{-1} lies below the x -axis.

This curve has its origin at (a_5, b_5) and ends at a point (a_6, b_6) at which T_0^4 and V_0^{-2} coincide. Like before, numerical computations give approximate values $(a_6, b_6) = (1.23772202, 0.918152634)$ and this case is given on Figure 2.14.

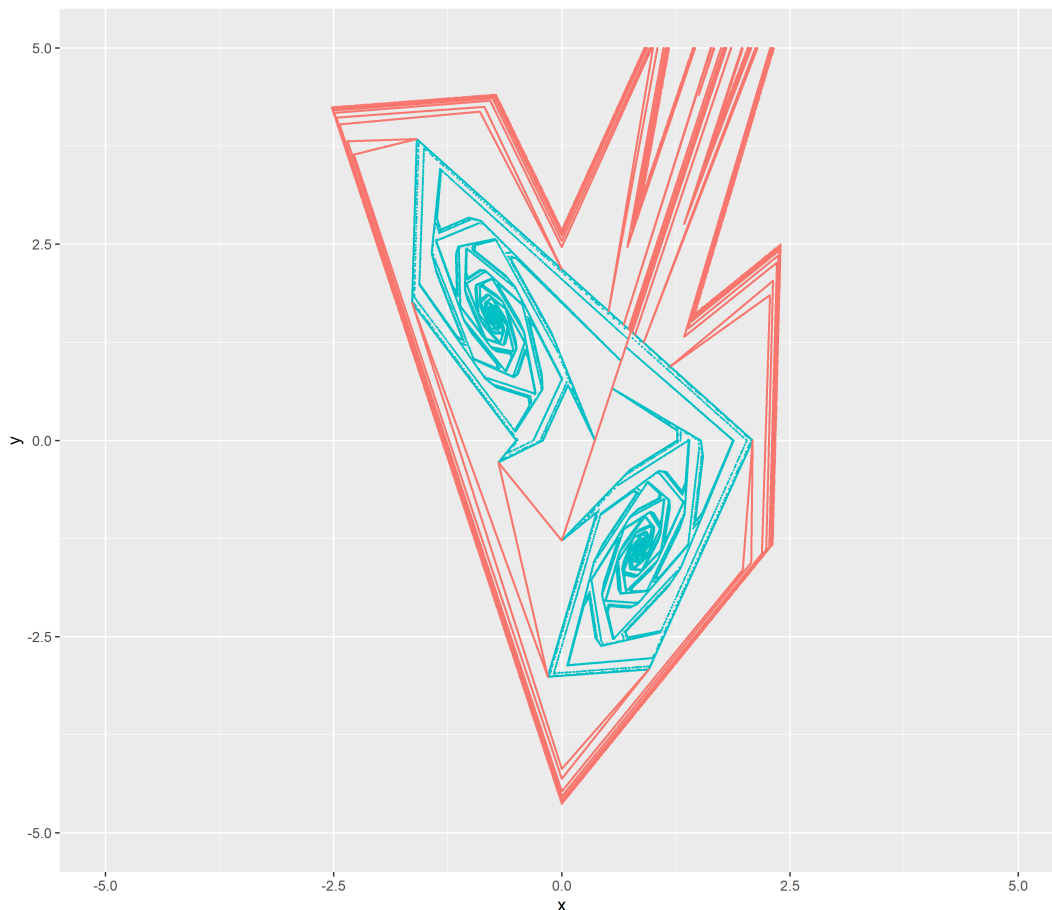


Figure 2.14: The stable (red) and unstable (blue) manifold in the border case $(a, b) = (a_6, b_6)$ (second endpoint of the curve C_6).

2.2.7. Seventh case: V_0^{-1} lies on $\overline{T_0^5 T_{-2}}^{(u)}$

As already mentioned, V_0^{-2} and T_0^4 coincide at (a_6, b_6) . Equivalently, V_0^{-1} and T_0^5 coincide so V_0^{-1} will be a homoclinic point in this case. Let $T_0^{2,4}$ be the point of intersection of segment $\overline{T_0^2 T_0^4}^{(u)}$ and the y -axis and let T_{-2} be image of the intersection of $\overline{T_0^4 L^2(T_0^{2,4})}^{(u)}$ and the y -axis. In this case, V_0^{-1} will lie on the segment $\overline{T_0^5 T_{-2}}^{(u)}$. As usual, by equating the slope coefficients of lines $T_0^5 V_0^{-1}$ and $T_0^5 T_{-2}$ we obtain the equation of the corresponding boundary curve in the form

$$C_7 \dots P_7(a, b) + Q_7(a, b) \sqrt{a^2 + 4b} = 0, \quad (2.10)$$

where polynomials P_7 and Q_7 are given by

$$\begin{aligned} P_7(a, b) = & 4ab^{10} + (-2a^3 - 6a^2 + 4a)b^9 + (-16a^5 - 8a^4 - 12a^3 - 2a^2 + 4a)b^8 \\ & + (6a^7 + 10a^6 - 22a^5 + 2a^4 - 26a^3 - 16a^2 + 8a + 4)b^7 \\ & + (-2a^8 + 32a^7 + 10a^6 - 16a^5 + 46a^4 + 2a^3 - 11a^2 - 12a)b^6 \\ & + (-8a^9 - 16a^8 + 80a^7 + 72a^6 - 64a^5 - 10a^4 + 22a^2)b^5 \\ & + (4a^{10} - 48a^9 - 160a^8 - 16a^7 + 60a^6 + 68a^5)b^4 \\ & + (8a^{11} + 80a^{10} + 132a^9 - 6a^8 - 72a^7)b^3 \\ & + (-12a^{12} - 76a^{11} - 64a^{10} - 26a^9)b^2 \\ & + (12a^{13} + 38a^{12} + 32a^{11})b + (-6a^{14} - 6a^{13}), \end{aligned}$$

$$\begin{aligned} Q_7(a, b) = & (-2a^2 + 2a)b^9 + (-4a^2 + 2a)b^8 + (2a^6 - 6a^5 - 2a^4 - 6a^3 + 2a^2 + 4a)b^7 \\ & + (2a^7 - 10a^5 - 14a^3 - 10a^2 - 3a + 2)b^6 + (16a^7 - 8a^5 + 16a^4 + 6a^3 - 2a^2)b^5 \\ & + (-4a^9 + 40a^7 + 32a^6 + 4a^5 - 12a^4)b^4 + (-24a^9 - 60a^8 - 26a^7 + 4a^6)b^3 \\ & + (4a^{11} + 28a^{10} + 32a^9 + 18a^8)b^2 + (-4a^{12} - 14a^{11} - 12a^{10})b + (2a^{13} + 2a^{12}). \end{aligned}$$

This curve emanates from (a_6, b_6) and ends at a point (a_7, b_7) at which T_0^5 lands on $\overline{V_0^{-2} V_0^{-3}}^{(s)}$. We approximately have $(a_7, b_7) = (1.23744761, 0.939287819)$ and Figure 2.15 represents this case.

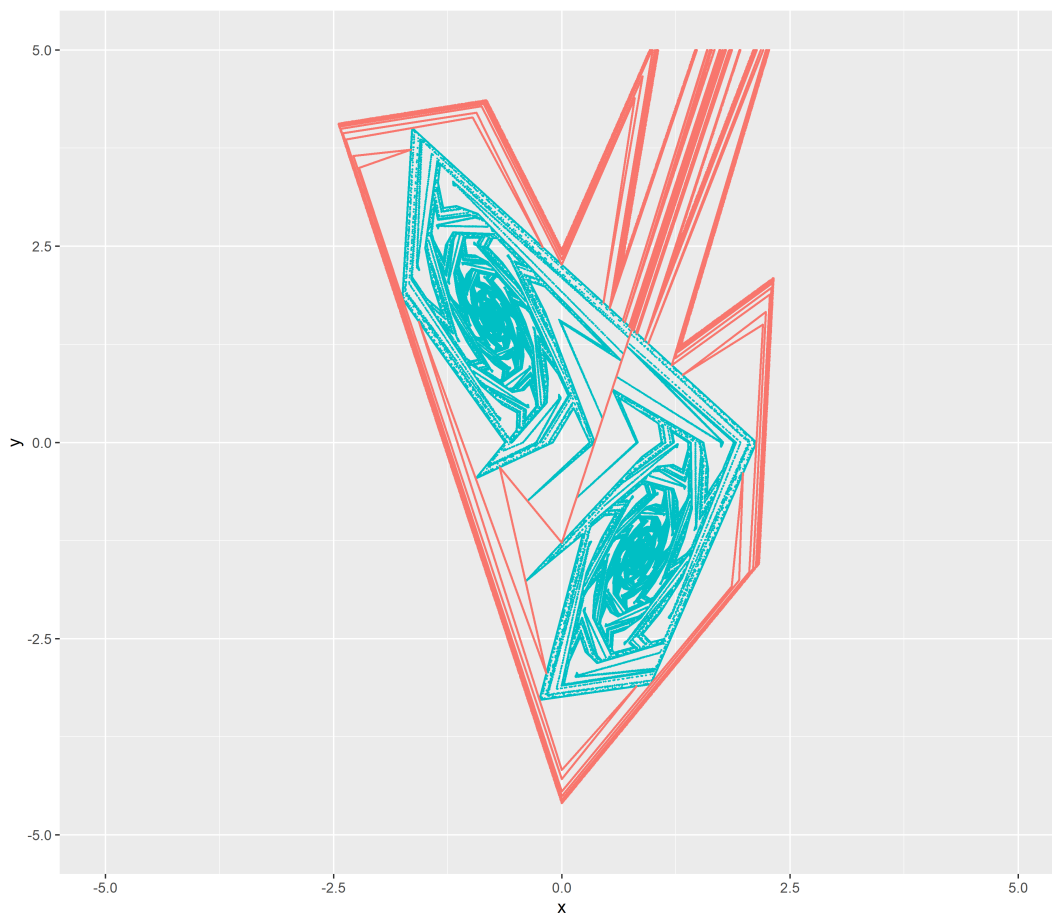


Figure 2.15: The stable (red) and unstable (blue) manifold in the border case $(a, b) = (a_7, b_7)$ (second endpoint of the curve C_7).

2.2.8. Eighth case: T_0^5 lies on $\overline{V_0^{-2}V_0^{-3}^{(s)}}$ in the third quadrant

By equating the slope coefficients of lines $V_0^{-2}V_0^{-3}$ and $V_0^{-3}T_0^5$ we obtain the equation of the eighth boundary curve:

$$C_8 \dots P_8(a, b) + Q_8(a, b)\sqrt{a^2 + 4b} = 0, \tag{2.11}$$

where

$$\begin{aligned} P_8(a, b) = & (-4a + 4)b^6 + (-15a^3 + a^2 + 4a)b^5 + (-24a^5 - 13a^4 + 4a^3 - 2a^2 + 4a)b^4 \\ & + (-5a^7 - 19a^6 - 6a^5 + 2a^4 + 14a^3)b^3 + (6a^9 - 24a^7 + 4a^6 + 24a^5 + 8a^4 + 4a^3)b^2 \\ & + (2a^{11} + 2a^{10} - 8a^9 + 12a^8 + 8a^7 - 4a^6 + 4a^4 + 4a^3 + 2a^2)b \\ & + (4a^{10} - 4a^8 - 4a^7 - 4a^6 - 4a^5 - 2a^4), \end{aligned}$$

$$\begin{aligned}
 Q_8(a,b) = & 2b^6 + (-a^2 - 3a)b^5 + (-10a^4 - 7a^3 + 2a)b^4 \\
 & + (-13a^6 - 7a^5 + 2a^4 + 2a^3 - 2a^2)b^3 \\
 & + (2a^8 + 4a^7 - 4a^5 + 8a^3 + 4a^2)b^2 \\
 & + (2a^{10} + 2a^9 - 12a^7 + 12a^5 + 8a^4 + 4a^3 + 4a^2 + 2a)b \\
 & + (-4a^9 + 4a^7 + 4a^6 + 4a^5 + 4a^4 + 2a^3).
 \end{aligned}$$

The second endpoint of this curve is a point (a_8, b_8) at which T_0^5 falls on the x -axis. As usual, numerical computations give approximate values $(a_8, b_8) = (1.09974148, 0.975240539)$ and this case is presented on Figure 2.16.

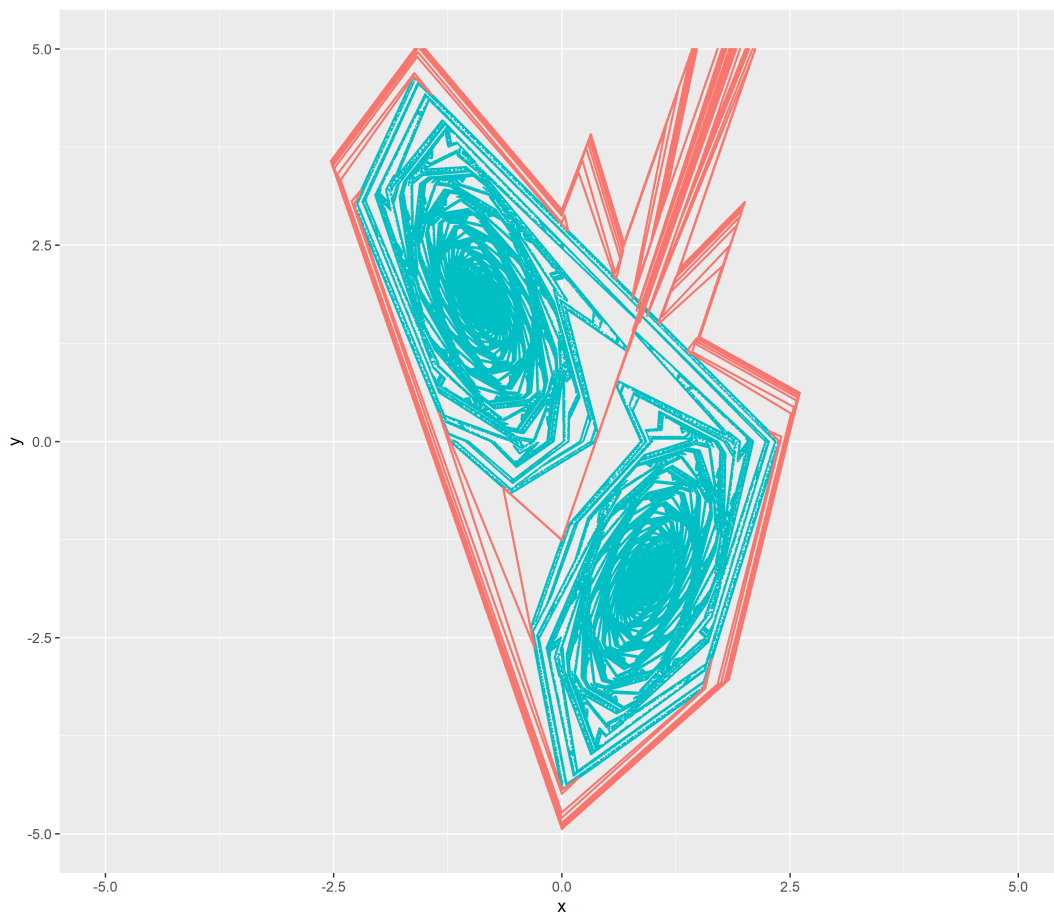


Figure 2.16: The stable (red) and unstable (blue) manifold in the border case $(a, b) = (a_8, b_8)$ (second endpoint of the curve C_8).

2.2.9. Ninth case: T_0^5 lies on $\overline{V_0^{-2}V_0^{-3}}^{(s)}$ in the second quadrant

The point T_0^5 will remain on the segment $V_0^{-2}V_0^{-3}$ but because T_0^4 will pass from the third to the fourth quadrant in this case, coordinates of T_0^5 need to be recalculated. The same computation as in the previous case results in the equation of the next boundary curve:

$$C_9 \dots P_9(a, b) + Q_9(a, b)\sqrt{a^2 + 4b} = 0, \quad (2.12)$$

where

$$\begin{aligned} P_9(a, b) = & -4b^6 + (17a^3 + 13a^2 - 4a)b^5 + (-4a^5 + 15a^4 + 8a^3 - 6a^2 - 4a)b^4 \\ & + (-13a^7 - 3a^6 + 26a^5 - 2a^4 - 2a^3 - 2a^2 - 4a)b^3 \\ & + (-2a^9 - 8a^8 - 12a^6 + 8a^5 - 8a^3)b^2 \\ & + (2a^{11} + 2a^{10} - 8a^9 - 4a^8 + 8a^7 - 4a^6 - 8a^5 - 4a^4 - 4a^3 - 2a^2)b \\ & + (4a^{10} - 4a^8 + 4a^6 + 4a^5 + 2a^4), \end{aligned}$$

$$\begin{aligned} Q_9(a, b) = & -2b^6 + (7a^2 + a)b^5 + (10a^4 + 5a^3 - 4a^2 - 2a)b^4 \\ & + (-5a^6 - 7a^5 + 2a^4 + 6a^3 - 2a^2 - 2a)b^3 \\ & + (-6a^8 - 4a^7 + 12a^5 + 2a^{10} + 2a^9 + 4a^7 + 4a^5 - 4a^3 - 4a^2 - 2a)b \\ & + (-4a^9 + 4a^7 - 4a^5 - 4a^4 - 2a^3). \end{aligned}$$

For the second endpoint of this curve, at which T_0^5 and V_0^{-3} coincide, we approximately have $(a_9, b_9) = (1.07356315, 0.967833586)$ and the corresponding case is given on Figure 2.17.

2.2.10. Tenth case: V_0^{-2} lies on $\overline{T_0^6 T_0^{6,8}}^{(u)}$

Notice that at the end of the previous case T_0^4 lies in the fourth and T_0^6 in the third quadrant - therefore, $\overline{T_0^4 T_0^6}^{(u)}$ intersects the y-axis. Let $T_0^{6,8}$ be the image of that intersection under L^2 .

We know that in this case V_0^{-3} will lie on the line segments whose endpoints are T_0^5 and the corresponding intersection of W_X^u with the x-axis (image of the intersection of $\overline{T_0^4 T_0^6}^{(u)}$ with the y-axis under L). Equivalently, V_0^{-2} lies on the segment $\overline{T_0^6 T_0^{6,8}}^{(u)}$. In this case we equate the slope coefficients of lines $V_0^{-2}T_0^6$ and $T_0^6 T_0^{6,8}$ and as a result we obtain

$$C_{10} \dots P_{10}(a, b) + Q_{10}(a, b)\sqrt{a^2 + 4b} = 0, \quad (2.13)$$

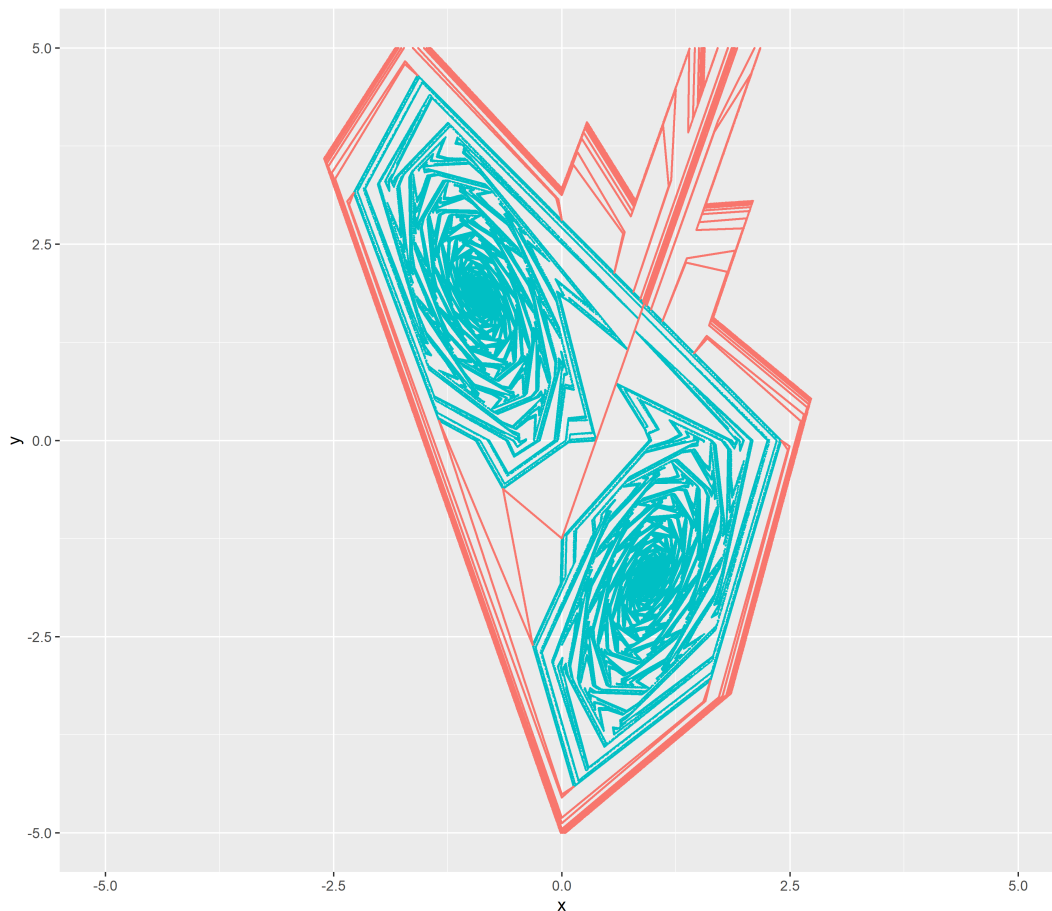


Figure 2.17: The stable (red) and unstable (blue) manifold in the border case $(a, b) = (a_9, b_9)$ (second endpoint of the curve C_9).

with

$$P_{10}(a, b) = \sum_{i=0}^{12} P_{10}^{(i)}(a)b^i, \quad Q_{10}(a, b) = \sum_{i=0}^{12} Q_{10}^{(i)}(a)b^i,$$

where polynomials $P_{10}^{(i)}$ and $Q_{10}^{(i)}$ are given by

$$P_{10}^{(12)}(a) = -2a^2 + 4a, \quad P_{10}^{(11)}(a) = -16a^4 - 14a^3 + 16a^2,$$

$$P_{10}^{(10)}(a) = 2a^6 - 30a^4 - 12a^3 + 16a^2 + 4a,$$

$$P_{10}^{(9)}(a) = 2a^8 + 2a^7 + 12a^6 + 6a^5 - 34a^4 + 6a^3 + 10a^2 + 4a,$$

$$P_{10}^{(8)}(a) = 2a^8 + 4a^7 + 52a^6 + 12a^5 - 58a^4 - 14a^3 - 14a^2 - 12a + 4,$$

$$P_{10}^{(7)}(a) = -2a^{10} - 2a^9 - 10a^8 + 122a^6 + 168a^5 + 102a^4 + 88a^3 + 5a^2 + 16a - 4,$$

$$P_{10}^{(6)}(a) = -6a^{10} - 8a^9 - 74a^8 - 240a^7 - 226a^6 - 198a^5 - 84a^4 - 93a^3 + a^2 + 4a + 4,$$

$$P_{10}^{(5)}(a) = 2a^{12} + 2a^{11} + 94a^9 + 260a^8 + 262a^7 \\ + 116a^6 + 22a^5 + 77a^4 + 20a^3 - 21a^2 - 20a - 4,$$

$$P_{10}^{(4)}(a) = 10a^{12} + 14a^{11} - 118a^{10} - 230a^9 - 160a^8 \\ + 110a^7 - 24a^6 - 156a^5 - 49a^4 + 81a^3 + 37a^2 + 8a,$$

$$P_{10}^{(3)}(a) = -2a^{14} - 14a^{13} + 92a^{11} + 137a^{10} - 58a^9 \\ - 160a^8 + 84a^7 + 205a^6 - 8a^5 - 102a^4 - 40a^3,$$

$$P_{10}^{(2)}(a) = 2a^{15} + 12a^{14} - 4a^{13} - 44a^{12} - 25a^{11} + 105a^{10} + 82a^9 - 70a^8 - 79a^7 - 5a^6 + 6a^5,$$

$$P_{10}^{(1)}(a) = -2a^{16} - 6a^{15} + a^{14} + 20a^{13} - 7a^{12} - 68a^{11} - 39a^{10} + 52a^9 + 59a^8 + 18a^7,$$

$$P_{10}^{(0)}(a) = a^{17} + a^{16} - 3a^{15} - 3a^{14} + 12a^{13} + 13a^{12} - 9a^{11} - 15a^{10} - 5a^9,$$

$$Q_{10}^{(12)}(a) = 2a, \quad Q_{10}^{(11)}(a) = -8a^3 - 2a^2, \quad Q_{10}^{(10)}(a) = -2a^5 - 4a^4 - 2a^3 + 8a^2,$$

$$Q_{10}^{(9)}(a) = 2a^7 + 2a^6 - 4a^5 - 14a^4 + 6a^3 + 10a^2 + 2a,$$

$$Q_{10}^{(8)}(a) = 6a^7 + 8a^6 - 4a^5 - 20a^4 + 10a^3 - 2a^2 + 2a + 2,$$

$$Q_{10}^{(7)}(a) = -2a^9 - 2a^8 + 14a^7 + 28a^6 - 6a^5 + 24a^4 + 18a^3 - 9a - 2,$$

$$Q_{10}^{(6)}(a) = -10a^9 - 12a^8 + 26a^7 - 4a^6 - 94a^5 - 90a^4 + 40a^3 + 17a^2 + 13a,$$

$$Q_{10}^{(5)}(a) = 2a^{11} + 2a^{10} - 32a^9 - 58a^8 + 100a^7 + 218a^6 + 35a^5 - 42a^4 - 109a^3 - 12a^2 - 3a + 2,$$

$$Q_{10}^{(4)}(a) = 14a^{11} + 54a^{10} - 6a^9 - 184a^8 - 200a^7 - 22a^6 + 112a^5 + 64a^4 + 35a^3 - 7a^2 - 3a - 2,$$

$$Q_{10}^{(3)}(a) = -2a^{13} - 18a^{12} - 36a^{11} + 44a^{10} + 163a^9 \\ + 108a^8 + 48a^7 - 48a^6 - 101a^5 - 38a^4 + 18a^3 + 12a^2,$$

$$Q_{10}^{(2)}(a) = 2a^{14} + 16a^{13} + 14a^{12} - 40a^{11} - 83a^{10} - 91a^9 - 14a^8 + 62a^7 + 75a^6 + 27a^5 + 4a^4,$$

$$Q_{10}^{(1)}(a) = -2a^{15} - 8a^{14} - a^{13} + 26a^{12} + 31a^{11} + 20a^{10} - a^9 - 42a^8 - 39a^7 - 12a^6,$$

$$Q_{10}^{(0)}(a) = a^{16} + a^{15} - 3a^{14} - 3a^{13} - 4a^{12} - 3a^{11} + 7a^{10} + 9a^9 + 3a^8.$$

The second endpoint of C_{10} is a point at which the points T_0^7 , V_0^{-2} and V_0^{-3} are collinear and for which we approximately have $(a_{10}, b_{10}) = (1.06317799, 0.982377305)$.

The stable and unstable manifold in this case are presented on Figure 2.18.

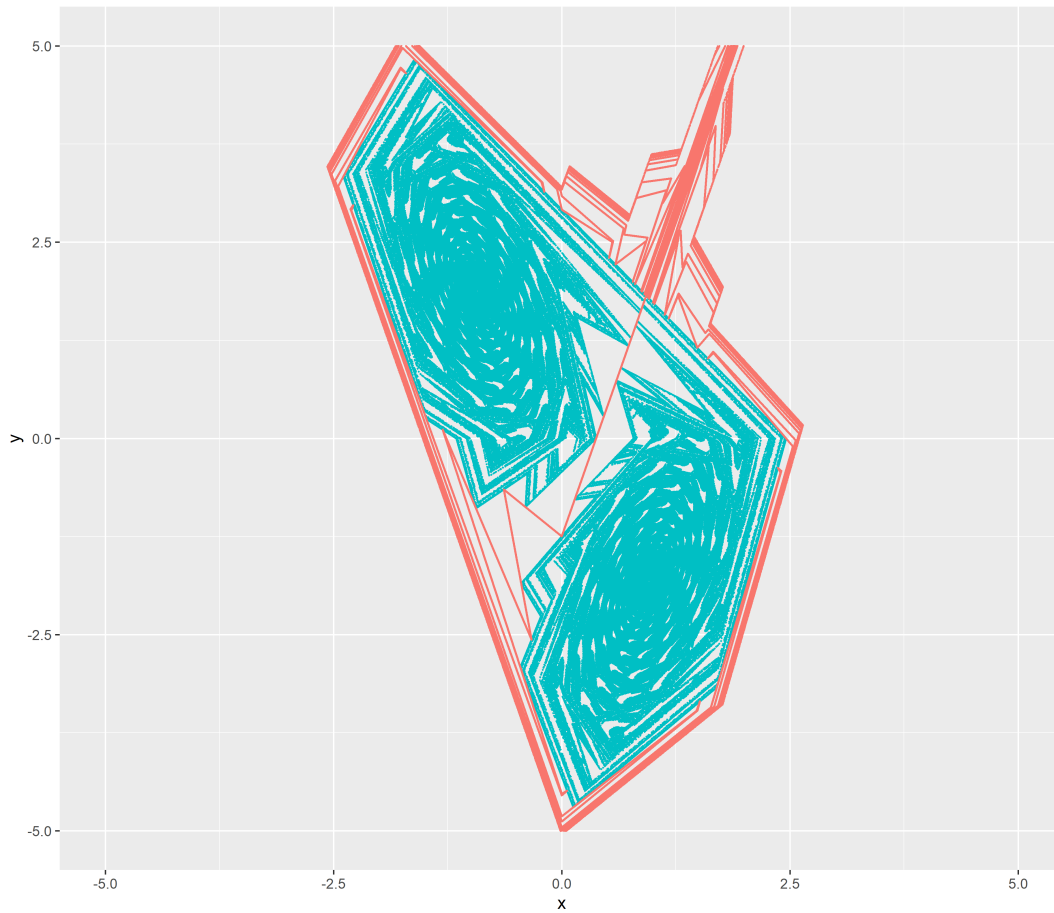


Figure 2.18: The stable (red) and unstable (blue) manifold in the border case $(a, b) = (a_{10}, b_{10})$ (second endpoint of the curve C_{10}).

2.2.11. Eleventh case: T_0^7 lies on $\overline{V_0^{-2}V_0^{-3}}^{(s)}$

After landing on $\overline{V_0^{-2}V_0^{-3}}^{(s)}$, T_0^7 will remain on that segment until it coincides with V_0^{-3} .

We equate the slope coefficients of $V_0^{-2}V_0^{-3}$ and $T_0^7V_0^{-3}$ and thus we obtain

$$C_{11} \dots P_{11}(a, b) + Q_{11}(a, b)\sqrt{a^2 + 4b} = 0, \tag{2.14}$$

where

$$\begin{aligned}
P_{11}(a,b) = & (8a-4)b^6 + (-7a^3+5a^2-4a)b^5 + (-4a^5+34a^4+16a^3+2a^2-4a)b^4 \\
& + (-7a^7-9a^6+40a^5-32a^4-2a^3+6a^2-4a)b^3 \\
& + (-5a^8-4a^7-26a^6+16a^5-6a^4-16a^3)b^2 \\
& + (a^{11}+a^{10}-6a^9+6a^8+6a^7-14a^6-6a^5+8a^4+4a^3)b \\
& + (4a^{10}-4a^8+4a^6+4a^5+4a^4+4a^3+2a^2),
\end{aligned}$$

$$\begin{aligned}
Q_{11}(a,b) = & -2b^6 + (5a^2+5a)b^5 + (14a^4-6a^3-2a)b^4 \\
& + (-9a^6-9a^5-12a^4+8a^3+2a^2-2a)b^3 \\
& + (-2a^8+a^7+26a^5-4a^4-2a^3+4a^2)b^2 \\
& + (a^{10}+a^9+2a^8-2a^7-2a^6+10a^5+2a^4-8a^3-4a^2)b \\
& + (-4a^9+4a^7-4a^5-4a^4-4a^3-4a^2-2a).
\end{aligned}$$

On this curve, similarly as in the sixth case, point V_0^{-3} will land on the x -axis at a point for which we approximately have $(a^{**}, b^{**}) = (1.03529028, 0.975731847)$ and remain in the third quadrant after that until it coincides with T_0^7 at the second endpoint of the curve, $(a_{11}, b_{11}) = (0.939255378, 0.968217486)$. This case is presented on Figure 2.19.

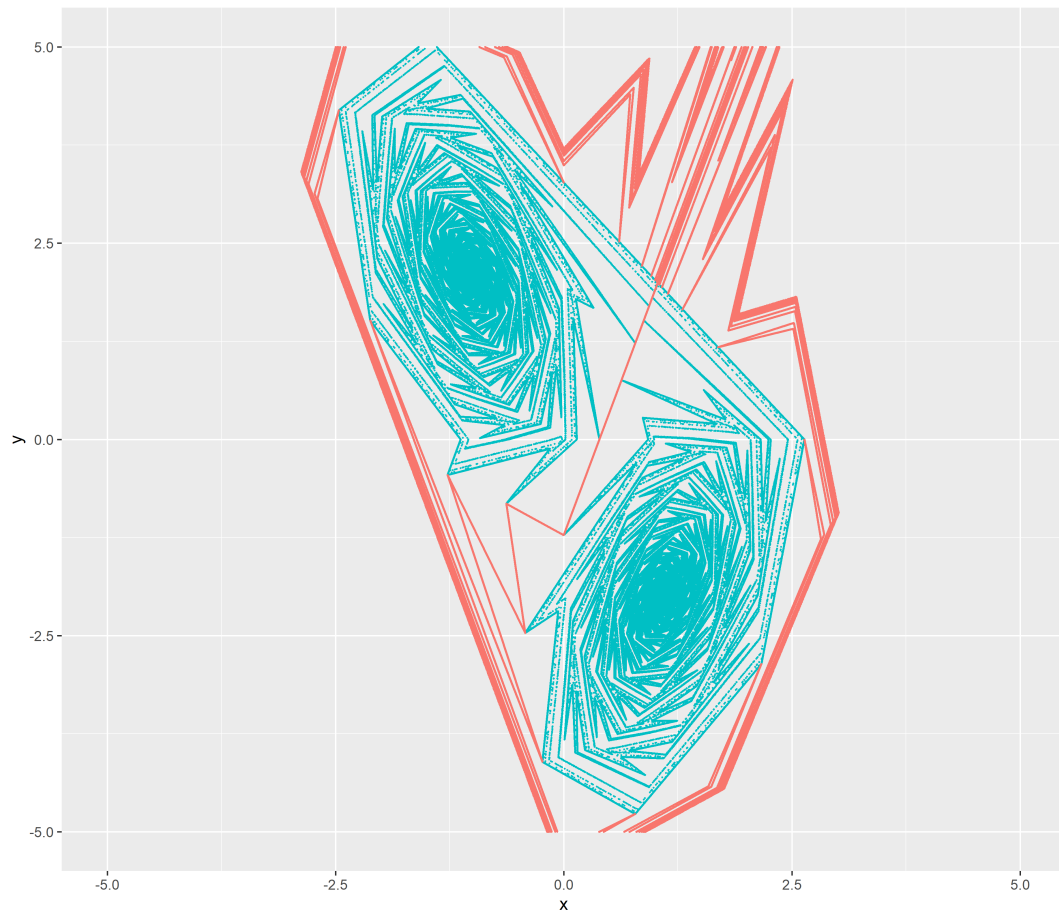


Figure 2.19: The stable (red) and unstable (blue) manifold in the border case $(a, b) = (a_{11}, b_{11})$ (second endpoint of the curve C_{11}).

3. ZERO ENTROPY FOR THE LOZI MAP

In this chapter we consider the zero entropy locus problem for the Lozi map when $b > 0$ and $a > 1 - b$. We show that the Lozi map has zero topological entropy, $h_{top}(L) = 0$, in a subset of a region in the parameter space for which the period-two orbit is attracting and there are no homoclinic points for the fixed point X . This result expands the one presented in [21].

3.1. RELATIONSHIP WITH THE ATTRACTING PERIOD-TWO CYCLE

If $a + b > 1$, the Lozi map L has two periodic points of prime period two, P in the fourth and P' in the second quadrant. These points are given by

$$P = \left(\frac{1+a-b}{a^2+(1-b)^2}, \frac{b(1-a-b)}{a^2+(1-b)^2} \right), \quad P' = \left(\frac{1-a-b}{a^2+(1-b)^2}, \frac{b(1+a-b)}{a^2+(1-b)^2} \right). \quad (3.1)$$

If $a < 1 + b$, these points are attracting. There are two specific things concerning their dynamics which occur on the border of existence of homoclinic points. Firstly, the differential of L^2 at these points has eigenvalues

$$\lambda_1 = \frac{1}{2} \left(-a^2 + 2b - a\sqrt{a^2 - 4b} \right), \quad \lambda_2 = \frac{1}{2} \left(-a^2 + 2b + a\sqrt{a^2 - 4b} \right).$$

In the case $a^2 < 4b$ we specially have a pair of complex conjugate eigenvalues which results in a rotation around the periodic point. Following the border of existence of homoclinic points for X described in the previous chapter, this occurs on the curve C_3 and persists on the rest of the border. The second specific property is when these hyperbolic periodic points become saddle points. This is achieved when $a > b + 1$ and the border of this area intersects curves C_1 , C_2 and C_3 only. All of this is given on Figure 3.1.

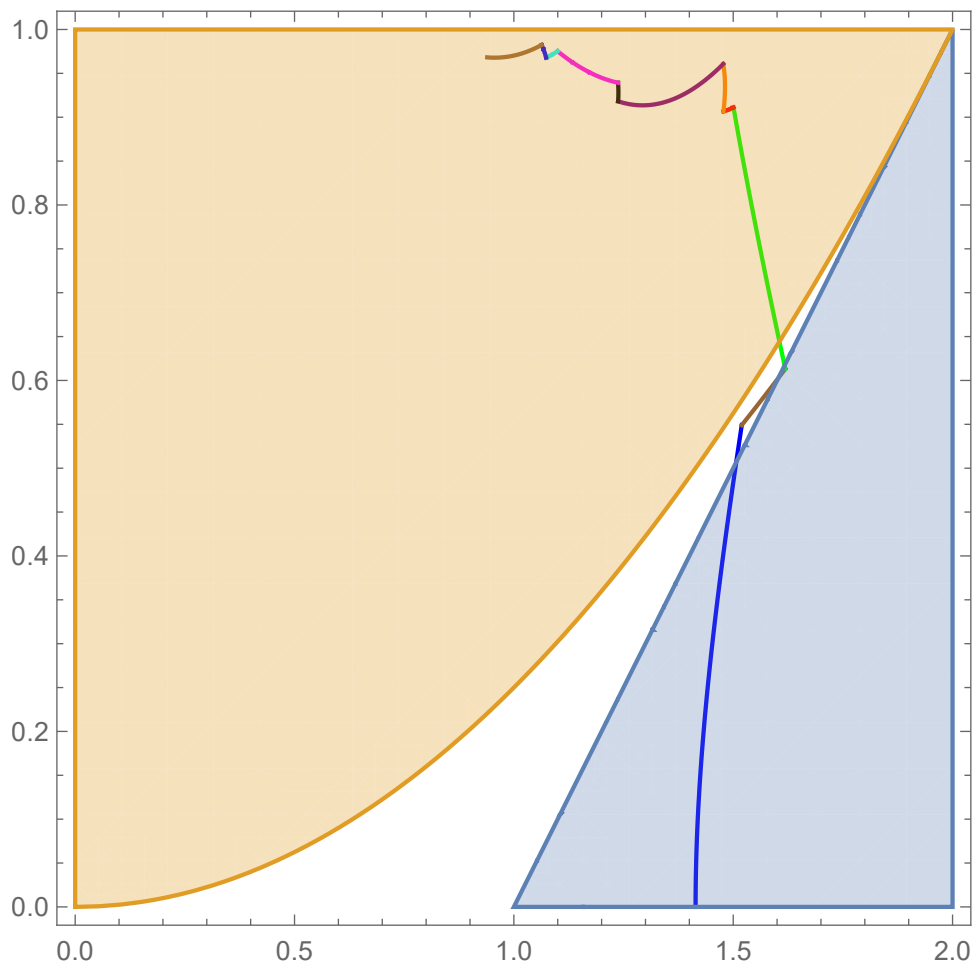


Figure 3.1: Areas in the parameter space where there is rotation around the periodic points of period 2 (yellow) and where these points are saddles (blue). Curves C_1 - C_{11} are presented in the same colors as on Figure 2.8. Values of parameter a are represented on the horizontal and those of b on the vertical axis.

From now on we will consider the region \mathfrak{R} in the parameter space such that $0 < b < 1$, $1 - b < a < 1 + b$ (period-two orbit $\{P, P'\}$ is attracting) and that there are no homoclinic points for the fixed point X . Additionally, we will also consider its subset R for which W_X^u does not intersect the coordinate axes at points other than T_0 and T_0^1 . These regions are represented on Figure 3.2.

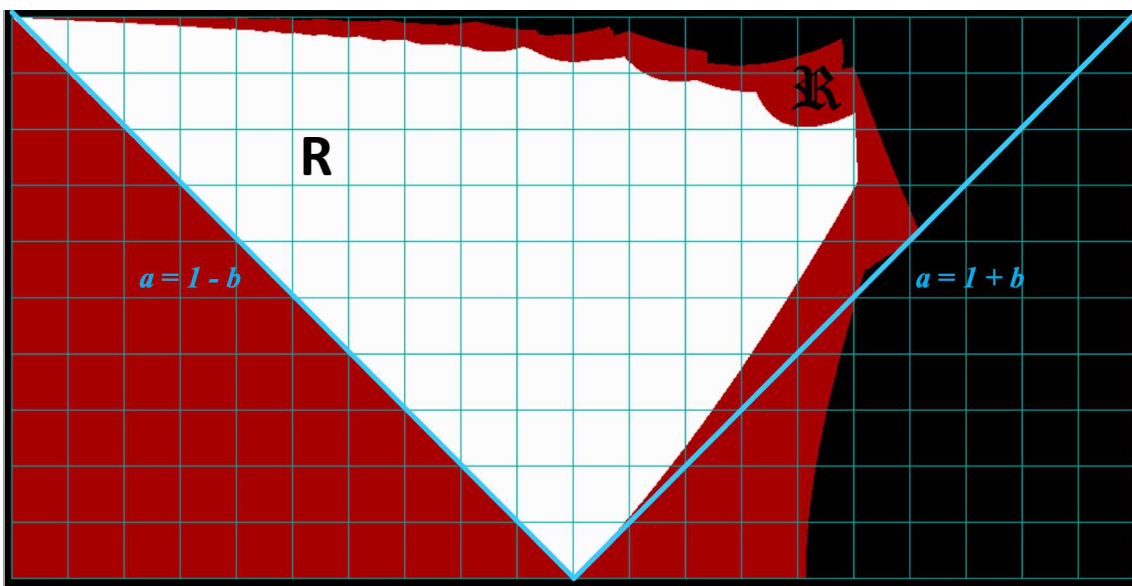


Figure 3.2: Regions R (white) and \mathfrak{R} (red and white, between the two blue lines) obtained numerically. Values of parameter a are represented on the horizontal and those of b on the vertical axis.

3.2. INVARIANT SETS FOR L^2

In this section we will consider parameter pairs $(a, b) \in \mathfrak{R}$ and first assume that W_X^u intersects the coordinate axes at points other than T_0 and T_0^{-1} .

From now on let $k \geq 2$ be the smallest integer such that T_0^{k-2} and T_0^k are not both in the right half-plane. If k is even, T_0^k lies in the third quadrant, and if k is odd, T_0^k lies in the first quadrant. In both cases T_0^{k-1} and T_0^{k+1} are not both contained in the upper half-plane. If k is even, T_0^{k+1} lies in the lower half-plane, and if k is odd, T_0^{k+1} lies in the first quadrant. In any case, the line segment $\overline{T_0^{k-2}T_0^k}$ intersects the y -axis and the line segment $\overline{T_0^{k-1}T_0^{k+1}}$ intersects the x -axis, see Figures 3.4 and 3.5.

Lemma 3.2.1. The intersection of the straight line segment $\overline{T_0^k T_0^{k+1}}$ and W_X^s consists of a single point.

Proof. Since one of the points T_0^k, T_0^{k+1} lies on W_X^{u+} , and the other one on W_X^{u-} , the line segment $\overline{T_0^k T_0^{k+1}}$ intersects W_X^{s-} (and $\overline{T_0^k T_0^{k+1}} \cap W_X^{s+} = \emptyset$).

If k is odd, points T_0^k, T_0^{k+1} lie both in the first quadrant. Since $[X, V_0]^{(s)}$ is a line segment and V_0 lies in the lower half-plane, $\overline{T_0^k T_0^{k+1}} \cap W_X^s$ is a single point.

If k is even, T_0^k lies in the third quadrant. If T_0^{k+1} lies in the fourth quadrant, then $\overline{T_0^k T_0^{k+1}}$ intersects the y -axis at one point, T_0^{k+2} lies in the first quadrant to the right of $[X, V_0]^{(s)}$ and $L(\overline{T_0^k T_0^{k+1}})$ is a polygonal line that consists of two line segments $\overline{T_0^{k+1}Q}$, $\overline{QZ^{k+2}}$ with $Q \in x$ -axis. Therefore, $L(\overline{T_0^k T_0^{k+1}})$ intersects W_X^{s-} in one point implying that $\overline{T_0^k T_0^{k+1}}$ also intersects W_X^s in a single point.

Let us now suppose that k is even and that the both points T_0^k, T_0^{k+1} lie in the third quadrant. Then $L(\overline{T_0^k T_0^{k+1}})$ is a line segment $\overline{T_0^{k+1}T_0^{k+2}}$. Let n_0 be as in Proposition 2.1.3. First note that it is not possible that $\overline{V_0^{-i}V_0^{-i-1}} \subset \overline{T_0^k T_0^{k+1}}$ for some $i \in \{0, \dots, n_0 - 1\}$, since in that case $\overline{V_0^{-i+1}V_0^{-i}} \subset \overline{T_0^{k+1}T_0^{k+2}}$, but $T_0^{k+1} \neq V_0^{-i}$ implies that the slopes of $\overline{T_0^{k+1}T_0^{k+2}}$ and $\overline{T_0^{k+1}V_0^{-i+1}}$ are different. Therefore, $\overline{T_0^k T_0^{k+1}} \cap W_X^{s-}$ consists of finitely many points.

Let us suppose, by contradiction, that $\overline{T_0^k T_0^{k+1}} \cap W_X^s$ contains at least two points. Let Q_1, Q_2 be the first two consecutive points of intersection, that is $[V_0, Q_1]^{(s)} \subset [V_0, Q_2]^{(s)}$ and that the only points of intersection in $[V_0, Q_2]^{(s)}$ are Q_1 and Q_2 . Then $\{L(Q_1), L(Q_2)\} \subset$

$\overline{T_0^{k+1}T_0^{k+2}} \cap W_X^{s-}$. Let $d_1, d_2 \in \{1, \dots, n_0 - 1\}$ be such that

$$Q_n \in \overline{V_0^{-d_n}V_0^{-d_n-1}}, \quad n = 1, 2 \quad (3.2)$$

(the case $d_1 = 0$ will be considered at the end of the proof). Then

$$L(Q_n) \in \overline{V_0^{-d_n+1}V_0^{-d_n}}, \quad n = 1, 2. \quad (3.3)$$

Since

$$\overline{V_0^{-d_1+1}V_0^{-d_1}} \cap \overline{T_0^kT_0^{k+1}} = \emptyset, \quad (3.4)$$

and hence

$$\overline{V_0^{-d_1+2}V_0^{-d_1+1}} \cap \overline{T_0^{k+1}T_0^{k+2}} = \emptyset, \quad (3.5)$$

it follows that $d_2 \neq d_1 + 1$. Namely,

$$\begin{aligned} d_2 = d_1 + 1 &\implies Q_1, L(Q_2) \in \overline{V_0^{-d_2+1}V_0^{-d_2}} = \overline{V_0^{-d_1}V_0^{-d_1-1}} \\ &\implies L(Q_1) \in \overline{V_0^{-d_1+1}V_0^{-d_1}} \implies V_0^{-d_1+1} \in \mathcal{G}, \end{aligned}$$

where \mathcal{G} is the region bounded by the line segments $\overline{T_0^kT_0^{k+1}}$, $\overline{T_0^{k+1}T_0^{k+2}}$ and the polygonal line $[T_0^k, T_0^{k+2}]^{(u)}$, implying that $[V_0^{-d_1+1}, X]^{(s)} \cap \overline{T_0^{k+1}T_0^{k+2}} \neq \emptyset$ contradicting (3.5) (if $d_1 = 1$, then $V \in \mathcal{G}$ and T_0^{k+2} lies in the fourth quadrant to the right of $\overline{V_0^1V_0} \subset \overline{XV_0}$).

Therefore, (3.2) and (3.3) for $n = 1$ imply that $V_0^{-d_1}$ lies in \mathcal{G} . Since Q_1 and Q_2 are two consecutive points of intersection of $\overline{T_0^kT_0^{k+1}}$ and W_X^{s-} , the polygonal line $[Q_1, Q_2]^{(s)}$ does not intersect \mathcal{G} at other points than Q_1 and Q_2 . By $d_2 \neq d_1 + 1$, we have $\overline{V_0^{-d_2+1}V_0^{-d_2}} \subset [Q_1, Q_2]^{(s)}$, which is a contradiction with (3.3) for $n = 2$ since every line segment that intersects $\overline{T_0^{k+1}T_0^{k+2}}$ also intersects \mathcal{G} . Therefore, $\overline{T_0^kT_0^{k+1}} \cap W_X^s$ is a single point.

If $d_1 = 0$, then $L(Q_1) \in \overline{V_0^1V_0} \subset \overline{XV_0}$ and $\overline{T_0^{k+1}T_0^{k+2}}$ intersects W_X^s at one point. Therefore, $\overline{T_0^kT_0^{k+1}} \cap W_X^s$ is also a single point. \blacksquare

Lemma 3.2.2. Let \mathcal{D} be the region bounded by the polygonal line $[T_0^k, T_0^{k+1}]^{(u)}$ and the line segment $\overline{T_0^kT_0^{k+1}}$. Then $L(\mathcal{D}) \subset \mathcal{D}$.

Proof. For every $i \in \{0, \dots, k-2\}$, let us consider the line l_i through points T_0^i, T_0^{i+2} . By the choice of k , straight line segments $\overline{T_0^iT_0^{i+2}}^{(u)}$ are all contained in the right half-plane for all even $i \leq k-3$, and they are contained in the left half-plane for all odd $i \leq k-3$.

Moreover, $L(M) \in \overline{XV}^{(s)}$, so $L(\overline{T_0^k T_0^{k+1}}) \subset \mathcal{D}$ and again $L(\mathcal{D}) \subset \mathcal{D}$. ■

Corollary 3.2.3. Let Z be the intersection of $[T_0^{k-2}, T_0^k]^{(u)}$ and the y -axis. Then $W_X^u \cap y\text{-axis} \subset \overline{ZT_0^{-1}}$ and $W_X^u \cap x\text{-axis} \subset \overline{L(Z)T_0}$.

Definition 3.2.4. We call a point Q a *turning point* if W_X^u transversally intersects the x -axis at Q . *Post-turning points* are forward images of turning points under L .

For example, T_0 is a turning point and T_0^i , $i \in \mathbb{N}$, are some post-turning points.

Lemma 3.2.5. There exists a turning point S such that $W_X^u \cap \overline{ST_0} = \{S, T_0\}$. If S lies in the right half-plane, let \mathcal{D}' be the region bounded by the polygonal line $[T_0, S]^{(u)}$ and the line segment $\overline{ST_0}$. If S lies in the left half-plane, let \mathcal{D}' be the region bounded by the polygonal line $[X, S]^{(u)}$ and the line segments $\overline{SV_0^1} \subset x\text{-axis}$ and $\overline{V_0^1 X}^{(s)}$. Then $L^2(\mathcal{D}') \subset \mathcal{D}'$.

Proof. Let us first assume that k is odd. Then T_0^{k+1} is in the first quadrant. Denote by d_1 the distance between T_0^{k+1} and $\overline{XV}^{(s)}$. If T_0^{k+1+i} , $i \in \mathbb{N}$, lies in the first quadrant, denote by d_{1+i} the distance between T_0^{k+1+i} and $\overline{XV_0}^{(s)}$. Note that $d_{1+i} = d_1 |\lambda_X^u|^i$, where λ_X^u is the eigenvalue of the differential DL at X with $|\lambda_X^u| > 1$. Thus, there exists the smallest $m \in \mathbb{N}$ such that $d_1 |\lambda_X^u|^m > \text{dist}(X, T_0^{-1})$, and hence T_0^{k+1+m} lies in the second quadrant. Consequently, T_0^{k+m+2} lies in the fourth quadrant and $[T_0^{k+m}, T_0^{k+m+2}]^{(u)}$ is a polygonal line that intersects the x -axis. It is easy to see that $\{S\} = [T_0^{k+m}, T_0^{k+m+2}] \cap x\text{-axis}$, see Figure 3.4.

Namely, since W_X^{u-} does not intersect the x -axis and W_X^{u+} does not intersect the y -axis, every polygonal line $[T_0^i, T_0^{i+2}]^{(u)}$ intersects at most one coordinate axis, and hence $[T_0^{k+m}, T_0^{k+m+2}]^{(u)}$ does not contain any post-turning points in the first quadrant except the boundary points. Therefore, $L^2(S), T_0^{k+m+2}, T_0^2 \in \mathcal{D}'$, and thus $L^2(\mathcal{D}') \subset \mathcal{D}'$.

Let us suppose now that k is even. If $W_X^{u-} \cap y\text{-axis} = \{T_0^{-1}\}$ (in that case T_0^{k+3} lies in the second quadrant), we have $W_X^{u+} \cap x\text{-axis} = \{T_0\}$, $\{S\} = [T_0^{k+1}, T_0^{k+3}]^{(u)} \cap x\text{-axis}$ lies in the left half-plane, and the proof follows.

Now suppose that W_X^{u-} intersects the y -axis in at least two points. If T_0^{k+3} lies in the first or fourth quadrant, at least one of the points T_0^{k+3}, T_0^{k+4} lies in the first quadrant, and as in the odd case, there exists $m \in \mathbb{N}$ such that T_0^{k+4+i} lies in the first quadrant for every $i < m$, and T_0^{k+4+m} lies in the second quadrant. Consequently again, $T_0^{k+4+m+1}$ lies in the fourth quadrant, $\{S\} = [T_0^{k+m+3}, T_0^{k+m+5}]^{(u)} \cap x\text{-axis}$ and $[T_0^{k+m+5}, T_0^{k+m+7}]^{(u)} \subset \mathcal{D}'$.

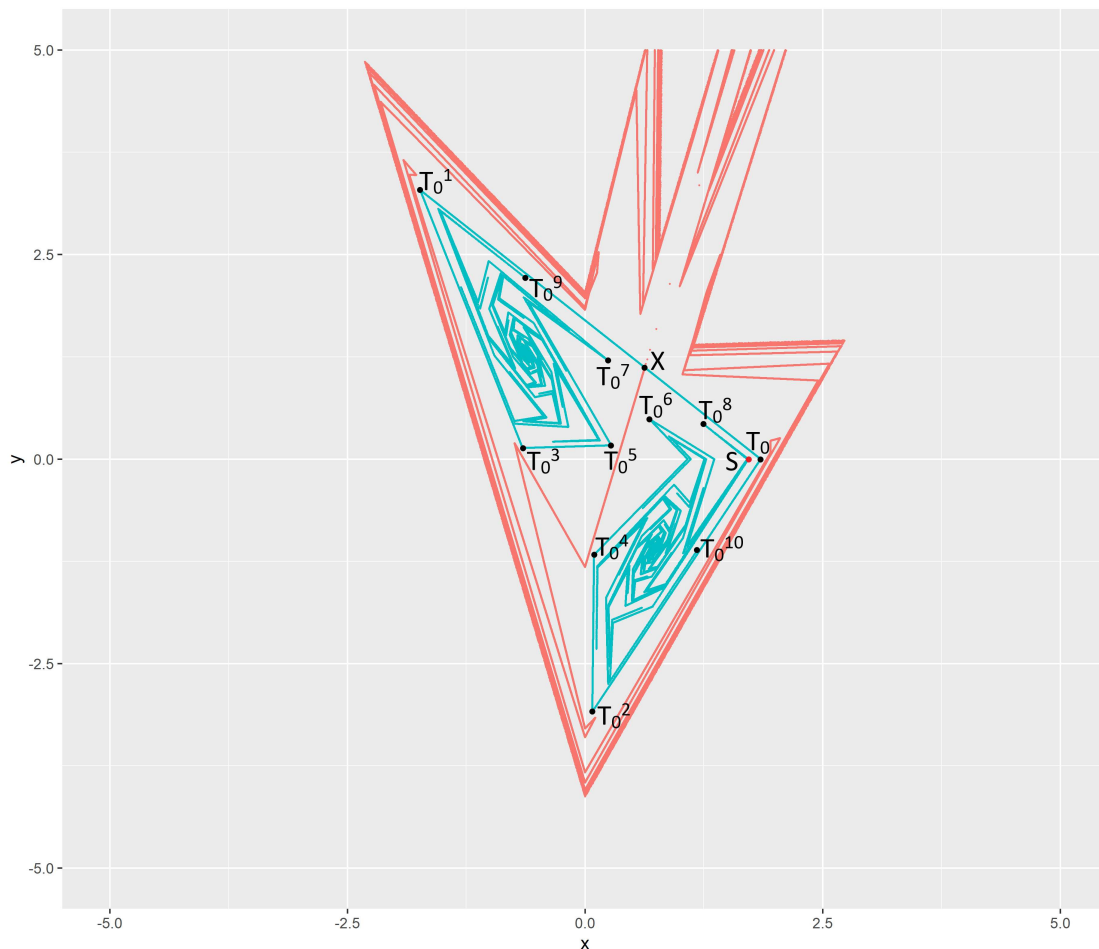


Figure 3.4: W_X^s (red) and W_X^u (blue) for parameter values $a = 1.48$, $b = 0.89$. In this case we have $k = 5$, $m = 3$.

Finally, suppose that T_0^{k+3} lies in the third quadrant. Then T_0^{k+4} lies in the fourth quadrant. If T_0^{k+5} lies in the second quadrant, T_0^{k+6} lies in the fourth quadrant. The polygonal line $[T_0^{k+4}, T_0^{k+6}]^{(u)}$ intersects the x -axis and contains finitely many turning and post-turning points in the first quadrant. Let Q be the post-turning point of $[T_0^{k+4}, T_0^{k+6}]^{(u)}$ that is the closest one to $\overline{XV_0}^{(s)}$. Then by the same argument as in the odd case, there exists $j \in \mathbb{N}$ such that $L^i(Q)$ lies in the first quadrant for every $i < j$, $L^j(Q)$ lies in the second quadrant and $L^{j+1}(Q)$ lies in the fourth quadrant. Then S is the rightmost point of $[T_0^{k+4+j-1}, T_0^{k+6+j-1}]^{(u)} \cap x\text{-axis}$ and $[T_0^{k+4+j+1}, T_0^{k+6+j+1}]^{(u)} \subset \mathcal{D}'$.

If T_0^{k+5} lies in the first quadrant, then as in the odd case, there exists $m \in \mathbb{N}$ such that T_0^{k+5+i} lies in the first quadrant for every $i < m$, T_0^{k+5+m} lies in the second quadrant, and consequently T_0^{k+m+6} lies in the fourth quadrant. Let us consider now the polygonal line

$[T_0^{k+m+4}, T_0^{k+m+6}]^{(u)}$. It contains finitely many turning and post-turning points in the first quadrant. If the distance between $\overline{XV_0^{(s)}}$ and each of these post-turning points is larger than the distance between $\overline{XV_0^{(s)}}$ and T_0^{k+m+4} , then L^2 maps all these points to the fourth quadrant and S is the rightmost point of $[T_0^{k+m+4}, T_0^{k+m+6}]^{(u)} \cap x$ -axis. If not, let us denote by Q the post-turning point of $[T_0^{k+m+4}, T_0^{k+m+6}]^{(u)}$ that is the closest one to $\overline{XV_0^{(s)}}$, see Figure 3.5.

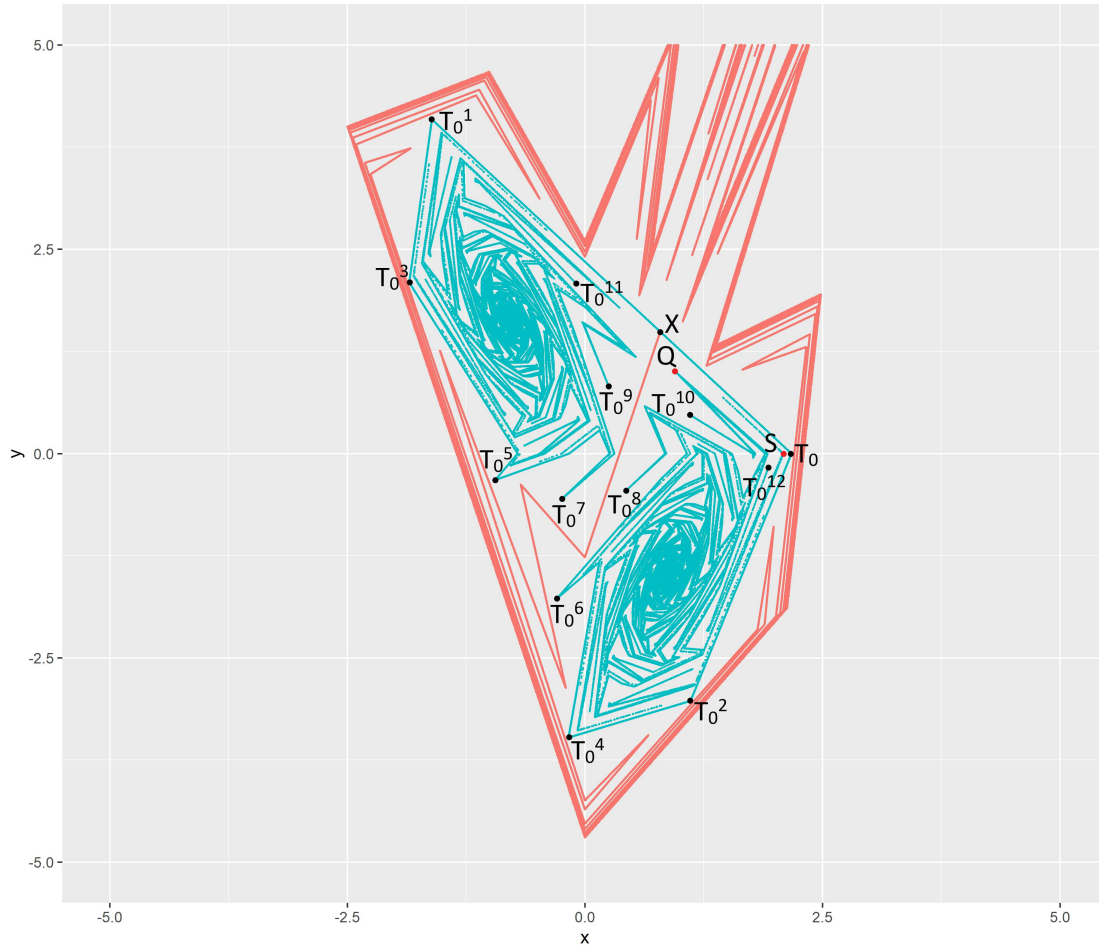


Figure 3.5: W_X^s (red) and W_X^u (blue) for parameter values $a = 1.2$, $b = 0.94$. In this case we have $k = 4$, $m = 2$, $j = 3$.

Then by the same argument as in the odd case, there exists $j \in \mathbb{N}$ such that $L^i(Q)$ lies in the first quadrant for every $i < j$, $L^j(Q)$ lies in the second quadrant and $L^{j+1}(Q)$ lies in the fourth quadrant. Then S is the rightmost point of $[T_0^{k+m+4+j-1}, T_0^{k+m+6+j-1}]^{(u)} \cap x$ -axis and $[T_0^{k+m+4+j+1}, T_0^{k+m+6+j+1}]^{(u)} \subset \mathcal{D}'$.

In any case, $L^2(\mathcal{D}') \subset \mathcal{D}'$. ■

Corollary 3.2.6. The polygonal line $[X, S]^{(u)}$ intersects the coordinate axes in finitely many points.

Let $M, N \in W_X^u$ be two different points. Let $0 < \varepsilon < \frac{1}{2} \text{dist}(M, N)$. Recall that $(M, N)^{(u)} = [M, N]^{(u)} \setminus \{M, N\}$. We define the point $M' \in (M, N)^{(u)}$ as *the first to M with* $\text{dist}(M, M') = \varepsilon$ if $\text{dist}(M, M') = \varepsilon$ and for every $Q \in (M, N)^{(u)}$ such that $\text{dist}(M, Q) = \varepsilon$ we have $(M, M')^{(u)} \subseteq (M, Q)^{(u)}$. Let $N' \in (M, N)^{(u)}$ be the first to N with $\text{dist}(N, N') = \varepsilon$. We define

$$B_\varepsilon((M, N)^{(u)}) := \bigcup_{Q \in [M', N']^{(u)}} B_\varepsilon(Q),$$

where $B_\varepsilon(Q)$ denotes the ball with center at Q and radius ε .

Corollary 3.2.7. For every $Q \in W_X^u$ there exists $\varepsilon > 0$ such that $B_\varepsilon((X, Q)^{(u)}) \cap W_X^u = (X, Q)^{(u)}$.

Proof. From Lemma 3.2.5 it follows that there exists $\delta > 0$ such that $B_\delta((T_0^{-1}, X)^{(u)}) \cap W_X^u = (T_0^{-1}, X)^{(u)}$. Since for every $Q \in W_X^u$ there exists $m \in \mathbb{N}$ such that $Q \in L^m((T_0^{-1}, X)^{(u)})$ and W_X^u is invariant, the proof follows. ■

3.3. MAIN RESULTS

For the main result about the zero entropy of the Lozi map, we will consider parameter pairs in the region R first.

Theorem 3.3.1. For $(a, b) \in R$, $h_{top}(L_{a,b}) = 0$.

Proof. Let $(a, b) \in R$. Let

$$T_0L := W_X^{u-} \setminus [X, T_0)^{(u)} \text{ and } T_0R := W_X^{u+} \setminus [X, T_0^1)^{(u)}.$$

Let us consider the convex hulls $\text{Conv}(T_0L)$ and $\text{Conv}(T_0R)$, we have $L(\text{Conv}(T_0L)) = \text{Conv}(T_0R)$ and $L(\text{Conv}(T_0R)) \subset \text{Conv}(T_0L)$. In both sets, $\text{Conv}(T_0L)$ and $\text{Conv}(T_0R)$, the map is globally linear, so their union is attracted to the periodic orbit $\{P', P\}$. This in particular means that $W_X^u \cup \{P', P\}$ is compact, connected and invariant.

Recall that W_X^{s+} denotes the upper connected component of the stable manifold of X (which starts at X and goes up), and let W_Y^{u+} denote the lower connected component of the unstable manifold of the other fixed point Y in the third quadrant (which starts at Y and goes down). Let us denote by \mathcal{M} the union of W_X^u , P' , P , W_X^{s+} , W_Y^{u+} and ∞ , $\mathcal{M} = W_X^u \cup \{P', P\} \cup W_X^{s+} \cup W_Y^{u+} \cup \{\infty\}$. Then \mathcal{M} is invariant, compact, connected in the extended plane and does not separate the extended plane, nor the plane.

Let us denote by U the complement of \mathcal{M} in the extended plane (that is, $U = \mathbb{S}^2 \setminus \mathcal{M}$). Then U is invariant by construction and does not contain any fixed points of L^2 . Also, U is open and simply connected in the plane and therefore homeomorphic to the open unit disc and moreover, to the plane. The Brouwer plane translation theorem (BPTT) says that if h is an orientation preserving homeomorphism of the plane which is fixed point free, then every point of the plane is contained in a properly embedded line l such that l does not intersect $h(l)$, and l is separating $h(l)$ from $h^{-1}(l)$. In our case, $L^2|_U$ satisfies the assumptions of BPTT and therefore every point of U is a wandering point for L^2 . This means that the non-wandering set of L^2 consists only of the fixed points of L^2 , and hence $h_{top}(L^2) = 2h_{top}(L) = 0$. ■

Remark 3.3.2. Notice that the proof of Corollary 2.1.6 implies that for all $(a, b) \in \mathfrak{R}$, L exhibits heteroclinic points since W_X^s and W_Y^u intersect. However, this does not pose an

obstruction for zero entropy since there is no heteroclinic cycle - namely, W_X^u and W_Y^s do not intersect (Lemma 4.2.1). For more details see [4, Theorem 2.2].

Now recall that for parameter pairs $(a, b) \in \mathfrak{R} \setminus R$, the unstable manifold W_X^u intersects the coordinate axes at additional points other than T_0 and T_0^{-1} . Therefore, one can not directly draw analogous conclusions for the sets $\text{Conv}(T_0L)$ and $\text{Conv}(T_0R)$ defined as in Theorem 3.3.1; namely, in this case W_X^u can accumulate on a set ℓ which can generate positive topological entropy. Our goal now is to present a result about zero topological entropy of the Lozi map outside the aforementioned accumulation set ℓ for which we will first further investigate the unstable manifold W_X^u together with that set.

Let the point S and polygon \mathcal{D}' be defined as in Lemma 3.2.5. Notice that the accumulation set ℓ of W_X^u can be represented as a union

$$\ell = \ell_L \cup \ell_R,$$

where $\ell_R = \ell \cap \mathcal{D}'$, $\ell_L = \ell \cap L(\mathcal{D}')$ if S lies in the right half-plane and $\ell_R = \ell \cap L(\mathcal{D}')$, $\ell_L = \ell \cap \mathcal{D}'$ otherwise. Observe that both ℓ_R and ℓ_L are L^2 - and L^{-2} -invariant.

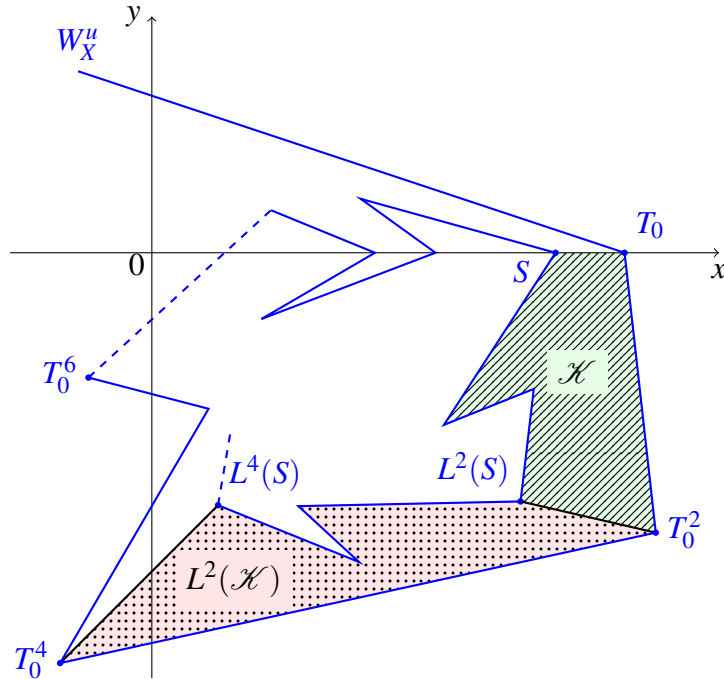


Figure 3.6: Polygon \mathcal{K} and its image under L^2 (Lemma 3.3.3).

Lemma 3.3.3. Define S and \mathcal{D}' as above. If S lies in the right half-plane, then

$$\ell_R = \bigcap_{k=0}^{\infty} L^{2k}(\mathcal{D}').$$

Proof. Since $\ell_R \subseteq \mathcal{D}'$, \mathcal{D}' is L^2 -invariant (Lemma 3.2.5) and ℓ_R is both L^2 - and L^{-2} -invariant, it directly follows that $\ell_R \subseteq \bigcap_{k=0}^{\infty} L^{2k}(\mathcal{D}')$. To prove the converse, let \mathcal{K} be the polygon with the boundary

$$\partial\mathcal{K} = \overline{ST_0} \cup [T_0, T_0^2]^{(u)} \cup [S, L^2(S)]^{(u)} \cup \overline{L^2(S)T_0^2}.$$

We see that $\text{Int}L^{2j}(\mathcal{K}) \cap \text{Int}L^{2k}(\mathcal{K}) = \emptyset$ for all $j, k \in \mathbb{N}_0$, $j \neq k$ (see Figure 3.6). Notice that

$$L^2(\mathcal{D}') = (\mathcal{D}' \setminus \mathcal{K}) \cup [S, L^2(S)]^{(u)} \cup L^2(\overline{T_0S}),$$

and similarly, for $k \in \mathbb{N}$,

$$L^{2k}(\mathcal{D}') = \left(\mathcal{D}' \setminus \left(\bigcup_{j=0}^{k-1} L^{2j}(\mathcal{K}) \right) \right) \cup [L^{2(k-1)}(S), L^{2k}(S)]^{(u)} \cup L^{2k}(\overline{T_0S}).$$

Moreover, $\mathcal{D}' \setminus \text{Int}L^{2k}(\mathcal{D}')$ contains $L^{2j}(\overline{T_0S})$ for all $j = 0, 1, \dots, k-1$. Hence, for every $i \in \mathbb{N}_0$ there exists $j \in \mathbb{N}_0$ such that $[T_0^{2j}, T_0^{2(j+1)}]^{(u)}$ is closer to ℓ_R than $L^{2i}(\overline{T_0S})$. Since $L^{2k}(\partial\mathcal{D}') = \partial L^{2k}(\mathcal{D}')$ for every $k \in \mathbb{N}$ and L^2 is dissipative, we see that for every point $Q \in \bigcap_{k=0}^{\infty} L^{2k}(\mathcal{D}')$ there exists a sequence of points in W_X^u which tends towards Q . Therefore, $Q \in \ell_R$ so we have $\bigcap_{k=0}^{\infty} L^{2k}(\mathcal{D}') \subseteq \ell_R$ which finishes the proof. ■

Remark 3.3.4. In the case when S lies in the left half-plane, one can analogously show that

$$\ell_L \cup \{X\} = \bigcap_{k=0}^{\infty} L^{2k}(\mathcal{D}')$$

by considering polygons $L^{2k}(\mathcal{K}')$, $k \in \mathbb{N}_0$, where the boundary of \mathcal{K}' is $\partial\mathcal{K}' = \overline{SV_0} \cup \overline{V_0V_0^{2(s)}} \cup [S, L^2(S)]^{(u)} \cup \overline{L^2(S)V_0^2}$. In either case, $\mathcal{D}' \cup L(\mathcal{D}')$ contains the periodic orbit $\{P, P'\}$ due to Lemma 3.2.5 and the Brouwer fixed point theorem, which allows us to conclude the following result.

Corollary 3.3.5. The periodic orbit $\{P, P'\}$ is contained in ℓ .

Similarly as in Theorem 3.3.1, we define the set

$$\mathcal{N} := W_X^u \cup \ell \cup W_X^{s+} \cup W_Y^{u+} \cup \{\infty\}$$

in the extended plane. By construction, \mathcal{N} is invariant, compact, connected in the extended plane and does not separate the extended plane nor the plane.

Let U' be the complement of \mathcal{N} in the extended plane ($U' = \mathbb{S}^2 \setminus \mathcal{N}$). Then U' is invariant by construction and, due to Corollary 3.3.5, does not contain any fixed points of L^2 .

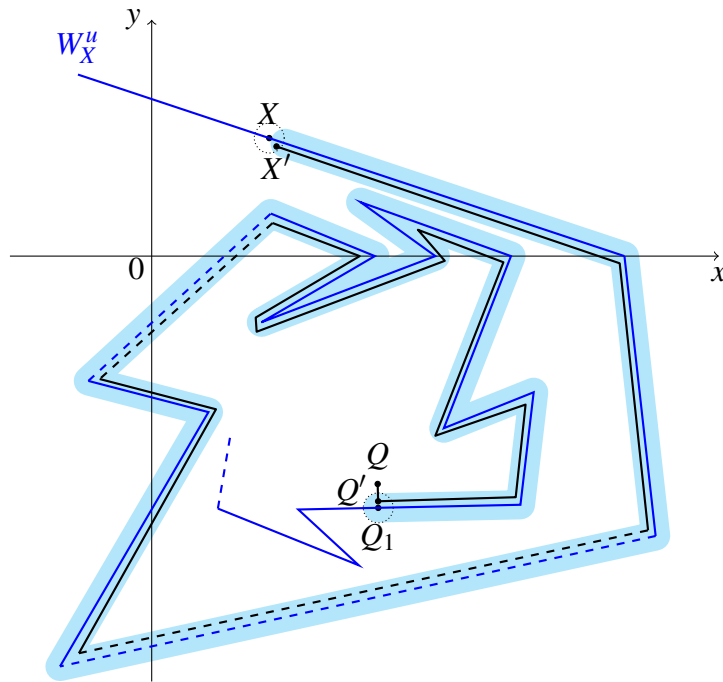


Figure 3.7: Construction of a path from Q to X' (Lemma 3.3.6). The path from Q' to X' is contained in an open neighborhood of $(X, Q_1)^{(u)}$ which contains only one arc component of W_X^u (Corollary 3.2.7).

Lemma 3.3.6. The set U' is pathwise connected.

Proof. Let \mathcal{D}' and S be defined as in Lemma 3.3.3. Notice that the set $\mathbb{S}^2 \setminus (\mathcal{N} \cup \mathcal{D}' \cup L(\mathcal{D}'))$ is open, connected and thus pathwise connected. Therefore, it suffices to show that the set $\mathcal{D}' \setminus (W_X^u \cup \ell)$ is pathwise connected (since this implies that the same holds for $L(\mathcal{D}') \setminus (W_X^u \cup \ell)$). In order to prove that, we will show that for any point Q lying in

$\mathcal{D}' \setminus (W_X^u \cup \ell)$, there is a path from Q to a point lying in an ε -neighborhood of the fixed point X for a specially chosen $\varepsilon > 0$ (see Figure 3.7).

Let $Q \in \mathcal{D}' \setminus (W_X^u \cup \ell)$ be fixed but arbitrary. Since $Q \notin \ell$, Lemma 3.3.3 implies that there exists a $k \in \mathbb{N}$ such that $Q \notin L^{2k}(\mathcal{D}')$. Let k_0 be the smallest such k . We then have $Q \in L^{2(k_0-1)}(\mathcal{D}')$ and $Q \notin L^{2k_0}(\mathcal{D}')$.

We know that

$$\partial L^{2j}(\mathcal{D}') = [T_0^{2j}, L^{2j}(S)]^{(u)} \cup L^{2j}(\overline{T_0 S})$$

for every $j \in \mathbb{N}_0$ and specially, for $j \in \{k_0 - 1, k_0\}$. Now observe the polygonal segment $[X, L^{2k_0}(S)]^{(u)}$. Since this is a closed set, there exists a point Q_1 lying on it such that

$$\text{dist}(Q, Q_1) = \min\{\text{dist}(Q, A) : A \in [X, L^{2k_0}(S)]^{(u)}\}.$$

By construction, we see that the straight line segment $\overline{QQ_1}$ does not intersect ℓ nor W_X^u at points other than Q_1 .

On the other hand, Corollary 3.2.7 implies the existence of an $\varepsilon > 0$ such that

$$B_\varepsilon((X, L^{2k_0}(S))^{(u)}) \cap W_X^u = (X, L^{2k_0}(S))^{(u)}.$$

In addition, the set $B_\varepsilon((X, L^{2k_0}(S))^{(u)}) \setminus [X, L^{2k_0}(S)]^{(u)}$ consists of two connected components only one of which has non-empty intersection with $\overline{QQ_1}$. We denote that connected component by \mathcal{B} . Notice that by construction $\mathcal{B} \cap \ell = \emptyset$.

Let Q' be any point lying on $\mathcal{B} \cap \overline{QQ_1}$ and let X' be any point lying on $(\mathcal{B} \cap B_\varepsilon(X)) \setminus W_X^{s+}$. Notice that X' can be chosen such that it lies outside of \mathcal{D}' . Since \mathcal{B} is open and connected, it is also pathwise connected so there exists a path $\mathbf{b} \subset \mathcal{B}$ from Q' to X' . By construction, the path \mathbf{b} lies in U' which finishes the proof. \blacksquare

Theorem 3.3.7. For all $(a, b) \in \mathfrak{R} \setminus R$, $h_{top}(L_{a,b}|_{\mathbb{R}^2 \setminus \ell}) = 0$.

Proof. Let U' and \mathcal{N} be defined as above. Lemma 3.3.6 implies that U' is connected and since its complement \mathcal{N} is also connected, it follows that U' is simply connected in the extended plane.

Therefore, by the Riemann mapping theorem we have that U' is homeomorphic to the open unit disc and moreover, to the plane. Now we see that $L^2|_{U'}$ satisfies the assumptions of the Brouwer plane translation theorem so every point of U' is a wandering point for

L^2 . As a consequence, the non-wandering set of the restriction $L^2|_{\mathbb{R}^2 \setminus \ell}$ consists only of its fixed points and hence $h_{top}(L^2|_{\mathbb{R}^2 \setminus \ell}) = 2h_{top}(L^2|_{\mathbb{R}^2 \setminus \ell}) = 0$. ■

Remark 3.3.8. For parameter pairs (a, b) such that the Lozi map $L_{a,b}$ exhibits transversal homoclinic points for the fixed point X , we have $h_{top}(L_{a,b}) > 0$; for more details, see [4, Theorem 2.1]. Therefore, in order to fully determine the zero entropy locus of the Lozi map in the case when the period-two cycle $\{P, P'\}$ is attracting, determining the structure of the accumulation set ℓ is of key interest. This motivates us to pose the following conjecture.

Conjecture 3.3.9. For all $(a, b) \in \mathfrak{R} \setminus R$, $\ell = \{P, P'\}$.

A positive answer to this hypothesis would imply that the whole region \mathfrak{R} is the zero entropy locus for the Lozi map when the periodic points of prime period two are attracting.

4. BASIN OF ATTRACTION

While considering the same parameter set \mathfrak{R} as in the previous chapter, in this chapter we construct the basin of attraction for the Lozi map, i.e. an invariant subset of the plane such that all points of its complement diverge (tend to infinity) under forward iterations of L . The main goal is to present a result analogous to the one presented in [1], where the basin of attraction on the Misiurewicz parameter set turned out to be bounded by the stable manifold W_Y^s of the fixed point Y in the third quadrant.

4.1. PERIOD TWO REVISITED

Recall that for $(a, b) \in \mathfrak{R}$, the Lozi map has two attracting periodic points of prime period two: P in the fourth and P' in the second quadrant. Their position relative to W_X^u and W_Y^s will be of interest in this chapter.

Remark 4.1.1 (Inequality of quadratic and arithmetic mean, $QM - AM$ inequality). Recall that if x and y are non-negative real numbers, then their quadratic mean is greater or equal to their arithmetic mean:

$$\sqrt{\frac{x^2 + y^2}{2}} \geq \frac{x + y}{2}. \quad (4.1)$$

The equality holds if and only if $x = y$; namely, (4.1) is equivalent to

$$2(x^2 + y^2) \geq (x + y)^2 \Leftrightarrow (x - y)^2 \geq 0.$$

Lemma 4.1.2 (Position of P and P' relative to W_X^u).

1. $P_x < T_{0,x}$, i.e. P lies to the left of T_0 ,
2. $P'_y < T_{0,y}^1$, i.e. P' lies below T_0^1 .

Proof. Since $P'_y = bP_x$, $T_{0,y}^1 = bT_{0,x}^1$ and $b > 0$, the second claim is a direct consequence of the first one. It remains to prove the first claim. We know that

$$P_x = \frac{1+a-b}{a^2+(1-b)^2}, \quad T_{0,x} = \frac{2+a+\sqrt{a^2+4b}}{2(a+1-b)},$$

and since the denominators are positive, $P_x < T_{0,x}$ is equivalent to

$$2(a+(1-b))^2 < (a^2+(1-b)^2)(2+a+\sqrt{a^2+4b}). \quad (4.2)$$

For $a+b > 1$ and $b < 1$ we have

$$a > 1-b \Rightarrow a^2 > 1-2b+b^2,$$

and therefore

$$2+a+\sqrt{a^2+4b} > 2+a+\sqrt{1+2b+b^2} = 3+a+b > 4. \quad (4.3)$$

Furthermore, (4.1) applied on a and $1-b$ gives

$$a^2+(1-b)^2 > \frac{1}{2}(a+(1-b))^2. \quad (4.4)$$

By multiplying (4.3) and (4.4) we obtain the desired inequality (4.2). ■

Now consider the case when W_X^u intersects the coordinate axes at points other than T_0 and T_0^{-1} . Specially, in that case we know there exists a point B on the negative y -axis or the positive x -axis such that the only intersections $[T_0, B]^{(u)}$ with the coordinate axes are T_0 and B - in other words, B is the first intersection of W_X^{u+} with the coordinate axes after T_0 . Let \mathcal{B} denote the polygon in the fourth quadrant with border $\partial\mathcal{B} = [T_0, B]^{(u)} \cup \overline{BO} \cup \overline{OT_0}$ (if B lies on the negative y -axis), or $\partial\mathcal{B} = [T_0, B]^{(u)} \cup \overline{BT_0}$ (if B lies on the positive x -axis), where O denotes the origin.

Lemma 4.1.3. Assume that W_X^u intersects the coordinate axes at points other than T_0 and T_0^{-1} and let B and \mathcal{B} be defined as above. Then $P \in \mathcal{B}$.

Proof. Suppose by contradiction that the converse holds. Since $[T_0, B]^{(u)}$ is closed, there exists a point B_1 lying on it such that

$$\text{dist}(P, B_1) = \min\{\text{dist}(P, A) : A \in [T_0, B]^{(u)}\}.$$

Notice that, by construction, W_X^u intersects $\overline{PB_1}$ at B_1 only. Since $B_1 \in [T_0, B]^{(u)}$, there exists $n \in \mathbb{N}$ such that $L^{-(2n)}(B_1)$ lies on $\overline{T_0 T_0^{-2}}$, i.e. in the first quadrant (specially, if $B_1 = T_0^{2k}$ for some $k \in \mathbb{N}_0$, we observe $L^{-2(k+1)}(B_1) = T_0^{-2}$). On the other hand, $\overline{PB_1}, L^{-2}(\overline{PB_1}) = \overline{PL^{-2}(B_1)}, \dots, L^{-2(n-1)}(\overline{PB_1}) = \overline{PL^{-2(n-1)}(B_1)}$ are all straight line segments in the fourth quadrant since L^{-2} acts on them as an affine map - that is why $L^{-2n}(\overline{PB_1}) = \overline{PL^{-2n}(B_1)}$ is also a straight line segment. However, due to Lemma 4.1.2, it intersects $[T_0, B]^{(u)}$, which is a contradiction (the only intersection of $\overline{PL^{-2n}(B_1)}$ with W_X^u is $L^{-2n}(B_1)$). ■

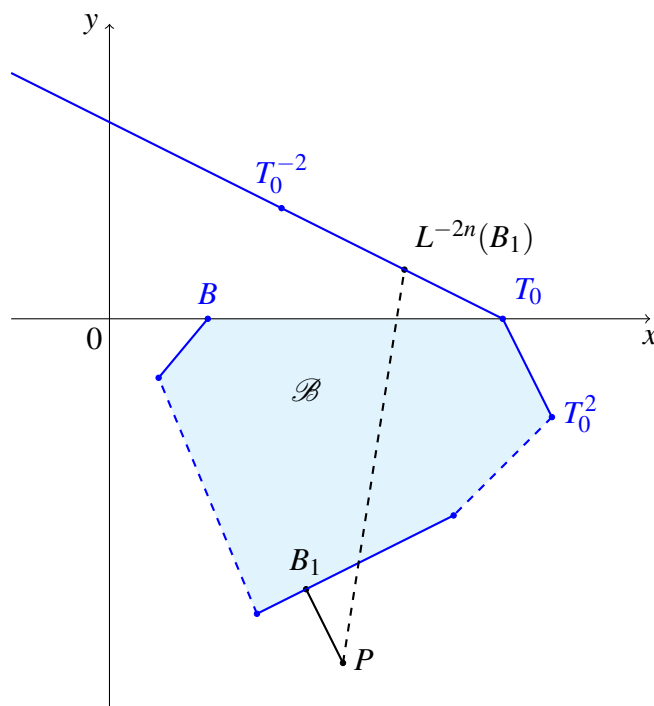


Figure 4.1: Lemma 4.1.3: P lying outside of \mathcal{B} would imply that the line segment $\overline{PL^{-2n}(B_1)}$ intersects the polygonal line $[T_0, B]^{(u)}$.

4.2. RELATIONSHIP BETWEEN W_Y^s AND W_X^s

In this section we observe in greater detail the structure of the stable manifold W_Y^s of the fixed point Y . In order to do that, we prove that W_Y^s intersects the positive x -axis at one point only and as a consequence, we fully describe that manifold in the first quadrant. Recall that from Corollary 2.1.6 it follows that W_X^s accumulates on W_Y^s . As we will see at the end of this section, W_Y^s also accumulates on W_X^s in the first quadrant.

Lemma 4.2.1. If there are no homoclinic points for X , then W_X^u and W_Y^s do not intersect.

Proof. Suppose by contradiction that W_X^u and W_Y^s have a non-empty intersection. Due to accumulation of W_X^s on W_Y^s (Corollary 2.1.6), this would imply that W_X^u also intersects W_X^s , which is a contradiction. ■

The stable manifold W_Y^s is an invariant polygonal line emanating from Y in the third quadrant and intersecting the negative y -axis for the first time at the point

$$R_0 = \left(0, \frac{a + 2b + \sqrt{a^2 + 4b}}{2(1 - a - b)} \right) = \left(0, -\frac{2b}{a + 2b - \sqrt{a^2 + 4b}} \right).$$

Moreover, we have $W_Y^s = \bigcup_{n=0}^{\infty} L^{-n}(\overline{YR_0})$ (see figure 4.2). As usual, we put $R_0^k = L^k(R_0)$ for all $k \in \mathbb{Z} \setminus \{0\}$ and specially, $R_0^0 = R_0$. Let W_Y^{s+} be the half of W_Y^s starting at Y and going down passing through R_0 ; also, let W_Y^{s-} be the other half starting at Y and going up through R_0^1 . Furthermore, for points $A_1, A_2 \in W_Y^s$, we denote by $[A_1, A_2]_Y^{(s)}$ the polygonal line contained in W_Y^s with A_1 and A_2 as endpoints.

Lemma 4.2.2. $R_{0,y} < P_y$, i.e. R_0 lies below P .

Proof. The following chain of equivalences holds

$$\begin{aligned} R_{0,y} < P_y &\Leftrightarrow -\frac{2b}{a + 2b - \sqrt{a^2 + 4b}} < \frac{b(1 - a - b)}{a^2 + (1 - b)^2} \\ &\Leftrightarrow \frac{2}{a + 2b - \sqrt{a^2 + 4b}} > \frac{a + b - 1}{a^2 + (1 - b)^2} \\ &\Leftrightarrow 2(a^2 + (1 - b)^2) > (a + b - 1)(a + 2b - \sqrt{a^2 + 4b}), \end{aligned} \tag{4.5}$$

since $a + 2b - \sqrt{a^2 + 4b} > 0$ due to

$$a + 2b > \sqrt{a^2 + 4b} \Leftrightarrow a^2 + 4ab + 4b^2 > a^2 + 4b \Leftrightarrow a + b > 1.$$

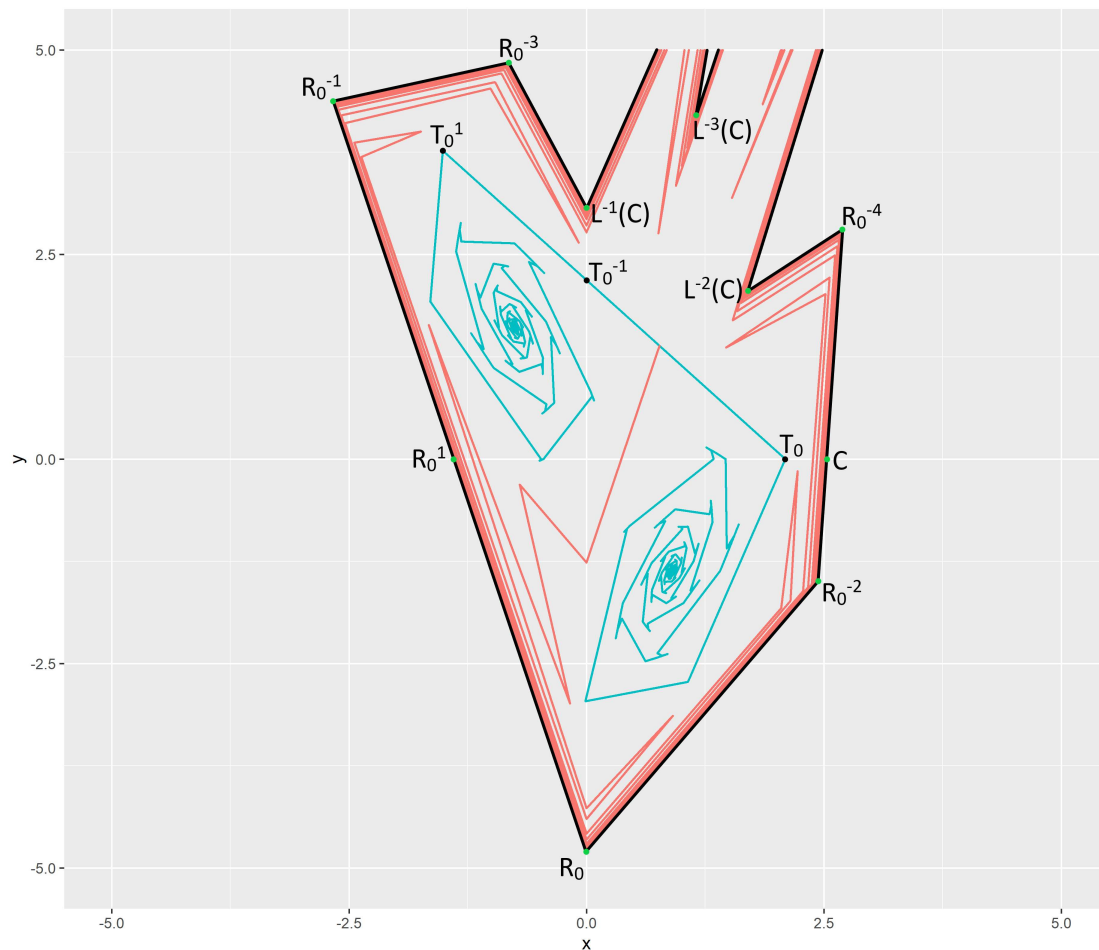


Figure 4.2: Unstable (blue) and stable (red) manifold of X together with the stable manifold of Y (black) for parameter values $a = 1.2, b = 0.9$. Notice that W_X^s accumulates on W_Y^s (Corollary 2.1.6). All breaking points of W_Y^s are iterates of points R_0 and C (intersection of W_Y^s with the positive x -axis, Proposition 4.2.3).

Due to $a > 1 - b$, we have

$$\sqrt{a^2 + 4b} > \sqrt{1 - 2b + b^2 + 4b} = 1 + b,$$

which is equivalent to

$$a + b - 1 > a + 2b - \sqrt{a^2 + 4b}. \quad (4.6)$$

Furthermore, by applying (4.1) on a and $1 - b$ we obtain

$$2(a^2 + (1 - b)^2) > (a + 1 - b)^2 > (a + b - 1)^2, \quad (4.7)$$

while the last inequality holds since both $a + 1 - b > 0$, $a + b - 1 > 0$ and $b < 1$. Finally,

$$2(a^2 + (1 - b)^2) \stackrel{(4.7)}{>} (a + b - 1)^2 \stackrel{(4.6)}{>} (a + b - 1)(a + 2b - \sqrt{a^2 + 4b}),$$

which proves the last inequality of (4.5). ■

Now observe the backward iterates of R_0 . Since R_0 lies on the negative y -axis, R_0^{-1} will lie on its preimage, $y = a|x| - 1$, in the second quadrant so R_0^{-2} lies in the fourth or first quadrant below the line $y = ax - 1$. In general, for $k \in \mathbb{N}$, if R_0^{-2k} lies in the fourth quadrant, R_0^{-2k-1} will lie in the second or third quadrant, and if R_0^{-2k+1} lies in the fourth quadrant below the line $x = 1 - \frac{a}{b}y$, R_0^{-2k} will lie in the fourth quadrant (see Figure 4.2). Therefore, one can think that for all $k \in \mathbb{N}$, all R_0^{-2k} would lie in the fourth and all R_0^{-2k+1} in the second quadrant, or that R_0^{-k} would lie in the third quadrant for some $k \geq -2$. However, the following proposition shows neither of that can happen.

Proposition 4.2.3. W_Y^s intersects the positive x -axis at a point right to T_0 .

Proof. 1° *Existence of the intersection point*

We will prove first that W_Y^s intersects the positive x -axis. Suppose by contradiction that the converse holds. We distinguish between two different cases of interest with respect to the intersection points of W_X^u with the coordinate axes - recall that there are always at least two such points, T_0 and T_0^{-1} .

A) *First case: W_X^u intersects the coordinate axes at points other than T_0 and T_0^{-1}*

Let B and \mathcal{B} be as in Lemma 4.1.3. Since W_X^u and W_Y^s do not intersect (Lemma 4.2.1), $\overline{R_0 R_0^{-2}}$ is contained in the fourth quadrant outside \mathcal{B} and the line segment $\overline{PR_0}$ thus intersects $[T_0, B]^{(u)}$ at a point A (see figure 4.3). Because $A \in [T_0, B]^{(u)}$, there exists a

positive integer n such that $L^{-2}(A), \dots, L^{-2(n-1)}(A)$ all lie in the fourth quadrant and $L^{-2n}(A)$ lies on $\overline{T_0 T_0^{-2}(u)}$ in the first quadrant. Notice that $\overline{PR_0^{-2}}, L^{-2}(\overline{PR_0^{-2}}) = \overline{PR_0^{-4}}, \dots, L^{-2(n-1)}(\overline{PR_0^{-2}}) = \overline{PR_0^{-2n}}$ are all straight line segments contained in the fourth quadrant so L^{-2} acts on them as an affine map - as a consequence, $L^{-2n}(\overline{PR_0^{-2}})$ is also a straight line segment which contains a point in the first quadrant. Therefore, $R_0^{-2(n+1)}$ is also contained in the first quadrant which implies that $[R_0^{-2}, R_0^{-2(n+1)}]_Y^{(s)}$ intersects the positive x -axis. This is a contradiction with our initial assumption.

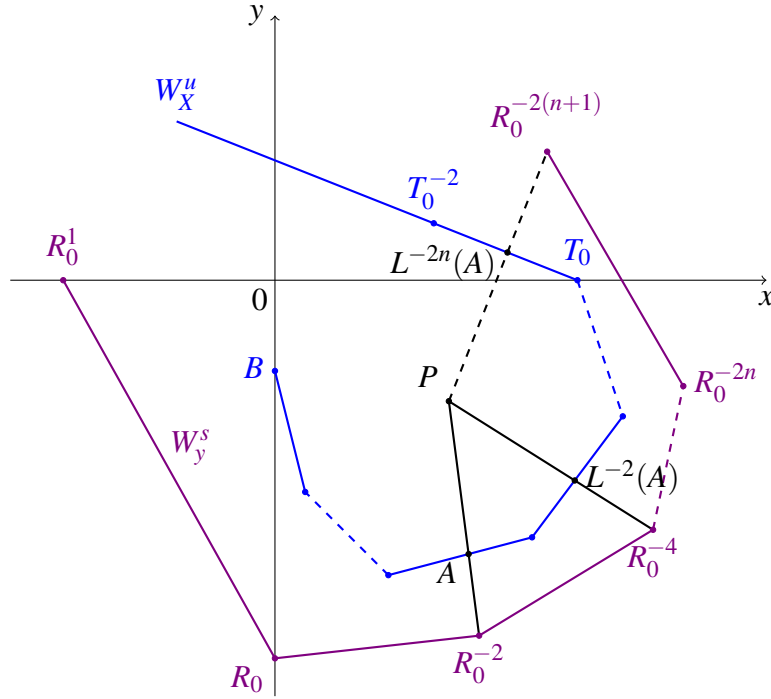


Figure 4.3: Proposition 4.2.3, case 1.1°.

B) *Second case: W_X^u intersects the coordinate axes at T_0 and T_0^{-1} only*

B1) *Claim: W_Y^s intersects the negative y-axis at R_0 only*

First we prove that W_Y^s does not intersect the third quadrant apart from the line segment $\overline{R_0 R_0^1}$. Suppose by contradiction that the converse holds. Then W_Y^{s-} intersects the negative x -axis and W_Y^{s+} the negative y -axis, i.e. there exists $j \in \mathbb{N}$ such that $R_0^{-2(j-1)}$ lies in the fourth and R_0^{-2j} in the third quadrant (see figure 4.4). Observe the smallest such j and the preimages of R_0^{-2j} under L . We claim that R_0^{-2j} lies above the straight line $R_0 R_0^1$. Otherwise, $[R_0^{-2(j-1)}, R_0^{-2j}]_Y^{(s)}$ would intersect the negative y -axis below R_0 which would imply that its image under L , $[R_0^{-(2j-3)}, R_0^{-(2j-1)}]_Y^{(s)}$, intersects the negative x -axis to the

left of R_0^1 . This is a contradiction since that polygonal segment, by the construction of j , lies in the preimage of the fourth quadrant, i.e. in the second or third quadrant above the line $y = -ax - 1$.

Therefore, if $R_0^{-2j}, R_0^{-(2j+1)}, \dots, R_0^{-(2j+n)}$ are all contained in the third quadrant for some $n \in \mathbb{N}$, L^{-1} acts on those points as an affine map and for every $i = 0, \dots, n$ we thus have

$$\text{dist}(R_0^{-(2j+i)}, W_Y^u) = \left(\frac{1}{|\lambda_Y^s|} \right)^i \text{dist}(R_0^{-2j}, W_Y^u),$$

where $|\lambda_Y^s| < 1$ is the eigenvalue of the differential of L at Y . It follows that distances of $R_0^{-(2j+i)}$ from W_Y^u in the third quadrant are unboundedly increasing so there exists $k \in \mathbb{N}$ such that R_0^{-2k} lies again in the fourth and $R_0^{-2(k-1)}$ in the third quadrant. Denote by Q the point of intersection of $[R_0^{-2(k-1)}, R_0^{-2k}]_Y^{(s)}$ and the negative y -axis - notice that $[R_0^{-(2k-1)}, R_0^{-(2k-2)}]_Y^{(s)}$ then intersects the negative x -axis at $L(Q)$ and $[R_0^{-2(k-2)}, R_0^{-2(k-1)}]_Y^{(s)}$ intersects the image of the negative x -axis, $x = 1 + \frac{a}{b}y$, at $L^2(Q)$ (so Q will lie below the image of the negative x -axis).

Now denote by \mathcal{J} the polygon with border $\partial \mathcal{J} = \overline{R_0 Q} \cup [R_0, Q]_Y^{(s)}$. We know that $\overline{QR_0^{-2k}}$ is contained in \mathcal{J} . In order for W_Y^{s+} to escape \mathcal{J} , $[R_0^{-2l}, R_0^{-2(l+1)}]_Y^{(s)}$ has to intersect the straight line segment $\overline{QR_0}$ for some $l \geq k$, but that would imply that its second preimage $[R_0^{-2(l-2)}, R_0^{-2(l-1)}]_Y^{(s)}$, a polygonal line contained in \mathcal{J} , intersects $\overline{R_0^2 L^2(Q)}$ which is contained outside \mathcal{J} . We conclude that $W_Y^{s+} \setminus [Y, R_0^{-2k}]_Y^{(s)}$ is contained in \mathcal{J} . Moreover, since Q lies below the image of the negative y -axis, $L^{-1}(\overline{QR_0}) = \overline{L^{-1}(Q)R_0^{-1}}$ is a straight line segment contained in the second quadrant below the image of the positive x -axis (due to the original assumption that W_Y^s does not intersect the positive x -axis). Therefore, $L^{-2}(\overline{QR_0}) = \overline{L^{-2}(Q)R_0^{-2}}$ is again a straight line segment contained in \mathcal{J} from which it follows that \mathcal{J} is L^{-2} -invariant.

Since that polygon is homeomorphic to the closed unit disc, Brouwer fixed point theorem (BFPT) implies that it contains a fixed point for L^{-2} . Since that fixed point can not be Y (W_Y^s would otherwise contain self-intersections) and the other two fixed points for L^{-2} lie in the upper half-plane, polygon \mathcal{J} contains P . However, since in this case W_X^u converges to P (Theorem 3.3.1), this would imply that W_X^u and W_Y^s intersect in the fourth quadrant, which is a contradiction with Lemma 4.2.1.

B2) Claim: W_Y^s eventually escapes the second and fourth quadrant

Since $[R_0, C]_Y^{(s)}$ is a closed set, there exists a point C_1 lying on it such that

$$\text{dist}(P, C_1) = \min\{\text{dist}(P, A) : A \in [R_0, C]_Y^{(s)}\}.$$

We claim that in this case $W_Y^{s+} \cap \overline{PC_1} = \{C_1\}$ (see Figure 4.5). Since W_Y^{s+} intersects the positive x -axis at C , there exists $j \in \mathbb{N}$ such that R_0^{-2j} lies in the first and $R_0^{-2}, \dots, R_0^{-2(j-1)}$ in the fourth quadrant (moreover, C is the intersection of $[R_0^{-2(j-1)}, R_0^{-2j}]_Y^{(s)} = \overline{R_0^{-2(j-1)} R_0^{-2j}}$ with the positive x -axis). Now observe further preimages of R_0 under L . If $R_0^{-2j}, R_0^{-(2j+1)}, \dots, R_0^{-(2j+n)}$ are all contained in the first quadrant for some $n \in \mathbb{N}$, L^{-1} acts on those points as an affine map and therefore for every $i = 0, \dots, n$,

$$\text{dist}(R_0^{-(2j+i)}, \overline{XV_0^1}^{(s)}) = \left(\frac{1}{|\lambda_X^u|} \right)^i \text{dist}(R_0^{-2j}, \overline{XV_0^1}^{(s)}),$$

$$\text{dist}(R_0^{-(2j+i)}, \overline{T_0T_0^{-1}}^{(u)}) = \left(\frac{1}{|\lambda_X^s|} \right)^i \text{dist}(R_0^{-2j}, \overline{T_0T_0^{-1}}^{(u)}),$$

where $|\lambda_X^u| > 1$ and $|\lambda_X^s| < 1$ are the eigenvalues of the differential of L at X . In other words, distances of $R_0^{-(2j+i)}$ from $\overline{XV_0^1}$ in the first quadrant are tending to zero and those from W_X^u are unboundedly increasing so there exists $k \in \mathbb{N}$, $k > 2j$, such that R_0^{-k} lies in the fourth and $R_0^{-(k-1)}$ in the first quadrant.

If the smallest such k is odd, then $[R_0^{-(k-2)}, R_0^{-k}]_Y^{(s)}$ intersects the positive x -axis at a point to the right of V_0^1 (since W_Y^s and W_X^s do not intersect) and since that part of the positive x -axis is a subset of the image of the negative y -axis, $[R_0^{-(k-1)}, R_0^{-(k+1)}]_Y^{(s)}$ intersects both the positive x -axis and the negative y -axis so $R_0^{-(k+1)} \in W_Y^{s+}$ lies in the third quadrant. Notice that the intersection of $[R_0^{-(k-1)}, R_0^{-(k+1)}]_Y^{(s)}$ lies to the left of C due to the fact that the distances of consecutive preimages of points in the first quadrant from $\overline{XV_0^1}^{(u)}$ are unboundedly decreasing. Now, by using analogous arguments as in the case 1.2.1°, we see that there exists a point Q on the negative y -axis such that $\overline{R_0Q} \cap W_Y^s = \{R_0, Q\}$ and that $W_Y^{s+} \setminus [Y, Q]_Y^{(s)}$ is contained in the polygon bounded by $\overline{R_0Q} \cup [R_0, Q]_Y^{(s)}$. Since P lies outside of that polygon, W_Y^{s+} does not intersect $\overline{PC_1}$ at points other C_1 .

If k is even, then $[R_0^{-(k-2)}, R_0^{-k}]_Y^{(s)}$ intersects the positive x -axis at a point to the right of V_0^1 and $R_0^{-k} \in W_Y^{s+}$ lies in the fourth quadrant. Notice that the intersection of $[R_0^{-(k-2)}, R_0^{-k}]_Y^{(s)}$ with the positive x -axis lies again to the left of C . Therefore, if $W_Y^{s+} \setminus [Y, R_0^{-k}]_Y^{(s)}$ is fully contained in the fourth quadrant, then it is contained in the polygon bounded by $\overline{R_0O} \cup \overline{OC} \cup [R_0, C]_Y^{(s)}$. Since $[R_0, C]_Y^{(s)}$ so W_Y^{s+} does not intersect $\overline{PC_1}$ at

points other than C_1 . On the other hand, if $W_Y^{s+} \setminus [Y, R_0^{-k}]_Y^{(s)}$ intersects the negative y-axis, then we obtain the same conclusion by applying arguments from the previous case.

Therefore, it follows that $W_Y^{s+} \cap \overline{PC_1} = \{C_1\}$. On the other hand, there exists $n \in \mathbb{N}$ such that $L^{2n}(C_1)$ lies on the line segment $\overline{R_0 R_0^2}$. In that case, $\overline{PC_1}, L^2(\overline{PC_1}) = \overline{PL^2(C_1)}, \dots, L^{2(n-1)}(\overline{PC_1}) = \overline{PL^{2(n-1)}(C_1)}$ are all straight line segments in the fourth quadrant since L^2 acts on them as an affine map - that is why $L^{2n}(\overline{PC_1}) = \overline{PL^{2n}(C_1)}$ is also a straight line segment. Lemma 4.2.2 now implies that this line segment intersects $[R_0, C]_Y^{(s)}$, which is a contradiction (its only intersection with W_Y^{s+} is $L^{2n}(C_1)$). ■

Now observe the point from the previous proposition - we denote it by C . There exists $n_0 \in \mathbb{N}$ such that C lies on $[R_0^{-(n_0-2)}, R_0^{-n_0}]_Y^{(s)} = \overline{R_0^{-(n_0-2)} R_0^{-n_0}}$ (moreover, n_0 is even) and $\overline{CR_0^{-n_0}}$ is contained in the first quadrant. As a consequence, $L^{-1}(C)$ lies on the positive y-axis and $L^{-1}(\overline{CR_0^{-n_0}}) = \overline{L^{-1}(C)R_0^{-(n_0+1)}}$ is a straight line segment lying in the preimage of the first quadrant above the line segment $\overline{T_0 T_0^{-1}}^{(u)}$ - therefore, it is again fully contained in the first quadrant. Inductively, we see that the same holds for all further preimages of that line segment and since L^{-1} acts as an affine map in the upper half-plane, $L^{-n}(\overline{CR_0^{-n_0}}) = \overline{L^{-n}(C)R_0^{-(n_0+n)}}$ is a straight line segment for every $n \in \mathbb{N}$.

Recall that W_X^{s+} denotes the half of W_X^s which is a half-line in the first quadrant starting at X and going to infinity. Note that W_X^{s+} does not intersect W_Y^s . We will first prove a result analogous to those in Lemmas 2.1.1(3) and 2.1.2(4) from which, due to linearity of L^{-1} in the first quadrant, it will follow that W_Y^s approaches W_X^{s+} .

Lemma 4.2.4 (Convergence of slope coefficients - upper half-plane).

1. Let α be a line segment in the upper half-plane which lies on a straight line whose slope coefficient equals k_1 . Then the image of α under L^{-1} lies on a straight line whose slope coefficient equals

$$k_2 = b \cdot \frac{1}{k_1} + a.$$

2. The sequence $(k_n)_{n \in \mathbb{N}_0}$ given by the recurrence

$$k_{n+1} = b \cdot \frac{1}{k_n} + a, \quad n \geq 0, \tag{4.8}$$

with $k_0 \neq \frac{1}{2}(a - \sqrt{a^2 + 4b})$, converges and

$$\lim_{n \rightarrow \infty} k_n = \frac{1}{2}(a + \sqrt{a^2 + 4b}).$$

Proof. If (x_1, y_1) and (x_2, y_2) are two points lying on α , then, due to $y_1 > 0$ and $y_2 > 0$, we have

$$L^{-1}(x_1, y_1) = \left(\frac{1}{b}y_1, x_1 - 1 + \frac{a}{b}y_1 \right), \quad L^{-1}(x_2, y_2) = \left(\frac{1}{b}y_2, x_2 - 1 + \frac{a}{b}y_2 \right),$$

and consequently,

$$k_2 = \frac{x_2 - 1 + \frac{a}{b}y_2 - x_1 + 1 - \frac{a}{b}y_1}{\frac{1}{b}(y_2 - y_1)} = b \cdot \frac{x_2 - x_1}{y_2 - y_1} + \frac{\frac{a}{b}(y_2 - y_1)}{\frac{1}{b}(y_2 - y_1)} = b \cdot \frac{1}{k_1} + a,$$

which proves the first claim.

For the second one, as in Lemma 2.1.2, we put

$$j_n := \frac{k_n - M_1}{k_n - M_2},$$

where

$$M_1 := \frac{1}{2}(a + \sqrt{a^2 + 4b}), \quad M_2 := \frac{1}{2}(a - \sqrt{a^2 + 4b})$$

are the roots of the equation $M^2 - aM - b = 0$, i.e. fixed points of the function

$$f: \mathbb{R} \setminus \{0\} \rightarrow \mathbb{R}, \quad f(x) = b \cdot \frac{1}{x} + a,$$

which defines recurrence (4.8). Since $k_0 \neq M_2$, j_n is well-defined for all $n \in \mathbb{N}_0$. Now we have

$$j_{n+1} \stackrel{(4.8)}{=} \frac{b \cdot \frac{1}{k_n} + a - M_1}{b \cdot \frac{1}{k_n} + a - M_2} = \frac{b \cdot \frac{1}{k_n} - b \cdot \frac{1}{M_1}}{b \cdot \frac{1}{k_n} - b \cdot \frac{1}{M_2}} = \frac{M_2}{M_1} \cdot j_n$$

for all $n \in \mathbb{N}_0$. Since $a, b > 0$, we see that $M_1 > 0$, $M_2 < 0$ and $|M_2| < |M_1|$ so for $\mu := \frac{M_2}{M_1}$ we have $-1 < \mu < 0$. Consequently, $\lim_{n \rightarrow \infty} |j_n| = \lim_{n \rightarrow \infty} |\mu|^n |j_0| = 0$, so

$$\lim_{n \rightarrow \infty} k_n = \lim_{n \rightarrow \infty} \frac{M_1 - M_2 j_n}{1 - j_n} = M_1,$$

which proves the second claim. ■

As expected, the limit of the sequence (k_n) from the previous lemma corresponds to the slope coefficient of W_X^{s+} . Hence, if all preimages of a straight line segment lie in the first quadrant and its slope is not parallel to the unstable direction at X , the slopes of its preimages will converge to the stable direction at X .

Lemma 4.2.5. Intersections of preimages of the positive y -axis with the first quadrant converge to $W_X^{s+} \cup \overline{XV_0^1}^{(s)}$.

Proof. Since T_0^{-1} lies on the positive y -axis, $T_0^{-(n+1)}$ lies on the intersection of the n -th preimage of the positive y -axis with the first quadrant. Now the claim follows from the fact that $\lim_{n \rightarrow \infty} T_0^{-n} = X$ and Lemma 4.2.4(2). ■

Corollary 4.2.6. Preimages of $\overline{CR_0^{-n_0}}$ converge to W_X^{s+} .

Proof. Since $L^{-1}(C)$ lies on the positive y -axis, its further preimages lie on the preimages of that axis in the first quadrant. The proof now follows by applying Lemmas 4.2.4(2) and 4.2.5. ■

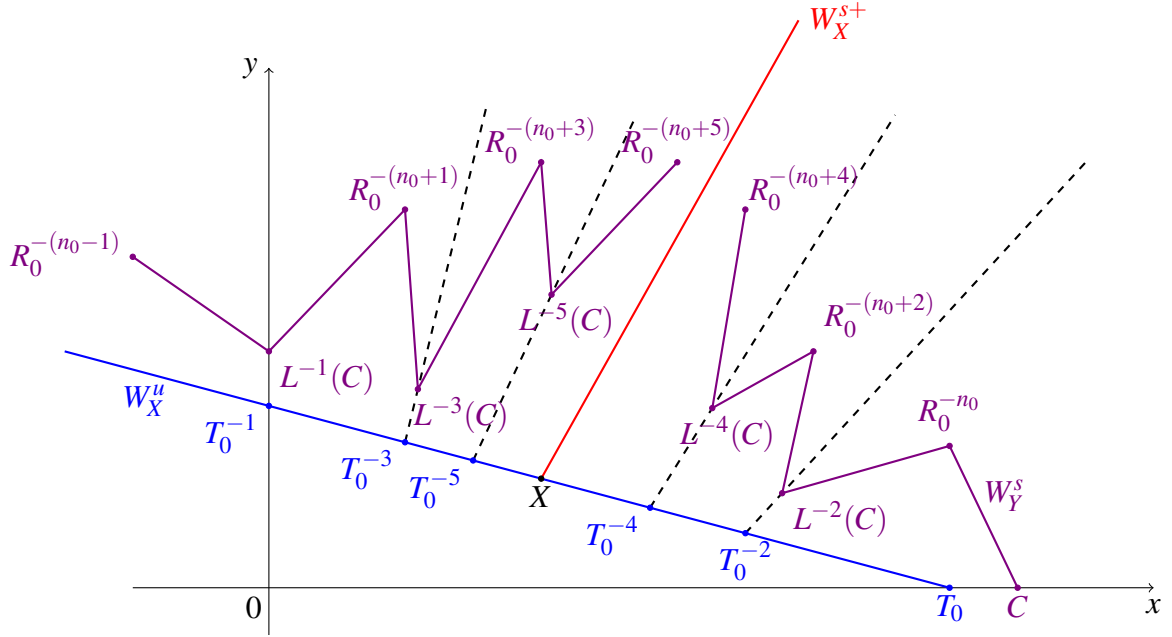


Figure 4.6: Corollary 4.2.6: for every $n \in \mathbb{N}$, $T_0^{-(n+1)}$ and $L^{-(n+1)}(C)$ lie on the n -th preimage of the positive y -axis (dashed lines) which converge to W_X^{s+} above the line segment $\overline{T_0 T_0^{-1}}^{(u)}$ (blue) due to Lemma 4.2.5. As a consequence, preimages of $\overline{CR_0^{-n_0}}$ also converge to W_X^{s+} .

Due to the convergence to W_X^{s+} , we see that points on W_Y^s tend to infinity in the first quadrant because L^{-1} stretches all vectors parallel to the stable direction at X by the factor $\frac{1}{|\lambda_X^s|} > 1$ when it acts as an affine map. Hence, $W_X^{s+} \cup \overline{XV_0^1}^{(s)}$ divides the first

quadrant into two connected components and W_Y^s separates each one of them. Since the intersection of W_Y^s with the union of the second, third and fourth quadrant is the polygonal line $[C, L^{-1}(C)]_Y^{(s)}$ which separates each one of them, we obtain the following result.

Corollary 4.2.7. W_Y^s separates the plane.

4.3. APPROACHING INFINITY

Corollary 4.2.7 implies that $\mathbb{R}^2 \setminus W_Y^s$ consists of two connected components - we will denote by \mathcal{A}_1 the one containing the fixed point X and by \mathcal{A}_2 the other one. Notice that \mathcal{A}_1 also contains W_X^u (Lemma 4.2.1) and W_X^s .

Lemma 4.3.1. Periodic orbit $\{P, P'\}$ is contained in \mathcal{A}_1 .

Proof. If W_X^u intersects the coordinate axes at points other than T_0 and T_0^{-1} , this is a direct consequence of Lemma 4.1.3. If W_X^u intersects the coordinate axes at T_0 and T_0^{-1} only, we obtain the result as a consequence of the fact that points on W_X^u accumulate on that periodic orbit (Theorem 3.3.1). ■

Our goal in this section is to prove that \mathcal{A}_1 contains all the "interesting dynamics" for the Lozi map.

Lemma 4.3.2. \mathcal{A}_1 and \mathcal{A}_2 are L -invariant.

Proof. We will prove first that \mathcal{A}_1 is invariant. We do that by dividing \mathcal{A}_1 into several regions \mathcal{R}_i such that L acts as an affine map on each one of them (see Figure 4.7):

1. Let \mathcal{R}_1 be the intersection of \mathcal{A}_1 with the part of the first quadrant above the line $\overline{T_0 T_0^{-1}(u)}$. Then $\mathcal{R}_1 \setminus W_X^{s+}$ can be partitioned into a union of polygons Δ_n , $n \in \mathbb{N}_0$, such that

$$\partial\Delta_n = \overline{T_0^{-n} T_0^{-(n+2)}(u)} \cup \overline{T_0^{-(n+2)} L^{-(n+2)}(C)} \cup \overline{T_0^{-n} L^{-n}(C)} \cup [L^{-n}(C), L^{-(n+2)}(C)]_Y^{(s)}.$$

Note that the border of each Δ_n consists of parts of W_X^u , W_Y^s and preimages of the positive y -axis (specially, $\partial\Delta_0$ also contains a part of the positive x -axis, $\overline{T_0 C}$, and $\partial\Delta_1$ that of the positive y -axis, $\overline{T_0^{-1} L^{-1}(C)}$, see Figure 4.6).

Since $L(\partial\Delta_{n+1}) = \partial\Delta_n$ by construction and L acts on every Δ_n as an affine map, we have $L(\Delta_{n+1}) = \Delta_n$ for every $n \in \mathbb{N}_0$. Specially, $L(\Delta_0)$ is a polygon with border $\overline{L^{-1}(C) T_0^{-1} \cup T_0^{-1} T_0^1(u)} \cup \overline{T_0^1 L(C)}$ which is contained in \mathcal{A}_1 (W_Y^s intersects $\overline{T_0^1 L(C)}$ at $L(C)$ only). This, together with $L(W_X^{s+}) = W_X^{s+}$, proves that $L(\mathcal{R}_1) \subset \mathcal{A}_1$.

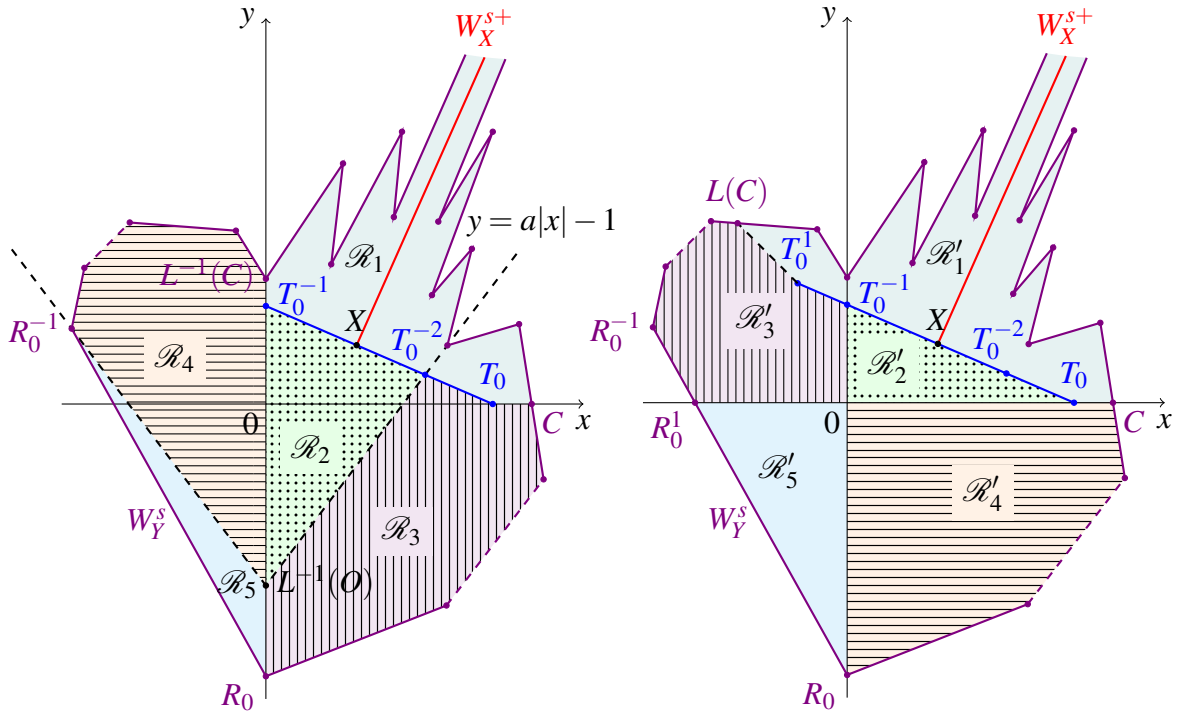


Figure 4.7: Regions \mathcal{R}_i and their images $\mathcal{R}'_i = L(\mathcal{R}_i)$ from Lemma 4.3.2.

2. Let \mathcal{R}_2 be the triangle $L^{-1}(O)T_0^{-1}T_0^{-2}$ in the first and fourth quadrant (where O is the origin). Then $L(\mathcal{R}_2)$ is the triangle $OT_0^{-1}T_0$ which is contained in \mathcal{A}_1 due to Proposition 4.2.3.

3. Let \mathcal{R}_3 be the polygon in the first and fourth quadrant with border

$$\partial\mathcal{R}_3 = \overline{R_0L^{-1}(O)} \cup \overline{L^{-1}(O)T_0^{-2}} \cup \overline{T_0^{-2}T_0^{(u)}} \cup \overline{T_0C} \cup [C, R_0]_Y^s.$$

Then \mathcal{R}_3 is mapped to the polygon in the second quadrant with border

$$\partial L(\mathcal{R}_3) = \overline{R_0^1O} \cup \overline{OT_0^{-1}} \cup \overline{T_0^{-1}T_0^{(u)}} \cup \overline{T_0^1L(C)} \cup [L(C), R_0^1]_Y^s.$$

Since $W_Y^s \cup \overline{T_0^1L(C)} = \{L(C)\}$, $L(\mathcal{R}_3)$ is contained in \mathcal{A}_1 .

4. We denote by \mathcal{R}_4 the polygon in the second and third quadrant with border

$$\partial\mathcal{R}_4 = \overline{L^{-1}(C)L^{-1}(O)} \cup \overline{L^{-1}(O)R_0^{-1}} \cup [R_0^{-1}, L^{-1}(C)]_Y^s.$$

In this case \mathcal{R}_4 maps to the polygon with border $\overline{R_0O} \cup \overline{OC} \cup [C, R_0]_Y^s$ which is the intersection of \mathcal{A}_1 with the fourth quadrant.

5. Finally, by \mathcal{R}_5 we will denote the triangle in the second and third quadrant with vertices $L^{-1}(O)$, R_0 and R_0^{-1} . Its image $L(\mathcal{R}_5)$ is the triangle with vertices O , R_0^1 and R_0 , i.e. the intersection of \mathcal{A}_1 with the third quadrant.

For every $i = 1, 2, \dots, 5$, let $\mathcal{R}'_i = L(\mathcal{R}_i)$. Notice that the sets \mathcal{R}'_i also form a partition of \mathcal{A}_1 (see Figure 4.7), hence $L(\mathcal{A}_1) = \mathcal{A}_1$. Moreover, since L is bijective, we also have $L^{-1}(\mathcal{A}) = L^{-1}(L(\mathcal{A}_1)) = \mathcal{A}_1$, i.e. \mathcal{A}_1 is L^{-1} -invariant. Since W_Y^s is also L - and L^{-1} -invariant, the same holds for the complement of the union of these two sets, $\mathbb{R}^2 \setminus (\mathcal{A}_1 \cup W_Y^s) = \mathcal{A}_2$. Therefore, \mathcal{A}_2 is also L -invariant, which finishes the proof. ■

Theorem 4.3.3. All points in \mathcal{A}_2 diverge (tend to infinity) under forward iterations of L .

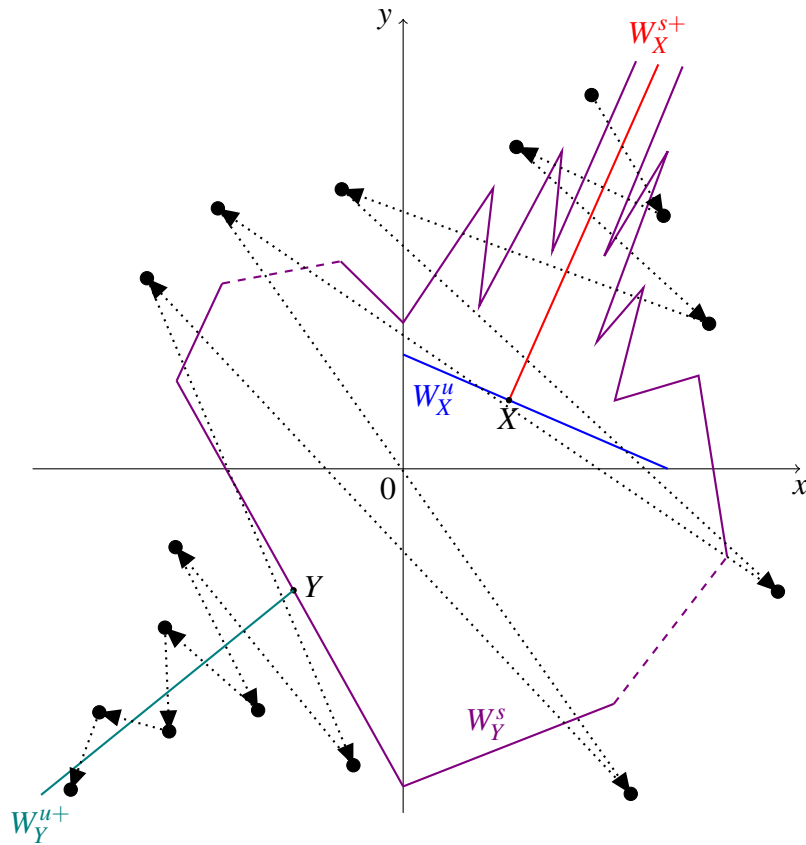


Figure 4.8: Dynamics of points in \mathcal{A}_2 (Theorem 4.3.3).

Proof. We will show that all points in \mathcal{A}_2 eventually end in the third quadrant under forward iterations of L from which they tend to infinity. Let Q be an arbitrary point of \mathcal{A}_2 .

Assume that Q is in the first quadrant and let $d_1 := \text{dist}(Q, W_X^{s+})$. For every $k \in \mathbb{N}$, if $L(Q), L^2(Q), \dots, L^k(Q)$ are all contained in the first quadrant, then

$$\text{dist}(L^i(Q), W_X^{s+}) = d_1 |\lambda_X^u|^i, \quad i = 1, 2, \dots, k.$$

Since $|\lambda_X^u| > 1$, distances of iterates of Q and W_X^{s+} are unboundedly increasing so there exists $k_0 \in \mathbb{N}_0$ such that $L^{k_0}(Q)$ lies in the second quadrant. In other words, all points in the intersection of \mathcal{A}_2 and the first quadrant eventually land in the second quadrant (their forward orbit can not be fully contained in the first quadrant).

Now assume that Q lies in the second quadrant. We know that the second quadrant maps to the union of the fourth and third quadrant. On the other hand, points in \mathcal{A}_2 lying in the fourth quadrant map to the second quadrant only (points in the fourth quadrant which map to the first quadrant all lie in \mathcal{A}_1 by Lemma 4.3.2). Therefore, it is possible that the entire forward orbit of Q is contained in the union of the second and fourth quadrant. However, in that case L^2 would act on Q as an affine map and since it has attracting fixed points P and P' in the fourth and second quadrant respectively, the forward orbit of Q would accumulate on those points. This is a contradiction with Lemma 4.3.1 and the invariance of \mathcal{A}_2 . Therefore, all points in \mathcal{A}_2 in the second quadrant also eventually end in the third quadrant.

If Q lies in the fourth quadrant, by previous discussions we see that it maps to the second quadrant so the previous argument also applies in this case.

Finally, if Q lies in the third quadrant, observe its forward iterations under L and their position relative to W_Y^s and W_Y^u . First note that the entire forward orbit of Q lies in the third quadrant (points from the third quadrant which map to the first one all lie in \mathcal{A}_1). Therefore, L acts on Q and all of its forward iterates as an affine map.

We know that the intersection of W_Y^u with \mathcal{A}_2 is a half-line, W_Y^{u+} , emanating from Y and going to infinity in the third quadrant. Hence, for all $k \in \mathbb{N}_0$,

$$\text{dist}(L^k(Q), W_Y^{u+}) = |\lambda_Y^s|^k \text{dist}(Q, W_Y^{u+}), \quad \text{dist}(L^k(Q), \overline{R_0 R_0^1}) = |\lambda_Y^u|^k \text{dist}(Q, \overline{R_0 R_0^1}).$$

Since $|\lambda_Y^s| < 1$ and $|\lambda_Y^u| > 1$, we see that distances of $L^k(Q)$ from W_Y^{u-} tend to zero and those from W_Y^s are unboundedly increasing. Therefore, $L^k(Q)$ tend to infinity in this case, which finishes the proof. ■

As a consequence, we see that the basin of attraction of the Lozi map is contained in \mathcal{A}_1 . In order to investigate this set in greater detail, we will first describe the structure of the unstable manifold W_Y^u of the fixed point Y .

As already mentioned in Corollary 2.1.6, the part of W_Y^u which is a part of a straight line passing through Y intersects the negative y -axis at a point which we denote by U_0^{-1} . The image of that point under L lies on the positive x -axis and is given by

$$U_0 = \left(\frac{2 - a + \sqrt{a^2 + 4b}}{2(1 - a - b)}, 0 \right) = \left(\frac{a + \sqrt{a^2 + 4b}}{a + 2b + \sqrt{a^2 + 4b}}, 0 \right).$$

Recall that W_Y^{u+} denotes the lower connected component of W_Y^u (which is a half-line emanating from Y and going down in the third quadrant) and W_Y^{u-} the other one. Under the given notation we see that

$$W_Y^{u-} = \bigcup_{n=0}^{\infty} L^n(\overline{YU_0}).$$

As usual, for every $n \in \mathbb{Z}$ we put $U_0^n = L^n(U_0)$ (and $U_0^0 = U_0$) and for points $A, B \in W_Y^u$ we define $[A, B]_Y^{(u)}$ and the other corresponding polygonal lines analogously as it was done for W_Y^s .

Moreover, from the proof of Corollary 2.1.6 it follows that $[Y, U_0]_Y^{(u)} = \overline{YU_0}$ and $[X, V_0]^{(s)} = \overline{XV_0}^{(s)}$ intersect at a unique point since both of these sets are straight line segments. This point lies in the fourth quadrant and will be denoted by D (see Figure 4.9).

Since the point D lies on the straight line segment $\overline{V_0V_0^1}^{(s)} \subset W_X^s$, we see that all forward images $L^n(D)$, $n \in \mathbb{N}$, lie in the first quadrant on $\overline{XV_0^1}^{(s)}$. On the other hand, D also lies on $\overline{U_0^{-1}U_0}$ so it follows that all forward images of $\overline{U_0^{-1}U_0}$ under L have a non-empty intersection with the first quadrant. In addition, if $L^n(\overline{U_0^{-1}U_0})$ is a straight line segment in the first quadrant for some $n \in \mathbb{N}$, then $L^{n+1}(\overline{U_0^{-1}U_0})$ is again a straight line segment which lies in the first and possibly in the second quadrant (in that case $L^{n+2}(\overline{U_0^{-1}U_0})$ has a breaking point on the positive x -axis). For every $k \in \mathbb{N}$, let k_n denote the slope coefficient of the part of $L^n(\overline{U_0^{-1}U_0})$ which is a straight line segment in the first quadrant and let k_0 be the slope coefficient of $\overline{U_0^{-1}U_0}$, $k_0 = \frac{1}{2}(-a + \sqrt{a^2 + 4b})$. Similarly as in Lemma 4.2.4, one can see that the sequence $(k_n)_{n \in \mathbb{N}_0}$ satisfies the recurrence

$$k_{n+1} = \frac{b}{k_n - a}, \quad n \in \mathbb{N}_0,$$

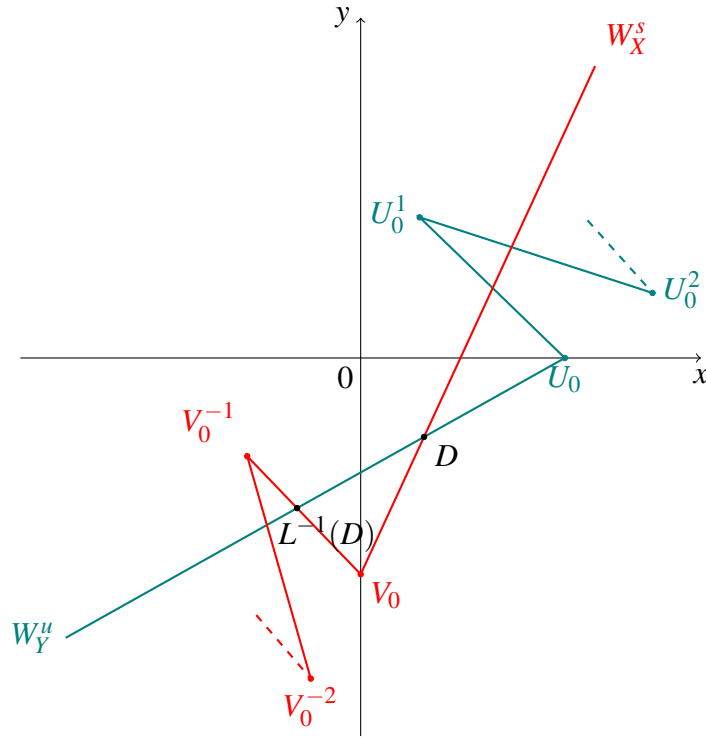


Figure 4.9: The unstable manifold of Y , W_Y^u , together with the stable manifold of X , W_X^s , and their point of intersection D in the fourth quadrant.

from which it follows that (k_n) converges and

$$\lim_{n \rightarrow \infty} k_n = \frac{1}{2} \left(a - \sqrt{a^2 + 4b} \right).$$

As one would expect, the limit is equal to the slope coefficient of the line segment $\overline{T_0^{-1}T_0}^{(u)}$. By taking into account that $\overline{U_0^{-1}U_0}$ contains the point D whose forward images under L converge to X , we see that parts of $L^n(\overline{U_0^{-1}U_0})$ in the first quadrant converge to $\overline{T_0^{-1}T_0}^{(u)}$ and we thus obtain the following result analogous to Corollary 2.1.6.

Corollary 4.3.4. W_Y^u accumulates on W_X^u .

Let \mathcal{B} be the triangle with vertices V_0 , D and $L^{-1}(D)$ (i.e. the boundary of \mathcal{B} is $[L^{-1}(D), D]^{(s)} \cup [L^{-1}(D), D]^{(u)}$). Then $L(\mathcal{B})$ lies in the first and fourth quadrant. In general, if $L^{2n}(\mathcal{B})$ lies in the first quadrant for some $n \in \mathbb{N}$, then $L^{2n+1}(\mathcal{B})$ lies again in the first and $L^{2n+2}(\mathcal{B})$ in the first and possibly second quadrant. If it intersects the second quadrant, then $L^{2n+3}(\mathcal{B})$ intersects the fourth quadrant.

Now assume that W_X^u intersects the coordinate axes at points other than T_0 and T_0^{-1} and let the point S and polygon \mathcal{D}' be defined as in Lemma 3.2.5.

Lemma 4.3.5. Let \mathcal{B} be defined as above. Then for every point $B \in \mathcal{B}$ there exists $k \in \mathbb{N}$ such that $L^k(B) \in \mathcal{D}'$.

Proof. We first prove that every point in \mathcal{B} eventually gets mapped to the second quadrant. Suppose by contradiction that the converse holds. Then there exists a point $B \in \mathcal{B}$ and $k_0 \in \mathbb{N}$ such that $L^{k_0+k}(B)$ lies in the first quadrant for all $k \in \mathbb{N}$. Since L acts on those points as an affine map, we have

$$\text{dist}(L^{k_0+k}(B), \overline{XV_0}^{(s)}) = |\lambda_X^u|^k \text{dist}(L^{k_0}(B), \overline{XV_0}^{(s)}), \quad k \in \mathbb{N}_0.$$

Since $|\lambda_X^u| > 1$, we see that distances between $L^{k_0+k}(B)$ and $\overline{XV_0}$ in the first quadrant are unboundedly increasing so $L^{k_0+k}(B)$ will lie in the second quadrant. This yields a contradiction with our assumption and proves the claim.

The claim of the lemma now follows from the previous claim and Corollary 4.3.4. ■

Observe again the backward orbit $(V_0^{-n})_{n \in \mathbb{N}_0}$ of the point $V_0 \in W_X^s$. Let $n_0 \in \mathbb{N}$ be such that $V_0^{-2n_0}$ lies in the fourth and $V_0^{-2(n_0+1)}$ in the first quadrant (we know that such n_0 exists by Proposition 4.2.3; if V_0^{-2} lies in the first quadrant, we take $n_0 = 1$). Let \mathcal{P} be the polygon with boundary (see Figure 4.10)

$$\begin{aligned} \partial \mathcal{P} = & \overline{V_0^{-2n_0} T_0} \cup \overline{T_0 T_0^{2(u)}} \cup \overline{T_0^2 V_0^{-2(n_0-1)}} \cup [V_0^{-2(n_0-1)}, L^{-2n_0+1}(D)]^{(s)} \\ & \cup [V_0^{-2n_0}, L^{-2n_0-1}(D)]^{(s)} \cup \overline{L^{-2n_0-1}(D) L^{-2n_0+1}(D)}. \end{aligned}$$

Since the straight line segment $\overline{T_0 V_0^{-2n_0}}$ intersects the x -axis at T_0 only, $L^{-2}(\overline{T_0 V_0^{-2n_0}}) = \overline{T_0^{-2} V_0^{-2(n_0+1)}}$ is again a straight line segment in the first quadrant and its preimages under L converge to W_X^{s+} due to Lemma 4.2.4. If we define the set \mathcal{R}_1 as in Lemma 4.3.2, the aforementioned convergence implies the following result.

Corollary 4.3.6. For every point of $Q \in \mathcal{R}_1 \setminus W_X^{s+}$ there exists $k \in \mathbb{N}$ such that $L^k(Q) \in \mathcal{P}$.

Define ℓ as the set of accumulation points of W_X^u , as in Theorem 3.3.7.

Theorem 4.3.7. The set $\mathcal{A}_1 \setminus W_X^s$ is the basin of attraction for ℓ .

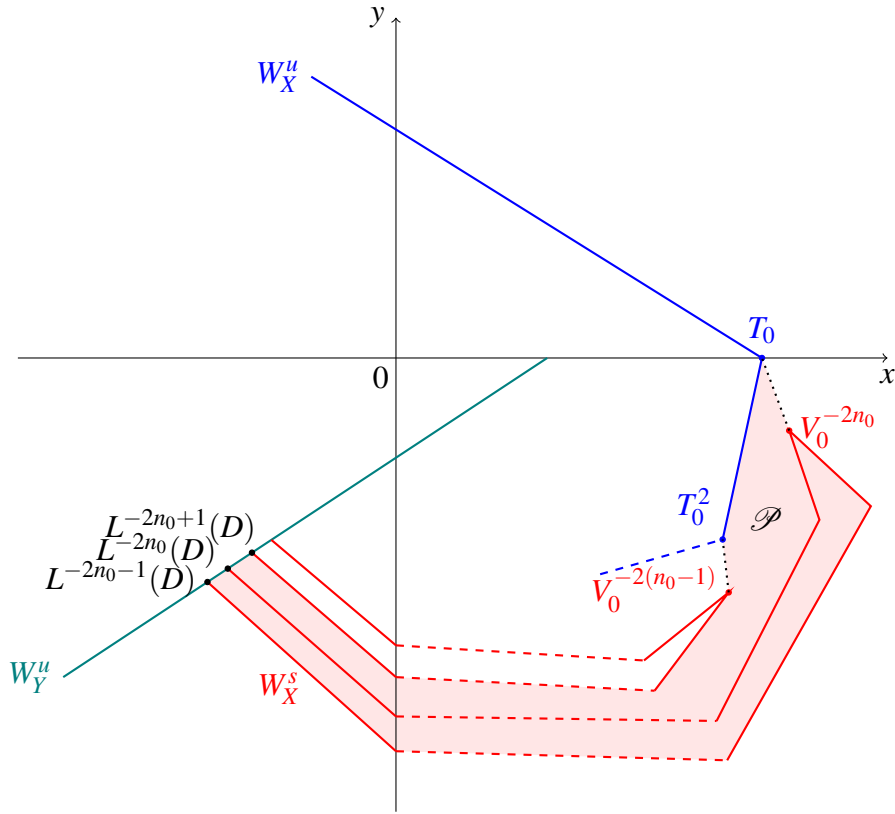


Figure 4.10: Polygon \mathcal{P} . Positive integer n_0 is chosen such that $V_0^{-2n_0}$ lies in the fourth and $V_0^{-2(n_0+1)}$ in the first quadrant. Point D is the intersection point of W_X^s and W_Y^u in the fourth quadrant.

Proof. Lemma 3.3.3 implies that it suffices to show that every point of $\mathcal{A}_1 \setminus W_X^s$ eventually get mapped to the polygon \mathcal{D}' . Due to Corollary 4.3.6 we see that this will follow if we prove that every point of \mathcal{P} eventually maps to \mathcal{D}' .

Observe that the polygonal line $[V_0^{-2n_0}, L^{-2n_0}(D)]^{(s)}$ divides \mathcal{P} into two parts, one of them being $L^{-2n_0}(\mathcal{B})$, where \mathcal{B} is the triangle from Lemma 4.3.5. From that same lemma it follows that all points from that part eventually get mapped to \mathcal{D}' .

Let Q be an arbitrary point from the other part of \mathcal{P} . If Q lies in the first quadrant (above the line segment $\overline{T_0 T_0^{-1}(u)}$), from the same argumentation as in Lemma 4.3.5 we see that there exists $k_1 \in \mathbb{N}$ such that $L^{k_1}(Q)$ lies in the second and $L^{k_1+1}(Q)$ in the fourth quadrant.

Now assume that Q lies in the fourth quadrant. We distinguish between two cases of interest. Firstly, if $L^{2k}(Q)$ all lie in the fourth and $L^{2k+1}(Q)$ in the second quadrant for all

$k \in \mathbb{N}_0$, then L^2 acts on those points as an affine map so the orbit of Q is mapped to the period-two cycle $\{P, P'\}$ and the claim follows. Otherwise, in the other case, there exists $k_2 \in \mathbb{N}$ such that $L^{k_2-2}(Q)$ lies in the fourth, $L^{k_2-1}(Q)$ in the second and $L^{k_2}(Q)$ in the third quadrant.

Let us now assume that Q lies in the third quadrant. If $L(Q), L^2(Q), \dots, L^k(Q)$ all lie in the third quadrant for some $k \in \mathbb{N}$, then L acts on these points as an affine map so

$$\text{dist}(L^j(Q), \overline{R_0 R_0^1}) = |\lambda_Y^u|^j \text{dist}(Q, \overline{R_0 R_0^1}), \quad j = 1, 2, \dots, k.$$

Since $|\lambda_Y^u| > 1$, distances between $L^j(Q)$ and W_Y^s are unboundedly increasing so there exists $k_4 \in \mathbb{N}$ such that $L^{k_4}(Q)$ lands in the fourth quadrant. From there, two things can happen: either all further iterates of $L^{k_4}(Q)$ lie in the second and fourth quadrant only (in which case we again see that they are attracted to the cycle $\{P, P'\}$), or there exists $k_5 \in \mathbb{N}$ such that $L^{k_5}(Q)$ lies in the first quadrant.

If $L^{k_5+1}(Q), \dots, L^{k_5+k}(Q)$ all lie in the first quadrant for some $k \in \mathbb{N}$, then L again acts on these points as an affine map so

$$\text{dist}(L^{k_5+j}(Q), \overline{XV_0^{(s)}}) = |\lambda_X^u|^j \text{dist}(L^{k_5}(Q), \overline{XV_0^{(s)}}), \quad j = 1, 2, \dots, k.$$

Therefore, the distances between $L^{k_5+j}(Q)$ and $\overline{XV_0^{(s)}}$ in the first quadrant are unboundedly increasing so there exists $k_6 \in \mathbb{N}$ such that $L^{k_6-1}(Q)$ lies in the second and $L^{k_6}(Q)$ in the fourth quadrant.

Notice that $L^{k_6}(Q)$ can lie in \mathcal{D}' . If not, all forward iterates of $L^{k_6}(Q)$ can lie in the second and fourth quadrant only from which we conclude by previous arguments that the orbit of that point is attracted to $\{P, P'\}$. Otherwise, $L^{k_6}(Q)$ lands in one of the polygons in the fourth quadrant outside \mathcal{D}' bounded by the x -axis and parts of the polygonal line $[T_0, S]^{(u)}$, where the point S is defined as in Lemma 3.2.5. Observe the parts of the x -axis that belong to the boundary of those polygons. Their intersections with $[T_0, S]^{(u)}$ all eventually get mapped to \mathcal{D}' and moreover, apart from those points, images of those parts under L^2 do not intersect $[T_0, S]^{(u)}$ at any other additional points. Those polygons are thus also eventually mapped to \mathcal{D}' which finishes the proof. ■

CONCLUSION

We studied the dynamics of the two-parameter family of Lozi maps in a region \mathfrak{R} in the parameter space for which there are no homoclinic points for the fixed point X in the first quadrant and the cycle of period two is attracting. Results about homoclinic points for X were presented first. We describe the zigzag structure of the stable manifold of X in the third quadrant as well as prove that in the border case there are only homoclinic tangencies. The construction of polygons bounded by the stable and unstable manifold of X which are mapped into each other under the Lozi map permits us to prove that all homoclinic points in the border case are iterates of two salient points T_0 and V_0 . Along with these results, we also compute the equations of curves in the parameter space which represent the border of the set of existence of homoclinic points for the fixed point X . The following question of interest was the zero entropy locus for the Lozi map. We further look into the structure of the unstable manifold of X , construct invariant polygons in part bounded by it and prove that the topological entropy of the Lozi map is zero for all parameter pairs in the region R for which the unstable manifold intersects the coordinate axes at T_0 and its preimage only. In addition, we prove the same result for parameter pairs in $\mathfrak{R} \setminus R$ when the Lozi map is restricted to the complement of the accumulation set ℓ of the unstable manifold of X and conject that ℓ consists of the period-two cycle only. Finally, considering the same parameter set \mathfrak{R} , we analyze the stable manifold of the other fixed point Y in the third quadrant and prove that it separates the plane into two connected components. By proving that all points in one of those connected components tend to infinity under the Lozi map, we see as a consequence that the basin of attraction of the period-two cycle is contained in the other one, \mathcal{A}_1 . We also prove that the set \mathcal{A}_1 , without the stable manifold of X , is the basin of attraction of the accumulation set ℓ .

BIBLIOGRAPHY

- [1] Baptista, D., R. Severino, and S. Vinagre: *The basin of attraction of Lozi mappings*. International Journal of Bifurcation and Chaos, 19(03):1043–1049, 2009. ↑ 3, 82.
- [2] Benedicks, M. and L. Carleson: *The dynamics of the Hénon map*. Annals of Mathematics, 133(1):73–169, 1991. ↑ 1.
- [3] Bonatti, C., L. J. Díaz, and M. Viana: *Dynamics beyond uniform hyperbolicity: A global geometric and probabilistic perspective*, volume 3. Springer Science & Business Media, 2004. ↑ 21.
- [4] Burns, K. and H. Weiss: *A geometric criterion for positive topological entropy*. Communications in mathematical physics, 172(1):95–118, 1995. ↑ 20, 77, 81.
- [5] Buzzi, J.: *Maximal entropy measures for piecewise affine surface homeomorphisms*. Ergodic Theory and Dynamical Systems, 29(6):1723–1763, 2009. ↑ 3.
- [6] Devaney, R. L.: *An introduction to chaotic dynamical systems*. CRC press, 2018. ↑ 7, 9.
- [7] Hénon, M.: *A two-dimensional mapping with a strange attractor*. Communications in Mathematical Physics, 50(1):69–77, 1976. ↑ 1.
- [8] Ishii, Y.: *Towards a kneading theory for Lozi mappings I: A solution of the pruning front conjecture and the first tangency problem*. Nonlinearity, 10(3):731, 1997. ↑ 2, 3, 4, 29, 30.
- [9] Ishii, Y.: *Towards a kneading theory for Lozi Mappings II: Monotonicity of the topological entropy and Hausdorff dimension of attractors*. Communications in mathematical physics, 190(2):375–394, 1997. ↑ 4.

- [10] Ishii, Y. and D. Sands: *Monotonicity of the lozi family near the tent-maps*. *Communications in mathematical physics*, 198(2):397–406, 1998. ↑ 4, 27.
- [11] Lozi, R.: *Un attracteur étrange(?) du type attracteur de Hénon*. *J. Physique*, 39(9):9–10, 1978. ↑ 1.
- [12] Misiurewicz, M.: *Strange attractor for the Lozi mappings*. *Ann. New York Acad. Sci.*, 357(1):348–355, 1980. ↑ 1, 50.
- [13] Mora, L. and M. Viana: *Abundance of strange attractors*. *Acta mathematica*, 171(1):1–71, 1993. ↑ 20.
- [14] Newhouse, S. E.: *The abundance of wild hyperbolic sets and non-smooth stable sets for diffeomorphisms*. *Publications Mathématiques de l’IHÉS*, 50:101–151, 1979. ↑ 21.
- [15] Newhouse, S. E.: *Homoclinic Phenomena*. American Mathematical Society, 350(10):4023–4040, 2006. ↑ 20, 21.
- [16] Poincaré, H.: *Les méthodes nouvelles de la mécanique céleste*, volume 3. Gauthier-Villars et fils, 1899. ↑ 19.
- [17] Pollicott, M. and M. Yuri: *Dynamical systems and ergodic theory*. Number 40. Cambridge University Press, 1998. ↑ 23, 24, 25, 27.
- [18] Pujals, E. R. and M. Sambarino: *Homoclinic tangencies and hyperbolicity for surface diffeomorphisms*. *Annals of Mathematics*, pages 961–1023, 2000. ↑ 22.
- [19] Robinson, C.: *Dynamical systems: stability, symbolic dynamics, and chaos*. CRC press, 1998. ↑ 9.
- [20] Smale, S.: *Differentiable dynamical systems*. *Bulletin of the American mathematical Society*, 73(6):747–817, 1967. ↑ 9, 19.
- [21] Yildiz, I. B.: *Monotonicity of the Lozi family and the zero entropy locus*. *Nonlinearity*, 24(5):1613–1628, 2011. ↑ 2, 4, 27, 28, 29, 66.

- [22] Yildiz, I. B.: *Discontinuity of topological entropy for Lozi maps*. Ergodic Theory and Dynamical Systems, 32(5):1783–1800, 2012. ↑ 3, 29.

CURRICULUM VITAE

Kristijan Kilassa Kvaternik was born on October 27, 1992, in Zagreb, Croatia, where he finished primary and secondary school. During secondary school, he attended mathematical competitions, winning a Bronze Medal at the Middle European Mathematical Olympiad in 2009.

In 2011 he started studies at the Department of Mathematics, Faculty of Science, University of Zagreb. He obtained his bachelor's degree in 2014 and his master's degree in Theoretical Mathematics in 2016 with master's thesis *Thurston geometries* under supervision of Prof. Dr. Željka Milin Šipuš. During his studies, he was a demonstrator at various courses, including Linear Algebra, Probability and Metric Spaces, and he received awards for exceptional success in studies in academic years 2013/2014 and 2015/2016.

In 2016 he enrolled in the PhD program in Mathematics at the same faculty under supervision of Prof. Dr. Sonja Štimac. In the same year he started working as a research and teaching assistant at the University of Zagreb: he first worked at the Department of Quantitative Methods at the Faculty of Organization and Informatics, then, since July 2017, at the Department of Applied Mathematics at the Faculty of Electrical Engineering and Computing where he is currently employed.

He was a member of the scientific project *Geometric, Ergodic and Topological Analysis of Low-dimensional Dynamical Systems* (project leader: Prof. Dr. Siniša Slijepčević) and is currently a member of the project *Dynamical and Ergodic Properties of Maps on Surfaces* (project leader: Prof. Dr. Sonja Štimac), both of them funded by the Croatian Science Foundation. During his PhD studies he participated in nine international summer schools and conferences where he presented a poster and gave three talks. He is an active member of the *Seminar for Dynamical Systems* at the Department of Mathematics, Faculty of Science, University of Zagreb.